VISUAL AND MOTION CUES IN LATERAL AND PITCH SIMULATOR STABILIZATION

by

JEN-KUANG HUANG

B.S., NATIONAL TAIWAN UNIVERSITY, 1975
S.M., MASSACHUSETTS INSTITUTE OF TECHNOLOGY, 1979

SUBMITTED IN PARTIAL FULFILLMENT OF THE
REQUIREMENTS FOR THE DEGREE OF
DOCTOR OF PHILOSOPHY

IN

ESTIMATION AND CONTROL

at the

MASSACHUSETTS INSTITUTE OF TECHNOLOGY

JANUARY 1983

Signature of Author_____
Department of Aeronautics and Astronautics, January 1983

Certified by_____
Thesis Committee Chairman, Laurence R. Young

Certified by_____
Charles M. Oman

Certified by_____
Robert V. Kenyon

Accepted by_____
Chairman, Departmental Graduate Committee

VISUAL AND MOTION CUES IN LATERAL AND PITCH SIMULATOR STABILIZATION

by

JEN-KUANG HUANG

Submitted to the Department of Aeronautics and Astronautics on January 7, 1983, in partial fulfillment of the requirements for the degree of Doctor of Philosophy in Estimation and Control.

ABSTRACT

The influence of the visual field on human control performance in the closed-loop task of nulling perceived self-motion has been studied during angular pitch rotation and linear lateral motion. Measurements were made of subject performance in nulling perceived tilt pitch angles in the face of a pseudo-random vestibular disturbance combined with four types of visual field motion. Time histories of subject response showed a position bias of the trainer in the direction of field rotation with a larger value for pitch backwards than for pitch forward. Based on the correlation between the vestibular input and the operator response, the high frequency stimulation is mainly processed through the semicircular canals rather than the otolith organs. The results also suggest that the subject tends to rely less on the otolith organs in pitch compared to the roll case.

A type of projector display system has been designed and built to provide the selected visual field cues during the lateral motion. Human control performance in the closed-loop task of nulling perceived self-velocity about the lateral axis has been measured. A better operator performance, which corresponds to a higher gain in the low frequency range, was found with the fixed visual field as compared to that in the dark. This results from the sensitive motion detection capability associated with a fixed spot being visible during the motion. Describing function

data, relating subject compensatory response to actual linear velocity in the dark, was corrected for the dynamics of the operator nulling behavior and the resulting estimator, which is mainly represented by the otolith organs, was linearly modelled in the frequency domain. A Bode plot of the estimator data showed good agreement up to 1.5 rad/sec with a dynamic model of the otolith perception system.

Two psychological tests were performed to provide quantitative measures of the extent of field dependence of the subjects. Although the results from over 30 subjects showed that sex is an important factor and that educational background is not an important factor in contributing to field dependence, all the subjects who participated in the lateral motion experiments tended to be field independent, irregardless of how well or poorly they performed the task.

Thesis Supervisor: Laurence R. Young
Title: Professor of Aeronautics and Astronautics

Thesis Supervisor: Charles M. Oman
Title: Senior Research Engineer, Aeronautics and Astronautics

Thesis Supervisor: Robert V. Kenyon
Title: Assistant Professor of Aeronautics and Astronautics

ACKNOWLEDGEMENT

I would like to thank first my wife, Tyng-Genn Huang, who accompanied me lovingly through the many hours and years leading to the completion of this thesis.

I also wish to express my special gratitude to Professor Laurence R. Young for his excellent guidance, friendly encouragement and support throughout this study. Dr. Charles M. Oman provided many stimulating discussions on the problems found in this research. Professor Robert V. Kenyon gave considerable insight on the visual system. I am grateful for all their help and comments regarding the thesis itself.

Many people in the Man Vehicle Laboratory were very helpful to me and I appreciate both their assistance and their time spent as subjects. In particular, I would like to thank Anthony P. Arrott for his help with the MIT sled and in providing the software programs at the beginning of this research. Paul A. Wetzel helped me to find subjects to participate in the psychological tests. Bob Renshaw and Earl Wassmouth were totally indispensable to the design, construction and maintenance of the equipment. I also gratefully acknowledge the help of Sherry Modestino, who, with the assistance of Margaret Armour, has been a tremendous aid in improving and typing the final manuscript.

I would also like to express my gratitude to Dr. Greg Zacharias who introduced me to the instrumentation during the early days of this thesis and helped me extend his experimental approach in this research.

Finally, I wish to thank my parents and my brother, Chi-Kuang, for their support from the beginning of my life.

This research was supported by NASA Grants NSG 2032, NAG 2-12, and NAG 2-88.

TABLE OF CONTENTS

CHAPTER I

INTRODUCTION

1.1 Research Scope and Objectives

This research is aimed at investigating the influence of the visual field on the characteristics of the vestibular system during rotatory and linear motion. From our experiments, we wished to provide a functional model to explain how vestibular motion cues are integrated with visual field motion cues to result in a subjective sensation of self motion in different axes of rotation and linear motion. In previous years, considerable research effort has been directed toward understanding how our sense of self-motion is determined by the sensory cues available to us. This concentration on vestibular function has met with considerable success in developing descriptive models which predict sensation as a function of actual motion. Efforts directed at determining how motion cues in the peripheral visual field affect sensation have emphasized the qualitative aspects of the cues which best elicit motion illusions, although some work has also been directed toward explaining the dynamics of such illusions. A natural extension of both visual and vestibular studies involves combined cue presentation; the research reported here is directed toward that goal.

Zacharias and Young (1981) first developed a quantitative cue conflict model that provided a functional explanation of how vestibular

rotatory motion cues are integrated with peripheral visual field motion cues to result in a subjective sensation of self-rotation about an earth-vertical axis. The fundamental ideas contained within this earth-vertical rotation model provide a solid base on which to extend functional modelling to combined visual-vestibular cues applied about other axes. On the other hand, the vestibular processing model proposed by Ormsby (1974) has met with some success in modelling combined semicircular canals and otolith cue response. To take advantage of the work in this area, this research is directed toward investigating the influence of combined visual and vestibular cues about other axes. Since the roll axis was previously investigated (Huang, 1979), the scope of this research is restricted to pitch axis sensation and lateral translational motion sensation.

Although in the pitch experiment, we follow a similar experimental approach to that used in the yaw experiments, the pitch case is significantly more complicated than either yaw or roll due to the position of the utricle which is a part of the otolith system. The additional involvement of the otolith cues comes about through two pathways: the change in head orientation relative to the vertical and the tangential linear acceleration resulting from the fact that the axis of rotation is well below the pilot's head. This experiment is also technically challenging to perform since a suitable "wash-out" circuit may have to be invoked in order to permit excursions which are large enough to excite the semicircular canals and otoliths and yet which do not run the risk of having the subject frequently drive the trainer to the fixed pitch angle limits. In addition to developing an input-output model of subjective

response due to combined visual and vestibular cues, this experiment can provided two profitable investigations. First is the investigation of the directional asymmetry found in pitch vection, which will be described in Section 1.3.1. Second, it may provide a further understanding of how information is processed through the vestibular system in the pitch axis as compared to those found in the roll case.

An analytically simpler case than the pitch experiment is the case of horizontal linear acceleration with supporting or conflicting visual cues, in which there is primarily only a visual-otolith interaction to be considered. This topic was studied not only because only qualitative studies have been found in the literature, as described in Section 1.3.2.1, but also because of the availability of a rail-mounted linear acceleration cart in the Man Vehicle Laboratory. Since considerably less work has been done in the field of translational motion sensation compared with that done in rotational motion sensation, our work is aimed at modelling both the otolith system and visual-otolith interaction.

It is anticipated that this research would be a significant contribution in both the basic area of understanding the properties of motion perception and the applications areas which rely on human motion perception models. Knowledge concerning human spatial orientation is important to the design and use of fixed and moving base aircraft simulators and trainers. For example, if the visual information is presented in the proper way, a sense of motion can be imparted when there is no actual motion. Such an approach may not only minimize the current trial and

error procedures used in simulator design, but may also indicate how simultaneous presentations of fairly simple visual and vestibular cues may be used to induce a relatively complex sensation of motion. Recently, Sivan et al. (1982) showed a method for designing moving flight simulators using an optimal control approach to minimize the difference of the physiological outputs of the vestibular organs of the pilot in an airplane and the pilot in the simulator. Modelling of motion perception has proved beneficial in this area.

In the following section, some background material is presented which is related to this research. Section 1.2 will briefly introduce the vestibular system -- its structure, function, and a review of the modelling work in this area, especially for the otolith system. Section 1.3 then introduces visually induced motion sensations related to this research, particularly pitch vection and linearvection. Finally, Section 1.4 provides a brief, chapter-by-chapter, outline.

1.2 The Vestibular System

The vestibular system, man's motion sensing center, is the non-auditory portion of the inner ear. It is one of the sensory systems which provides information on body orientation and balance relative to the environment. Considerable physiological research and histological studies have been directed toward the vestibular system and, because of its implications on man's orientation in space, its properties and functions are under intense investigation.

1.2.1 Structure and Function

This section will briefly introduce the basic structural organization and physiological function of the vestibular system. More detailed introductions are available from Young (1974), Guedry (1974), and Peters (1969).

As shown in Figure 1.1, the inner ear is functionally divided into two parts: (1) an auditory transducer called the cochlea, and (2) a non-auditory portion, the vestibular system. This membranous structure, also called the labyrinth, is enclosed in a cavity called the bony labyrinth in the temporal bone of the skull. The two components of the vestibular system, the semicircular canals and otoliths, will be described below.

1.2.1.1 The Semicircular Canal System

The semicircular canals consist of three approximately circular toroidal canals whose axes form a roughly orthogonal set. The membranous canals are suspended in a fluid which is called perilymph in the temporal bone of the skull. The semicircular canals are filled with a water-like fluid called endolymph, which, due to its inertia, tends to lag behind the motion of the canal walls when the head undergoes angular acceleration. At one end of each canal is an expanded section called the ampulla. It contains a gelatinous, elastically restrained "flapper valve" called the cupula, which is attached to the crista. The crista is a raised section of the inner wall of the ampulla, which contains a layer of sensory hair cells. When the endolymph moves relative to the canal, it tends to dis-

place the cupula. This displacement is detected by the hair cells on the crista and in turn produces a change in the firing frequency of the first order afferents which provide information to the central nervous system. All of the hair cells associated with a particular canal have the same polarization and hence all cause either excitation or inhibition. The canals on the right side are essentially coplanar with the canals on the left side and they are pairwise sensitive to angular motion about the same axes.

1.2.1.2 The Otolith System

The otolith organs are another part of the vestibular system located in the inner ear and are found in the vestibule of the bony labyrinth between the three semicircular canals and the cochlea. The otoliths are divided into two different organs, the utricle and the saccule (see Figure 1.1). The utricle is in the utricular sac, which is a relatively large, oblong chamber common to all three semicircular canals. The utricle lies in a plane inclined about 20° above the horizontal plane, while the saccule lies in an almost vertical plane. Each otolith organ contains beds of sensory hair cells and supporting cells called the maculae. The utricle and saccule maculae are oval in shape. Situated on top of the cilia of the hair cells is a gelatinous mass containing a large number of dense hexagonal prisms of calcium carbonate crystals called otoconia (Figure 1.2). The otoconia have a specific gravity of about 2.94 (Engstrom, 1968), while the specific gravity of the endolymph in which they are located is about 1.02 (Jongkees, 1967). Because of this

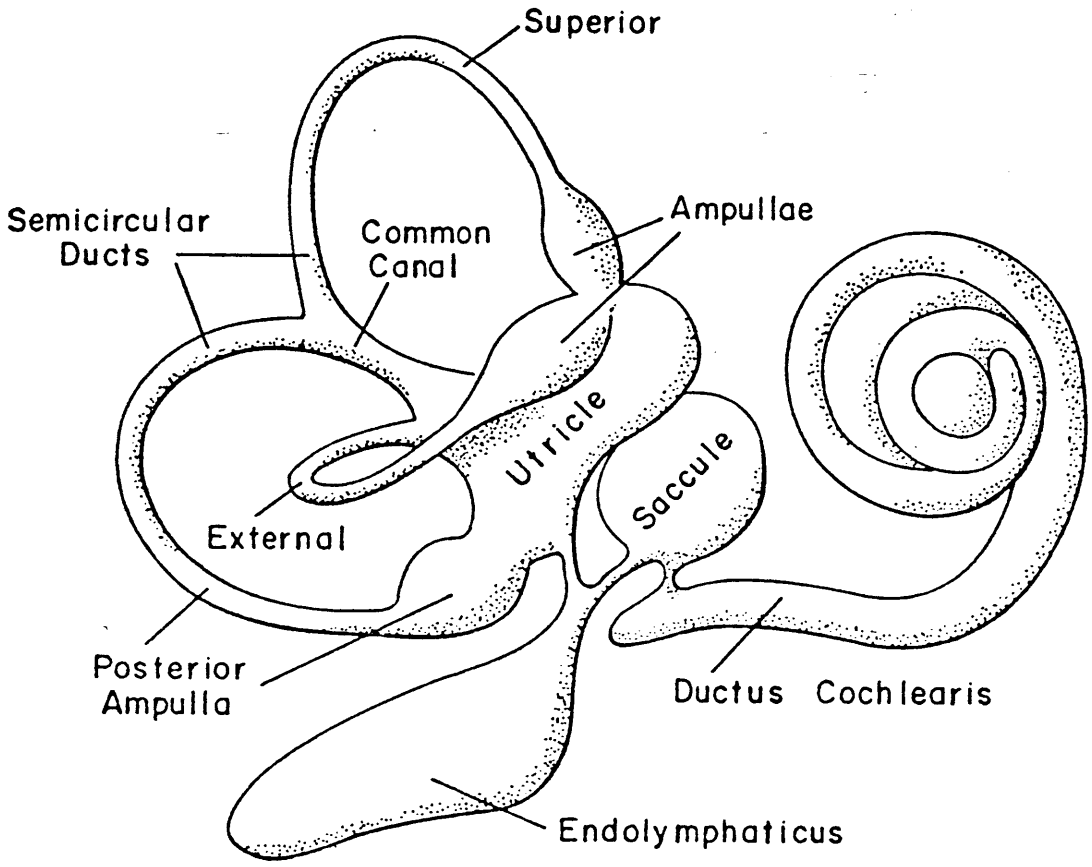

Figure 1.1: The Membranous Inner Ear (from Barnhill, 1940)

difference in density, the otoliths respond to linear accelerations, including gravity.

The utricles are oriented such that the major plane of their sensitivity is parallel to the plane of the horizontal semicircular canals. The saccular organs are oriented so that their plane of sensitivity is perpendicular to the horizontal canals and roughly parallel to the median plane. Unlike the semicircular canals, the hair cells in the otolith do not all have the same directional polarization and the orientation of the hair cells at various regions of the utricular and saccular maculae is not uniform (Figure 1.3). There is a raised portion of the maculae called the striola which runs in a curved manner across the macula. The functional striola have opposite polarizations. The utricular maculae are sensitive to displacements in any direction in the utricular plane and the afferent fibers innervating them have been shown to respond to tilt in any direction. The saccular macula, oriented principally in the vertical plane, has a similar structure. Although the functions of the saccular macula in man is still not entirely clear, it appears to respond to low-frequency vibration and to gravity and linear acceleration, especially along the longitudinal axis.

The adequate stimulus to the otoliths is linear acceleration. At the end of the nineteenth century, Breuer (1891) thought that a "sliding movement" was a sufficient stimulus to the maculae. At that time, some writers favored compression and others favored traction (Magnus, 1924; Quix, 1925; Mygind, 1948) on the hair cells from the weight of the

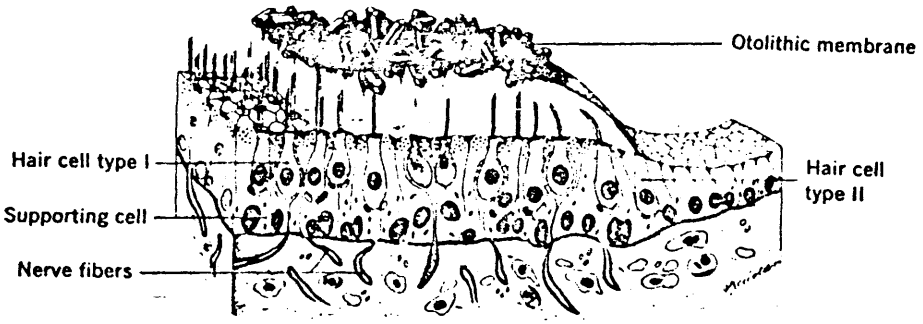

Fig. 1.2: Schematic drawing of macular epithelium. (From Iurato, 1967)

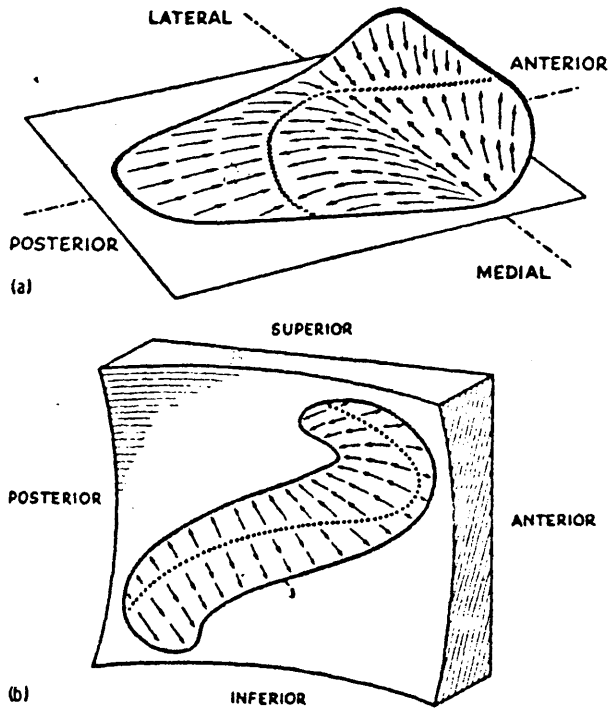

Fig. 1.3: Schematic representation of the direction of the sensory hairs. (a) in the utricular macula; and (b) in the saccular macula. (From Spoendlin, 1966)

otoconia as the effective physiological stimulus of the maculae. Today, most authors agree that the shear component is the most effective component of the stimulus (Von Holst, 1950a, 1950b; Meiry, 1965; Schöne, 1964; Von Bekesy, 1966). Recent evidence by Fernandez and Goldberg (1976a, b, c) also confirms the theory of shear forces.

1.2.2 Models of the Vestibular System

As compared to the effort devoted to studying rotational motion sensation (mainly detected by the semicircular canals), considerably less work has been done in the field of translational motion sensation (mainly detected by the otoliths). In this thesis, since modelling of the otolith system is involved, we will focus more on reviewing models of the otolith system than on those for the semicircular canals.

1.2.2.1 Models of the Semicircular Canals

It is generally accepted that the semicircular canals are the primary nonvisual sensors of rotational motion with respect to inertial space in the dark and also play a major role in detecting the high frequency components of angular motion in the light. The semicircular canals respond to angular acceleration as would a heavily damped torsion pendulum with some additional rate sensitivity and adaptation (Young and Oman, 1969; Goldberg and Fernandez, 1971; Young, 1974). The quantitative model of angular velocity sensation took the following form:

$$\frac{\hat{\omega}}{\omega} = \frac{\tau_L s}{(\tau_L s + 1)(\tau_s s + 1)} \frac{\tau_a s}{\tau_a s + 1} \tag{1.1}$$

where τ_L, τ_s, τ_a are the long time constant, the short time constant, and the adaptation time constant, respectively. The parameters and the threshold values are varied for different rotational axes (Hosman and Van der Vaart, 1978; Zacharias, 1978).

1.2.2.2 Models of the Otolith System

The otolith organ transduction dynamics are not as fully developed as for the semicircular canals and whether the sensation is caused by one of tilt, acceleration, or velocity, or some combination of the three is still not well defined. However, several models have been proposed for various parts of the otolith system and will be briefly discussed below.

It is well known that the otolith organs respond to static tilt away from the vertical. Fernandez et al. (1972) first started to study the details of the transduction geometry by statically tilting the otoliths and recording from the primary afferents. They showed that the firing rate of each responding unit was driven by the applied shear force of gravity, determined by head tilt, and by the unit's orientation within the otolith organ. Since the utricle and saccule are approximately planar surfaces, this implies that each organ can provide a vector measure of the specific force vector restricted to those components of the specific force vector contained within the organ's plane. Each unit was characterized by

a functional polarization vector, which defines the axis of greatest sensitivity. Force-response functions were obtained in the stimulus range of -4.92 to 4.92 g (Figure 1.4).

Forces were directed parallel to each units polarization vector. The normalized force response function can be described as a normal distribution function with three factors X_1, X_2, and X_3. X_1 and X_2 may correspond, respectively, to the transduction gain and receptor bias. X_3 might possibly be thought of as a mechanical gain relating effective force to displacement of the sensory hair bundle and d_{res} as the residual discharge (typically 5 to 20 spikes/sec).

Schöne (1964) performed a series of psychophysical experiments which investigated perception of the vertical as a function of specific force magnitude and direction. The results confirmed the static shear force sensitivity described above.

Ormsby and Young (1976) extended the stimulus response behavior by using a non-linear modification of the specific force processing. They proposed a functional model (Figure 1.5) which provides for linear transduction of utricular shear force, in combination with non-linear transduction of specific force perpendicular to the utricular plane. This latter transduction is possibly effected by the saccule.

The roll and pitch tilt illusions associated with the perception of static tilt in various specific force environments have been classified in such a way that this model is developed to account for the available

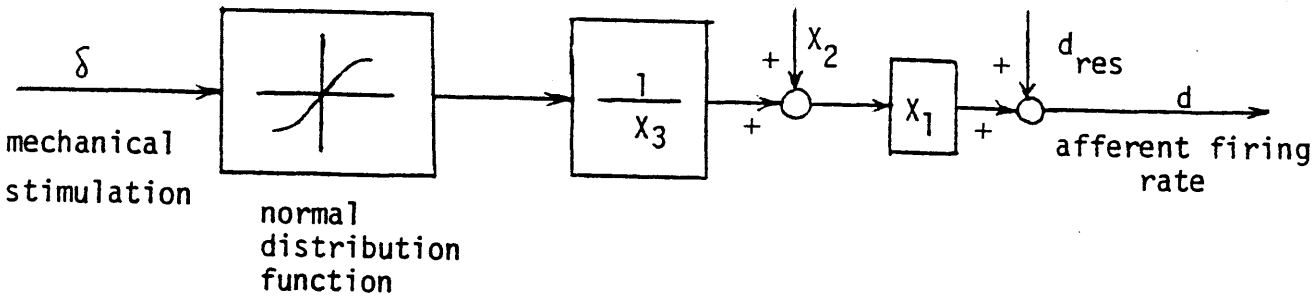

Figure 1.4: Static force-response relation model.

(Derived from Fernandez et al, 1976b)

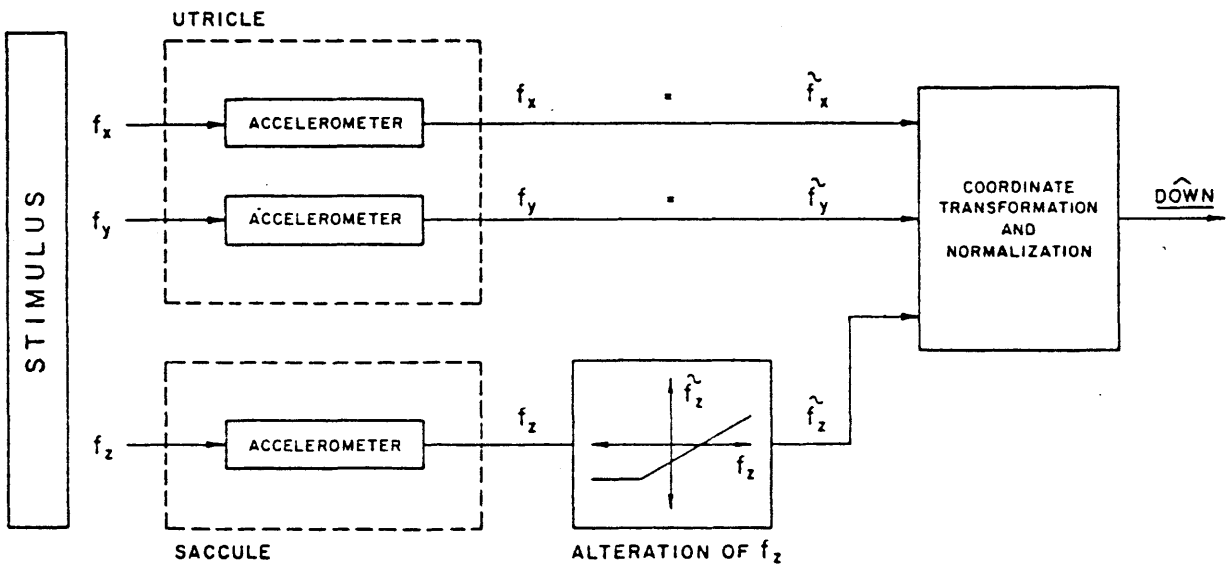

Figure 1.5: Model of perceived orientation.

(From Ormsby and Young, 1976)

experimental data. Finally, the perceived direction of "down" is given by a simple normalization of the transduced force vector, $\underline{f}$, according to

$$\hat{\underline{DOWN}} = \underline{f} \; / \; |\hat{\underline{f}}| \tag{1.2}$$

Meiry (1965) first investigated the dynamics of subjective sensation in response to time varying specific force cues. The frequency response of the utricle was studied by having subjects indicate, with a light-spring stick, the direction of motion during fore-aft linear sinusoidal motion within the frequency range 0.02 to 0.9 cps. By assuming that the saccule was irrelevant and that subjects were indicating the sign of their perceived velocity, he specified the stimulus-response phase relation dependence on stimulus frequency and constructed a linear "utricle" model which relates perceived velocity to actual velocity.

Peters (1969) raised the question of model output and suggested that the sensation measured in the experiment was not subjective velocity, but rather, subjective acceleration. Moreover, the long time constant of the otoliths, based on this model, was very long compared to those estimated by deVries (1950) and others (Jongkees and Groen, 1946).

Young and Meiry (1968) then proposed a revised model (Figure 1.6) of linear acceleration sensation which included a static component and provided a better fit to a greater range of observations by shortening the long time constant and adding a lead term. This revised linear model will act approximately as a velocity transducer over the mid-frequency range of

0.19 to 1.5 rad/s. The transfer function from specific force to perceived tilt or lateral acceleration has a static sensitivity of 0.4. The parameters of this model's transfer function might be justified by the known shear force transduction characteristics of the otolith organs.

The nonlinear equivalent model (Figure 1.7) incorporates a threshold and a more aptly positioned lead term. The threshold was added based on a minimum deviation of the otolith with respect to the macula rather than on the basis of a minimum output of the total model. In fact, the afferent recordings of Fernandez et al. (1972, 1976) suggest that neither a mechanical nor a neural threshold exists at the end organs. So this model may be interpreted as a functional characterization of input-output behavior rather than a detailed model of individual components along the sensory path. This model appears to fit latency detection curves as well as the data on the phase lag associated with counterrolling eye movements measured by Kellogg (1965) and Hannen et al. (1966). Recently, Lichtenberg et al. (1982) presented the first measurements of ocular counterrolling in humans induced by varying linear accelerations. The results showed that the transient ocular counterrolling response to a step acceleration followed by a deceleration shows good agreement with the model predictions. However, the sinusoidal ocular counterrolling response showed a greater phase lag than that predicted by the model at the three tested frequencies (0., 0.4, and 1.0 Hz).

Fernandez and Goldberg (1967c) showed a detailed look at afferent response to time-varying stimuli and suggested that otolith transduction

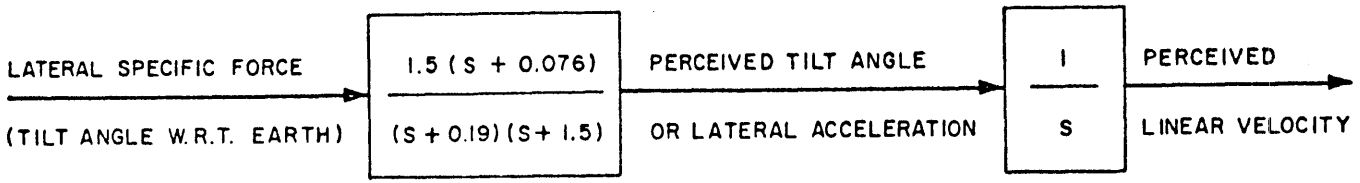

Figure 1.6: Revised otolith linear model. (From Young and Meiry, 1968)

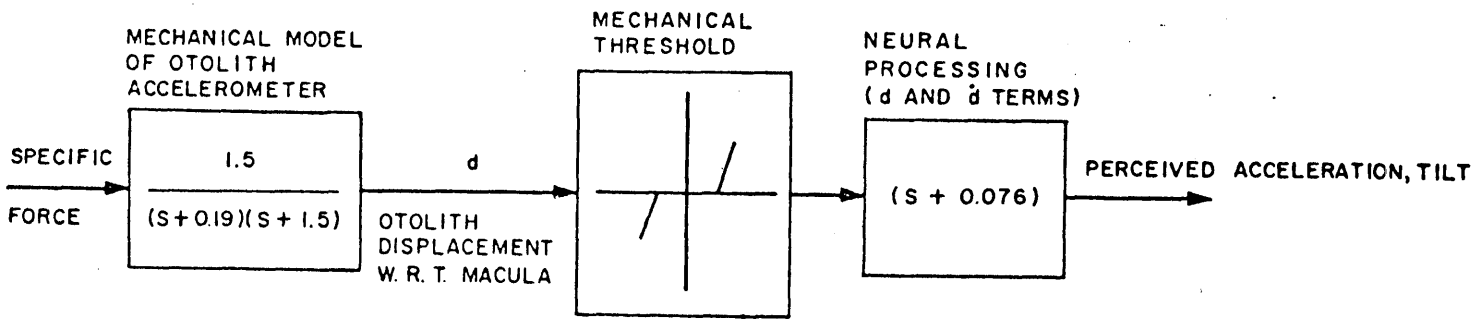

Figure 1.7: Revised otolith nonlinear model. (From Young and Meiry, 1968)

dynamics are not consistent with the subjective sensation model described above. Fernandez and Goldberg's model for the end organ includes a velocity-sensitive fractional exponent element, an adaptation element and a first order lag element associated with the mechanics of the otolith. Different dynamic responses from individual neurons can be accounted for by changes in the adaptation and velocity sensitive elements. The transfer function of the model is.

$$H(s) = \frac{1 + K_A\tau_A s}{1 + \tau_A s} \cdot \frac{1 + K_v(\tau_v s)^{K_v}}{1 + \tau_M s} \qquad (1.3)$$

τ_v is set equal to 40 seconds and large changes in τ_v can be cancelled out by small changes in K_V. With both excitatory and inhibitory sine wave stimulus, the parameters of the model were obtained by fitting the model to the Bode plots. For regular units responding to excitatory sine wave stimuli, the following average (N=16) parameters were obtained: K_V = 0.188, K_A = 1.12, τ_A = 69 seconds (based on units with $K_A > 1.5$), τ_M = 16 msec.

This model implies a long time constant in the range of 5 to 30 msec which is more than two orders of magnitude smaller than that associated with the subjective sensation model. Obviously, the long integration time seen in the subjective response must be found other than at the end organ. Substantial phase lags have been found at the level of the vestibular nuclei (Melvill Jones and Milsum, 1970).

Finally, Ormsby (1974) presents an optimal control model similar to Meiry'smodel but in modern control format. Borah et al. (1978) also

developed a multisensory (visual, vestibular, tactile and proprioceptive) Kalman filter time history model. This model has predicted some of the important qualitative characteristics of human dynamic spatial orientation under combined wide field visual motion and platform motion.

1.3 Visually Induced Motion Sensation

The phenomenon of visually induced motion sensation is a common one easily observed when gazing at moving clouds, streaming water, or when a train moves on the adjacent track in a railway station. This compelling sensation of body movement can even affect postural balance. Visually induced self motion has been explored for rotations about the earth vertical axis (circularvection) as well as for rotations about the horizontal axis (pitch or roll vection). Visually induced linear motion sensation (linearvection) can be evoked in a stationary subject by projection of a visual scene moving linearly in a sagittal plane at the periphery of the visual field. The effective field for generating a sensation of motion may be a large striped or checkerboard pattern as well as quasi-natural stimuli such as motion pictures taken from a moving vehicle (Gibson, 1947) or a swinging room surrounding the subject (Wood, 1895; Lishman and Lee, 1973). The general characteristics of visually induced motion in the absence of vestibular cues has been reviewed by Young (Henn et al., 1980, p. 557). One additional characteristic which was not mentioned is the dependence of the visually induced self-rotation on perceived linear surround motion, rather than angular motion in the horizontal plane. Wist et al. (1975) found that with the angular speed of the surround held

constant, the perceived speed of self-rotation increased linearly with increasing perceived distance of this surround.

The interaction between visual and vestibular cues is now established from psychophysical and electrophysiological data. An essential result is that vision can contribute to the sensation of self motion during rotation at a constant velocity whereas the labyrinthine receptors, whose specific stimulus is acceleration, can only signal changes of velocity. Effects of visual-vestibular interaction on self-motion perception, postural control and the generation of nystagmus have been recently reviewed by Dichgans and Brandt (1972) and Henn et al. (1980). However, since we are particularly focusing on the visually induced pitch and lateral motion sensations in this research, pitch vection and linearvection will be discussed in more detail in the following sections.

1.3.1 Pitch Vection

Pitch vection is an illusion which results from viewing a large pattern that moves around the y axis (the axis that is perpendicular to the saggital plane). Just like circularvection, the induced pitch motion is opposite to the direction of the pattern motion. However, in contrast to circularvection, subjects experience only a limited displacement despite a continuous sensation of self motion. This characteristic is similar to roll vection and the constraint on displacement may be caused by the inputs from the otoliths and somatosensory graviceptors, which are in conflict with the visual effect. This hypothesis has been confirmed by

Young et al. (1975). By using a full field (360°) flight simulator projection system, the visually induced pitch tilt illusion showed a similarity to roll vection in terms of its dependence on stimulus speed and head position. This vection increased for the head rolled 90° to the side or inverted, and decreased for the head pitched 25° forward. This is mainly caused by the conflict between the visual cues and the otolith information. As described in Section 1.2.1.2, with the head positioned 25° forward, the dominant plane of the utricular maculae is approximately horizontal and the sensitivity would thereby be maximized. With the head oriented away from the erect position, the utricular graviceptors are placed in relatively less sensitive positions, and consequently appear to be less effective in inhibiting the visual tilt illusion. However, pitch stimuli were found to produce a sensation of tilting to a steady pitch angle which was much stronger for pitch forward than backward. No corresponding left-right asymmetry was found in roll vection (Huang, 1979; Young et al., 1975). This directional asymmetry was found in this research and is discussed further in Section 2.5.1.

1.3.2 Linearvection

Helmholtz (1896) and Fischer and Kornmüller (1930) probably were the first to observe the influence of linearvection on postural balance, a phenomenon that was later rediscovered by Lee and Aronson (1974) and Lestienne (1977). In the following, we will briefly discuss horizontal and vertical linearvection and finally a neurophysiological study on linearvection.

1.3.2.1 Horizontal Linearvection

Berthoz et al. (1975, 1977, 1980) and Pavard and Berthoz (1977) found that although the general characterization of horizontal linearvection is qualitatively similar to that of circularvection, a number of interesting differences are apparent.

Threshold

The threshold for the appearance of linearvection was measured as a function of image luminance and velocity. The luminance thresholds were very close to the absolute luminance thresholds for image detection. Leibowitz and Dichgans (1977) found similar results found similar results for circularvection. The velocity threshold for forward linearvection (about 1 to 3 cm/sec) was of the order of magnitude of image velocity detection by the visual system. The velocity threshold for backward linearvection (below 1.5 cm/sec) was found to be systematically smaller than that for forward linearvection.

Onset Latency

Latencies for linearvection are consistently shorter than those for circularvection (1 to 14 seconds). With the scene velocity in the range 0.1 to 1 m/sec, the latencies are found to range around 1.5 sec (Berthoz et al., 1975) or 2.7 seconds (Chu, 1976), irrespective of stimulus velocity.

Saturation Velocity

Saturation velocities for linearvection seem to be similar to those of

circularvection as may be calculated from the data of Berthoz et al.

After Effect

There is a very small visual after effect induced by prolonged linearvection compared to the striking after effect observed, for instance, after exposure to a rotating disk in the frontal plane. However, a visual after effect may be observed when the subject associates locomotion with linearvection.

Frequency Response

Bode plots of the input sinusoidal image velocity and output linearvection showed that the frequency response falls off rapidly at frequencies above 0.1 Hz.

Adaptation

Slow adaptation was found for linearvection. However long time adaptation has not been investigated.

Characteristics of the Visual Field

The detailed characteristics of the visual field and its placement are more important for linearvection than for circularvection (Lestienne et al., 1977). Perceived forward velocity depends strongly on the spatial frequency of the moving pattern as well as its velocity. In addition, the position of the field is critical. As it moves further backward and peripherally, the effects become much stronger, just as for circularvection.

Asymmetric Sensitivity

An important asymmetry is related to increased sensitivity for backward linearvection (Chu, 1976; Lestienne et al., 1977).

Berthoz et al. (1975) also investigated the nature of visual-otolith interaction qualitatively. A cart was moved with a triangular velocity waveform (corresponding to steps of constant acceleration of 0.4 m/sec^2 and a varied duration range of 1.6 to 3 seconds). The subjects were required to signal the direction of their linear movement with all or none responses. The results showed that with a confirming visual field (the velocity of the visual stimulus is opposite to the cart velocity), there was 100 percent correct direction detection for subjects; with a stationary visual field (the visual world is fixed relative to the cart), subjects gave 75 to 80 percent correct detection; and with a constant backward visual field velocity of 0.4 m/sec, the detection remained good. However, the detection decreased very sharply (down to 50 percent) with increasing visual field velocity in the conflicting situation of an opposite movement between the visual scene and the cart. They also observed a reduction in the dominance over conflicting vestibular cues with repeated trials and showed that visual vestibular interaction is modifiable. As a result, the conflicting situations in which visual cues contradict vestibular and other proprioceptive cues showed a dominance of vision which supports the idea of an essential although not independent role of vision in self motion perception.

1.3.2.2 Vertical Linearvection

Chu (1976) and Chao (1974) examined some of the characteristics of vertical linearvection which was elicited through projection of vertically moving uniformly spaced horizontal stripes on the side windows of the Link trainer cabin.

Onset Latency

Shorter latencies (average 3.15 sec, standard deviation 0.88 sec) were found compared to those for circularvection.

Saturation Velocity

The speed of the stripes which induced maximum sensation of vertical linearvection was found to be 30 cm/sec which is comparable to the saturation velocity in horizontal linearvection.

After Effect

Chao (1974) reported that all subjects encountered an after effect sensation (sinking or rising) which persisted for no more than one or two seconds after the stripes were halted. This result is similar to those found in horizontal linearvection.

Frequency Response

When subjects are exposed to periodic sinusoidal stripe velocities, their response (vertical linearvection) decreases with increasing frequency. A sharp drop in gain was observed for frequencies above 0.1 Hz which is also the same break frequency found in horizontal linearvection. The phase lag increases with increasing frequency and levels off to approximately 60°

due to the predictable nature of the sinusoidal input. The linearvection response to vertically moving stripes with pseudorandom velocity was also found to be frequency dependent . However, the gain decays more rapidly for frequencies above 1.2 Hz and the phase lag was larger than that of the sinusoidal response.

Asymmetric Sensitivity

It was shown that visually induced downward moving sensations are stronger than the sensation of moving upward.

1.3.2.3 Neurophysiological Study for Linearvection

Illusions of self motion, such as circularvection and linearvection, as well as the phenomenon of visually induced motion sickness, suggest that visual-vestibular interactions are important in self motion perception. So far, neurophysiological evidence for such interactions have been found in the case of circularvection, from several studies of the vestibular nerve, the vestibular nuclei of the goldfish and the medial and lateral vestibular nuclei of the rabbit, the cat and the monkey (see Dichgans et al., 1978). However, very little neurophysiological evidence has been reported for visual vestibular interaction under conditions similar to those which elicit linearvection in humans. Daunton et al. (1979) recently presented data obtained from otolith dependent units in cat vestibular nuclei which respond to both visual and vestibular stimulation. Vestibular stimulation consisted of sinusoidal linear acceleration (0.59 Hz; 0.15 g) in the fore-aft, right-left, or up-down directions.

Visual stimulation was provided by a flower and dot pattern covering a large frame which surrounded the linear acceleration platform on the front, sides and bottom. Extracellular recordings of single unit activity showed an increased gain under the combined visual-vestibular condition as compared with the vestibular-only condition. However, the phase shifts observed showed little consistency in direction or magnitude. Only 76 percent of the 45 otolith dependent units sampled in the vestibular nuclei of the cat were modulated by visual stimulation. Waespe and Henn (1977) found 100 percent of the canal dependent units sampled in the vestibular nuclei of the monkey were modulated by visual stimulation. Daunton et al. discussed the possibility that this discrepancy is due to different states of alertness, different species and different neural mechanisms underlying the perception. As a result, visual vestibular interactions are found to take place in a single otolith dependent unit in the cat vestibular nuclei and these interactions could provide a neurophysiological basis for the phenomenon of linearvection, and perhaps for visually induced motion sickness.

1.4 Thesis Organization

This thesis is organized into five chapters.

Chapter 2 describes an experiment investigating the influence of the visual field on the characteristics of the vestibular system during pitch rotation. Subjects were asked to perform a closed-loop task of nulling perceived tilted pitch angles in the face of a wideband vestibular distur-

bance applied to the trainer drive combined with low-frequency visual motion cues. The results, shown in time histories of subject response, provide an understanding of the effect of the asymmetrical pitch vection on subject performance. The frequency response helps us to understand how low-frequency visual cues dominate the low-frequency motion perception. Finally, how the information is processed through the semicircular canals as compared to the otoliths is further analyzed.

In order to study visual vestibular interactions during lateral motion, Chapter 3 describes how a visual display system was designed and constructed to conform with the specifications of a rail mounted linear acceleration cart -- the "MIT sled". The detailed specifications of this projector display, accompanied by a set of reflecting mirrors, are also provided.

Chapter 4 continues the study and is aimed at developing a quantitative functional model of motion sensation dependence on low-frequency visual motion cues and wideband vestibular motion cues during lateral linear acceleration. The overall describing function found in the dark presentation was corrected for the dynamics of the operator nulling behavior, and the resulting estimator, which is mainly represented by the otolith organs, was linearly modelled in the frequency domain and compared to another dynamic model of the otolith perception system. Another experiment with time-varying visual stimuli was also performed in order to develop a human operator dual-input describing function, but its further analysis was precluded by the lack of subjects' compensatory response to

the conflicting visual motion cues. Finally, the extent of field dependence of the subjects was studied by performing two psychological tests -- the rod and frame test and the embedded figures test. The results were compared to the general population as well as to the MIT community.

Chapter 5 summarizes the major findings of the research and provides suggestions for further research.

CHAPTER II

VISUAL FIELD INFLUENCE ON MANUAL PITCH STABILIZATION

As discussed in the introduction, our main objective is to study the interaction of visual and vestibular stimuli in a closed loop nulling task about the pitch axis. Specifically, we wish to demonstrate the effect of visual field influence on manual pitch stabilization in three aspects. First, the effect of the asymmetrical pitch vection on the subject's performance will be studied. Second, we want to show how low-frequency visual cues dominate low-frequency sensation and how they can be used to augment the AC transduction characteristics of the vestibular system. Finally, we will examine how the information is processed through the vestibular system to result in a subjective sensation of pitch rotation.

This chapter is organized into six sections. Section 2.1 shows the experimental approach to monitor subject performance in the closed-loop position nulling task. Sections 2.2 and 2.3 then provide a description of the experimental apparatus and protocol respectively, while Section 2.4 shows the subject response in time histories and in the frequency domain with different visual motion cue stimuli. This section also provides the correlations between the input stimuli and the output subject response. Section 2.5 provides a further discussion of the results and, finally, Section 2.6 summarizes them.

2.1 Experimental Approach

The method used in this experiment involves giving the subject the task of closed-loop control over his own sensed position. This is an extension to pitch of the method used for yaw (Zacharias and Young, 1981), and roll (Huang, 1979). The subject was instructed to maintain the trainer straight and level by means of a position control wheel which commands the pitch platform drive of a platform on which the subject was seated. The task requires the subject matching his sensation, mainly derived from visual and vestibular motion cues, with the sensation of sitting upright. To avoid a null response from the subject, a pseudo-random disturbance signal is added to the platform drive, so that disturbance compensation must be performed throughout the course of the run. The overall block diagram of the experiment is illustrated in Figure 2.1. It is important to point out that during the pitch axis experiments, the estimator shown in the diagram of the subject involves both the semi-circular canals and the otolith organs.

There are several different visual fields that could be considered in this experiment. First, it is interesting to observe the response when the visual field motion exactly confirms the vestibular sensation. This is obtained by rotating the visual field with respect to the subject in the opposite direction of the actual platform motion. A second choice can be motivated by a desire to observe operator response with a reliance mainly upon vestibular cues, that is, when deprived of visual motion cues. However, one should notice that the motion sensation in the dark is

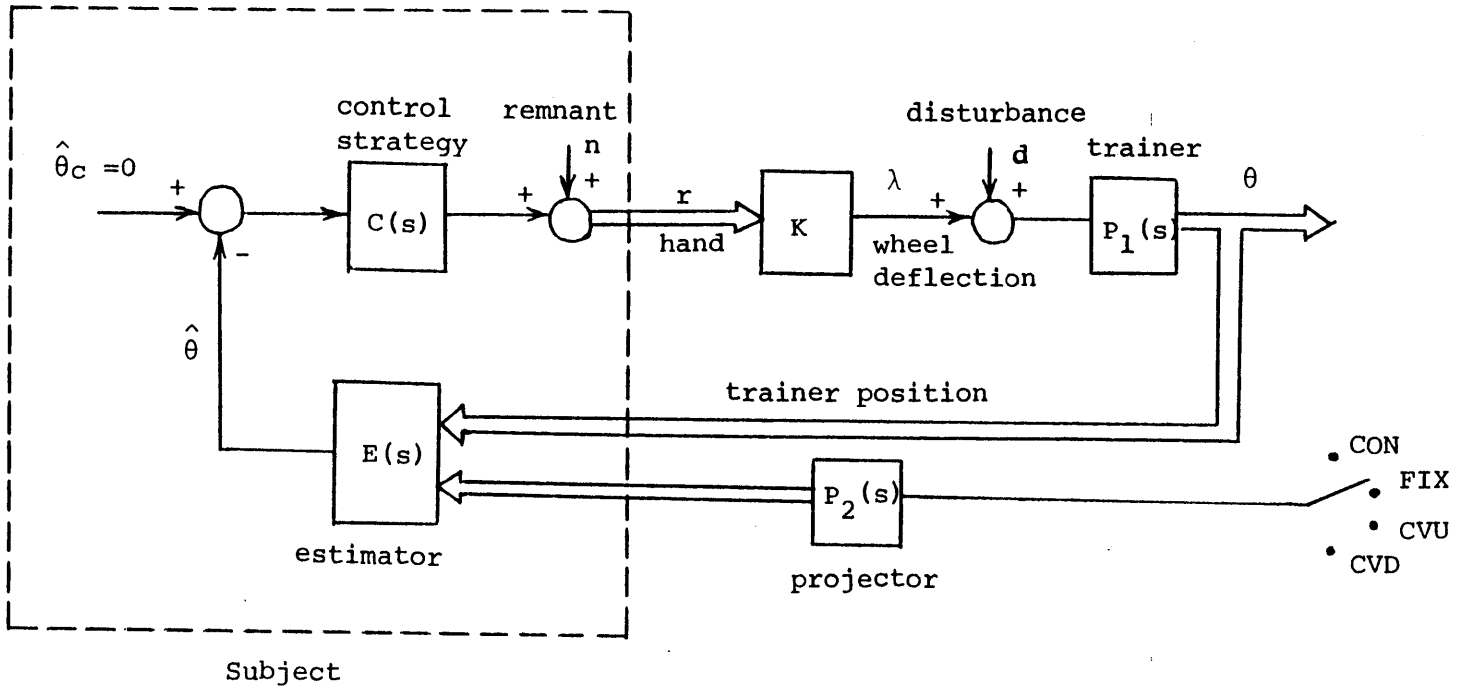

Figure 2.1: Closed-loop position nulling task in the pitch experiment

different from that observed in a motionless visual field (Huang and Young, 1981; Waespe et al., 1980). Finally, one is interested in observing the subjective response to low frequency visual motion cues, the most obvious of which is a constant velocity field motion, i.e. one of zero frequency. Because of the asymmetrical pitch vection (Young et al., 1975), both directions of constant speed field motion will be tested.

These choices motivate the visual field stimuli illustrated in the block diagram and are labelled as follows:

(1) CON (counterrotating): The front window of the trainer is uncovered. The subject can see the laboratory through the front window.

(2) FIX (fixed): A field fixed with respect to the subject, so that reliance is mainly on vestibular cues.

(3) CVD (constant velocity down): A field moving at constant velocity 8°/s downward with respect to the subject, independent of actual trainer position.

(4) CVU (constant velocity up): A field moving at constant velocity 8°/s upward with respect to the subject, independent of actual trainer position.

By measuring subject responses during the nulling task, in particular his control of platform position and wheel deflection, the differences due to operation in these four visual field environments will be compared. Time histories of subject response, frequency response and correlations between platform and wheel signals can be derived from this method. For

now, however, it is appropriate to describe some of the details of the experiment.

2.2 Subjects and Apparatus

2.2.1 Subjects

Six subjects participated in this experiment, five males and one female, aged 25 to 36, in normal health. None of the subjects had experience in pitch manual control.

2.2.2 Apparatus

2.2.2.1 Platform

The Link GAT-1 trainer was used with a GPS-290T analog computer. The analog block diagram is shown in Appendix B. A digital prefilter implemented on the PDP-11 computer is used to avoid resonance in the trainer drive at high frequencies ($\geq$ 1 Hz). The overall closed loop position transfer function of the trainer can be approximated by a simple second order system

$$P(s) = \omega_n^2 e^{-\tau_d s} / (s^2 + 2\xi_n \omega_n s + \omega_n^2) \qquad (2.1)$$

where the break frequency is 0.382 Hz, the damping ratio is 0.85 and the time delay is 0.3 seconds. The dynamic characteristics of the trainer are plotted in Figure 2.2. In pitch, the maximum trainer angle is 18° upward and 10° downward. In order to have 14° excursion in both directions, the trainer is tilted 4° upward and this position is used as the referenced zero position. The headrest and the seat inside the trainer are tilted so that the subject sits in an erect position when the trainer is at the referenced zero point. In addition to the safety belt, there is another belt used to tighten the subject's chest on the seat.

2.2.2.2 Projector

During FIX, CVD, and CVU presentations, the visual motion cue is provided to the subject on the translucent front window of the trainer, upon which is projected a horizontal stripe pattern via a trainer-mounted slide projector, lens, reflecting mirror, and servo-drive system (Murphy, 1972; Morrison, 1975). The drive allows velocity control of a film loop passing through the projector and containing the stripe pattern, and thus velocity control of the projected image on the front window.

When the subject is seated in the trainer looking forward, with his head supported by the headrest, the front window subtends approximately 63° horizontally and 28° vertically, measured from the subject's eye position. Alternating black and white horizontal stripes subtend angles of approximately 12°. The two side windows of the trainer are covered with a black cloth, so that the subject can see the front window only.

Since the level of illumination is not an important factor in producing the sensation of yaw rotation (Huang and Young, 1981), only one level of illumination is used (about 1.5 ft candles measured on the front window of the trainer).

2.2.2.3 Control Wheel

A control wheel (diameter 66", length 12") cut from a long pipe is used for nulling the trainer pitch motion. This balanced wheel is mounted directly in front of the subject so that the subject can easily rotate it (the axis of the wheel lies in the y axis). Since the surface of this wheel is polished quite well, it provides neither visual nor tactile cues as to the center (and hence zero commanded position), although mechanical stops limit the total wheel deflection to 85° in either direction. A full deflection of the wheel results in a trainer pitch position of 14°, trainer pitch direction corresponding to the direction of wheel deflection.

2.2.2.4 Disturbance

The disturbance signal is generated by the real time operation of a PDP-11 digital computer which creates the signal by summing 12 sinusoids and providing timed digital-to-analog conversion for subsequent analog computer scaling and summation with the subject's wheel signal (Figure 2.1). Details of the analog circuitry are given in Appendix B and a listing of the digital programs are given in Appendix A.

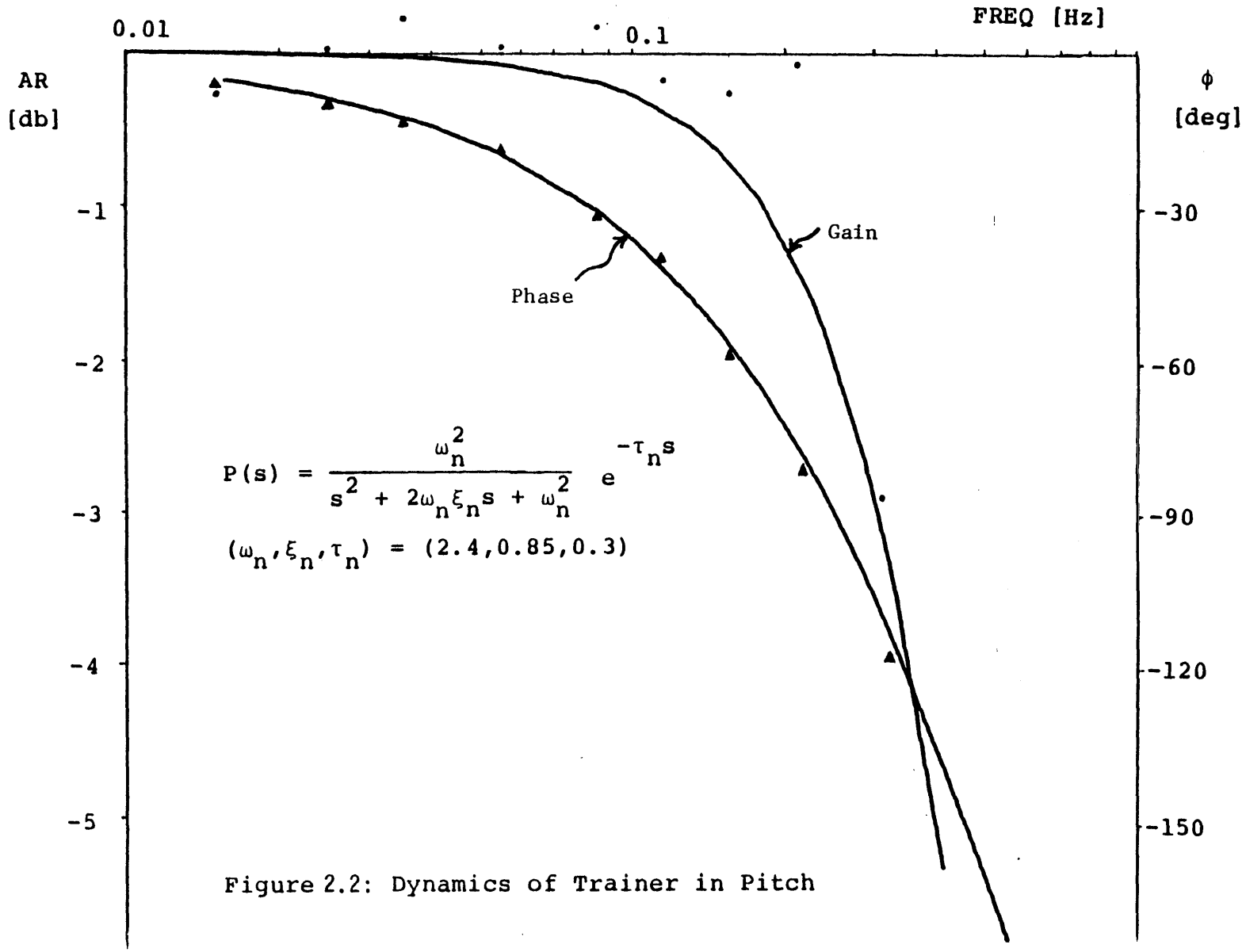

Figure 2.2: Dynamics of Trainer in Pitch

The disturbance d is a pseudo random zero mean signal with a period of 200.7 seconds, spanning the frequency range from 0.015 to 0.683 Hz. The disturbance amplitude is chosen to approximate a smooth power spectral density function. The stimulus acceleration spectrum is shown in Figure 2.3 where each spectral component is a prime multiple of a base frequency of 1/200.7 Hz, so that the signal is periodic with a period of 200.7 seconds. The time history is shown in Figure 2.4.

2.2.2.5 Supplementary Equipment

Additional equipment used in the experimental design included a four channel strip chart recorder to record the basic variables of the closed-loop task: disturbance input, trainer position, subject wheel deflection, and visual field velocity. In addition, a headphone-microphone set is provided for communication with the subject and for audio cue elimination during a run, by means of music from an FM band tuner.

2.3 Experimental Procedure

All six subjects were instructed to use the pitch position nulling method to keep the trainer as level as possible by concentrating on their sensation of motion. Before the experiment, with no wheel input, the front window of the trainer was covered and the disturbance signal was injected into the trainer so that the subject, first standing outside the trainer and then seated inside, could obtain some estimate of the amplitude and frequency content of the signal he would be asked to null. The

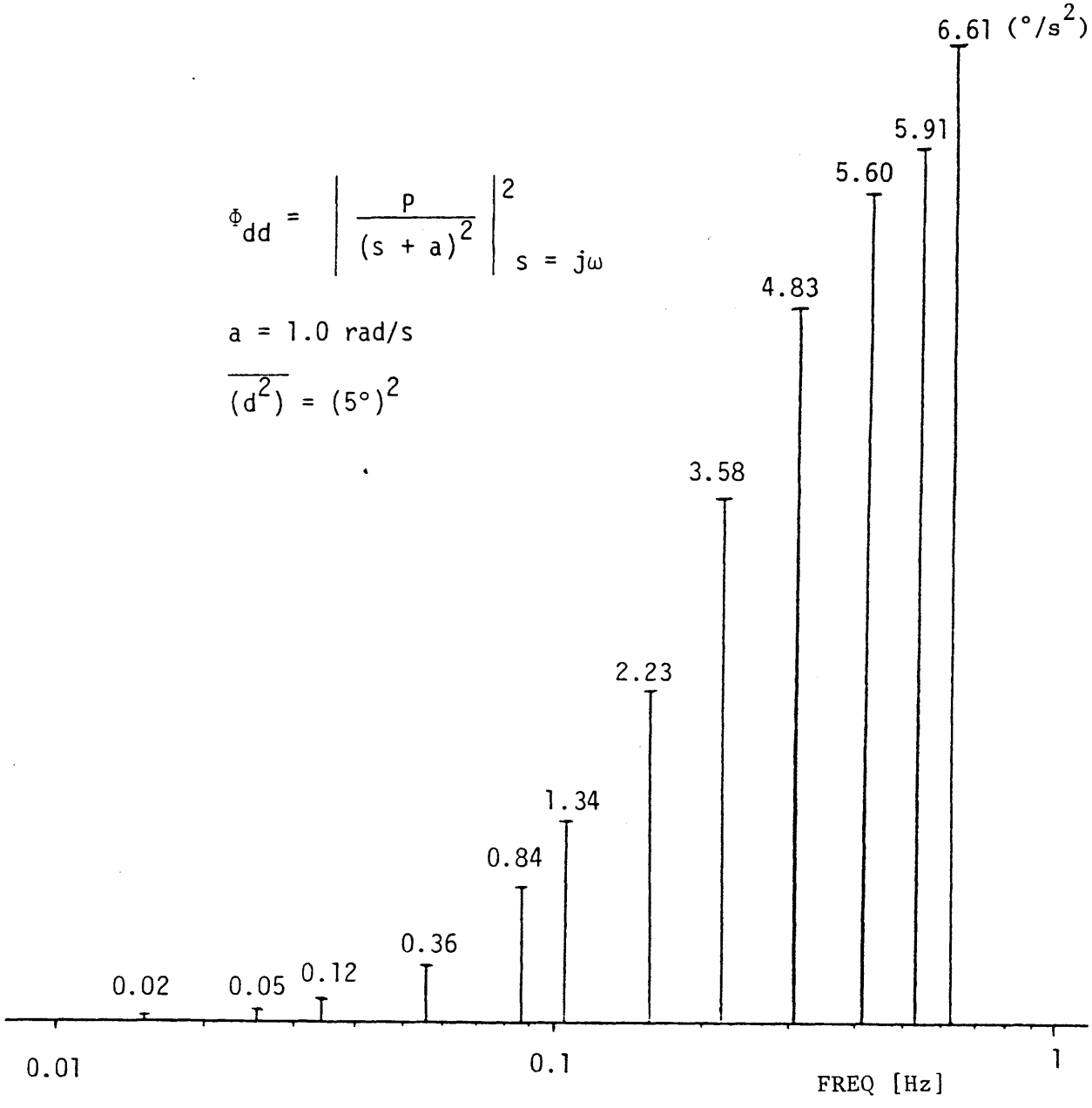

Figure 2.3: Stimulus acceleration spectrum in pitch experiment

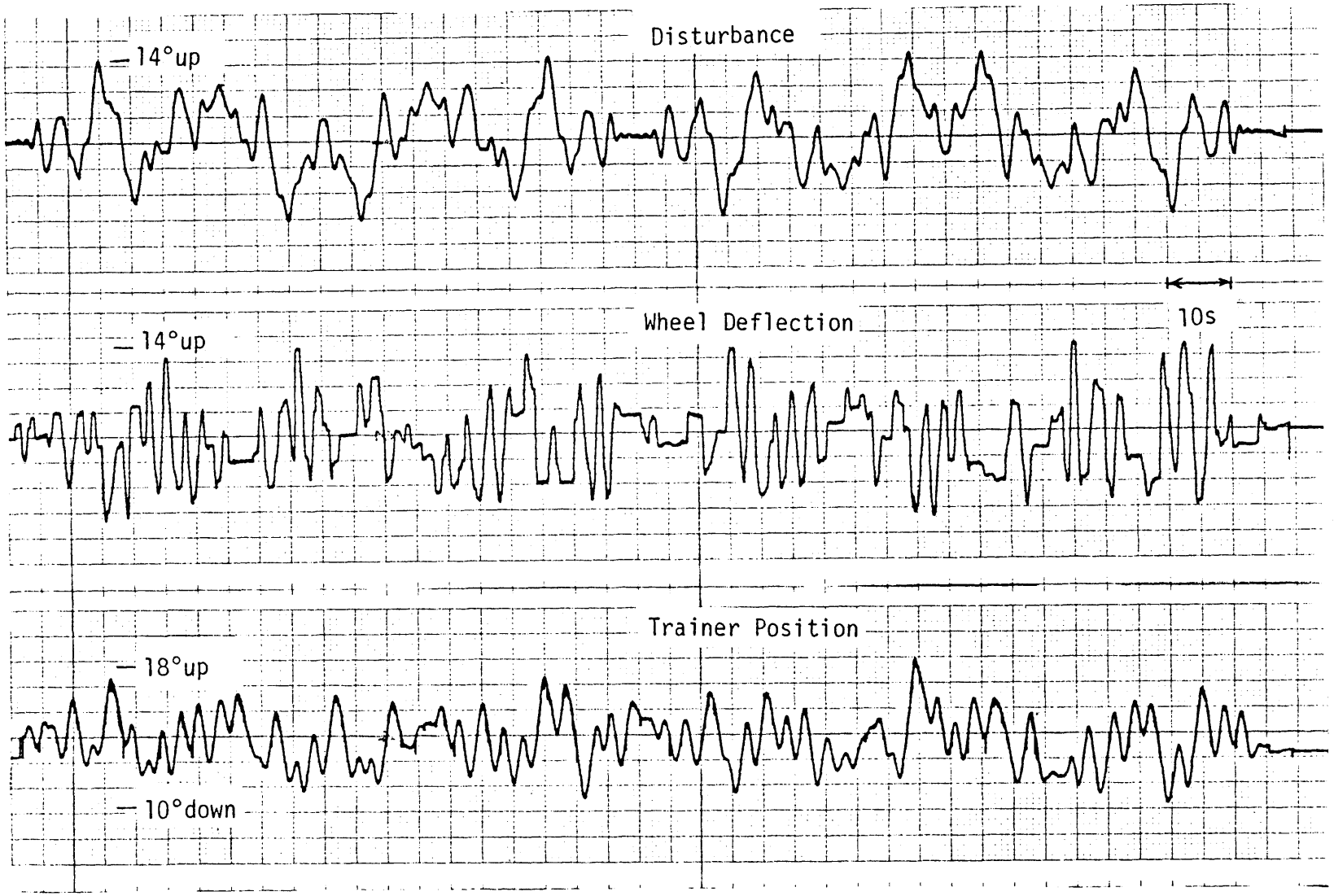

Figure 2.4: Counterrotating visual field (CON) in pitch experiment

subject was seated in the trainer, the safety belts were tightened, and the head restraint adjusted to fit his head. Then, without a disturbance input, the subject was asked to rotate the wheel to drive the trainer in both directions, so that he could see how well the wheel controlled the trainer. Finally, the subject was given a practice session in the CON presentation which provided confirming visual cues. During this time, the subject wore the headphone and the music volume was adjusted to a comfortable level for the subject, which assured that the motor sounds from the trainer were inaudible.

There were eight runs for each subject with a random order of visual presentations (two runs of each visual field: CON, FIX, CVD and CVU). Because of previous results showing the differing effects on pitch vection of motion in the upper or lower visual field (Young and Oman, 1974), we used two field position. For each initial run of FIX, CVD, and CVU, the subject was instructed to look at the upper edge of the front window. For each second run of FIX, CVD, and CVU, he was instructed to look at the lower edge. Because operator bias may occur during CVD and CVU presentations, the CON visual display was presented for 30 seconds prior to each run to ensure nominal subject performance. Between each run, there was a one minute rest.

2.4 Results

As mentioned at the beginning of this chapter, the major objective here is to study the effect of the visual field influence on manual pitch

stabilization in three aspects. First, Section 2.4.1 will briefly discuss four sample strip chart histories, one for each visual field type, and will motivate a further look at the asymmetrical pitch vection on subject performance. Section 2.4.2 will propose a human operator describing function which adequately models the subject's dynamic behavior observed during the course of the assigned position nulling task. This describing function will show how low frequency visual cues dominate low frequency sensation and how they can be used to augment the AC transduction characteristics of the vestibular system. Finally, Section 2.4.3 will show the correlations between the trainer position and wheel deflection signals in each visual presentation.

2.4.1 Time Histories of Subject Response

Figure 2.4 shows a set of typical histories of the disturbance signal sent to the trainer, the subject's compensatory control wheel deflection and the trainer pitch position. Since the visual field is counterrotating (CON), that is stationary in the laboratory, operator performance in this situation results in a well-met task objective with the trainer being maintained at zero-mean position throughout the run. Similarly, Figure 2.5 illustrates performance in the fixed visual field, where the visual field is held stationary with respect to the subject (FIX). Because the otolith organ is very sensitive to tilt, the subject can still maintain the trainer at a zero-mean position throughout the run. (This is in marked contrast to yaw, where substantial drift occurs in the FIX condition

(Zacharias, 1977).) Figure 2.6 illustrates performance in a constant velocity field rotating at 8°/s downward with respect to the subject (CVD). The trainer position does not have a significant bias caused by pitch vection. Figure 2.7 illustrates performance in a constant velocity field rotating at 8°/s upward with respect to the subject (CVU). It can be seen that after 10 seconds, the subject begins to bias the trainer upward about 6°. This is caused by pitch vection and will be discussed later. All the subjects mentioned that they did not have any linear-vection during CVD and CVU presentations.

The average values of trainer position for CON and FIX were calculated throughout the entire run. For CVD and CVU, the average values of trainer position were calculated starting from t = 20 seconds through the end of the run. By subtracting the average value in CON from the average values in FIX, CVD and CVU (i.e. using the average value in CON as the reference value), we calculated the final average values in FIX, CVD and CVU on a subject by subject basis. For each subject, the average values for each visual field condition in the first run (looking at the upper edge of the window) are nearly the same as for those in the second run (looking at the lower edge of the window), so these data were pooled. Figure 2.8 shows the averaged trainer pitch tilt angle induced by pitching visual stimulus for each subject. The mean value for each visual presentation is connected by a solid curve. There is a significantly higher ($p < 0.05$ (t-test)) average value of the trainer position in CVU (average = 5.06°, σ = 1.93°) than in CON (average = -0.002°, σ = 0.93°) and FIX (average = 1.06°, σ = 1.38°). On the other hand, the average value of the

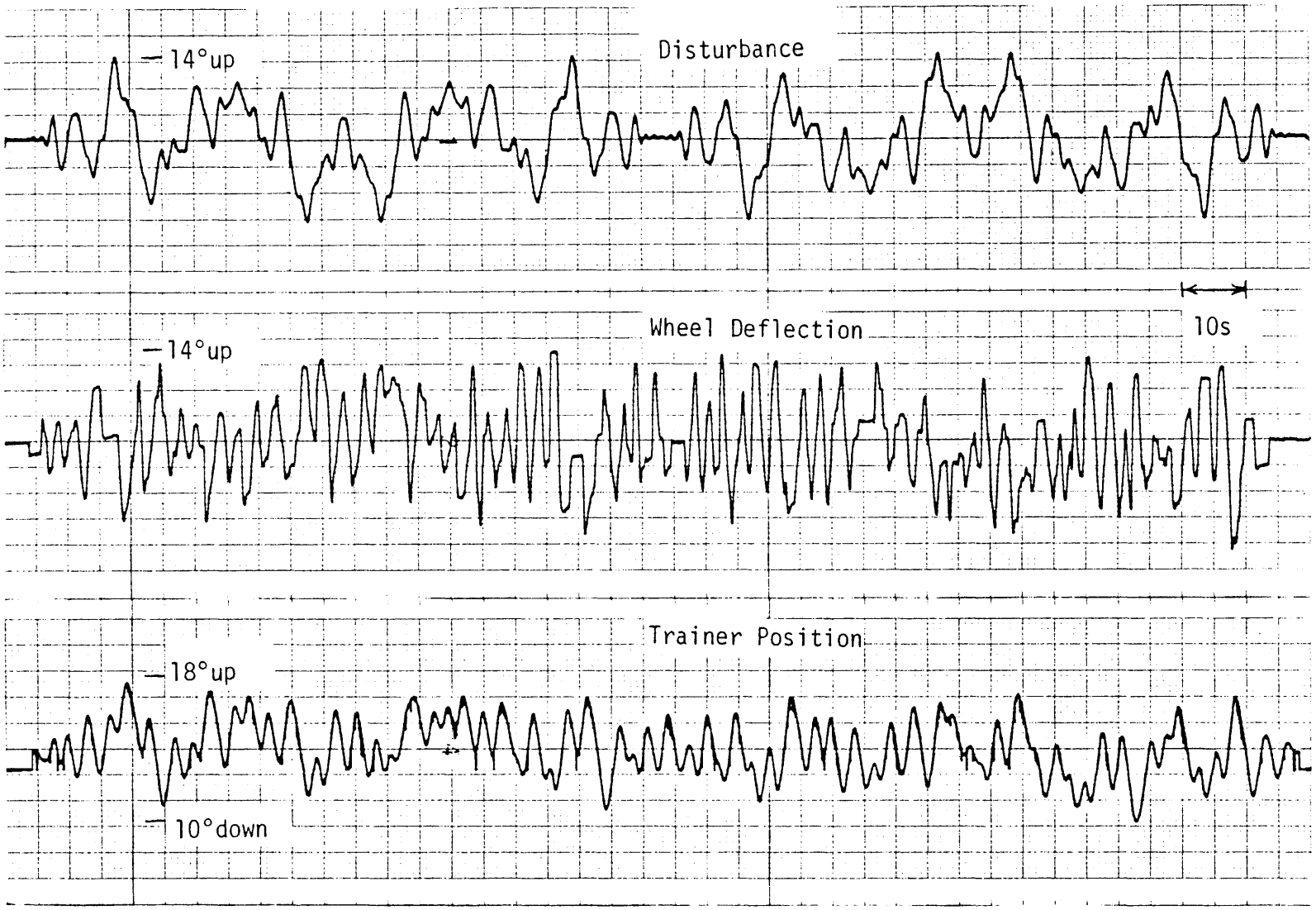

Figure 2.5: Stationary visual field (FIX) in pitch experiment

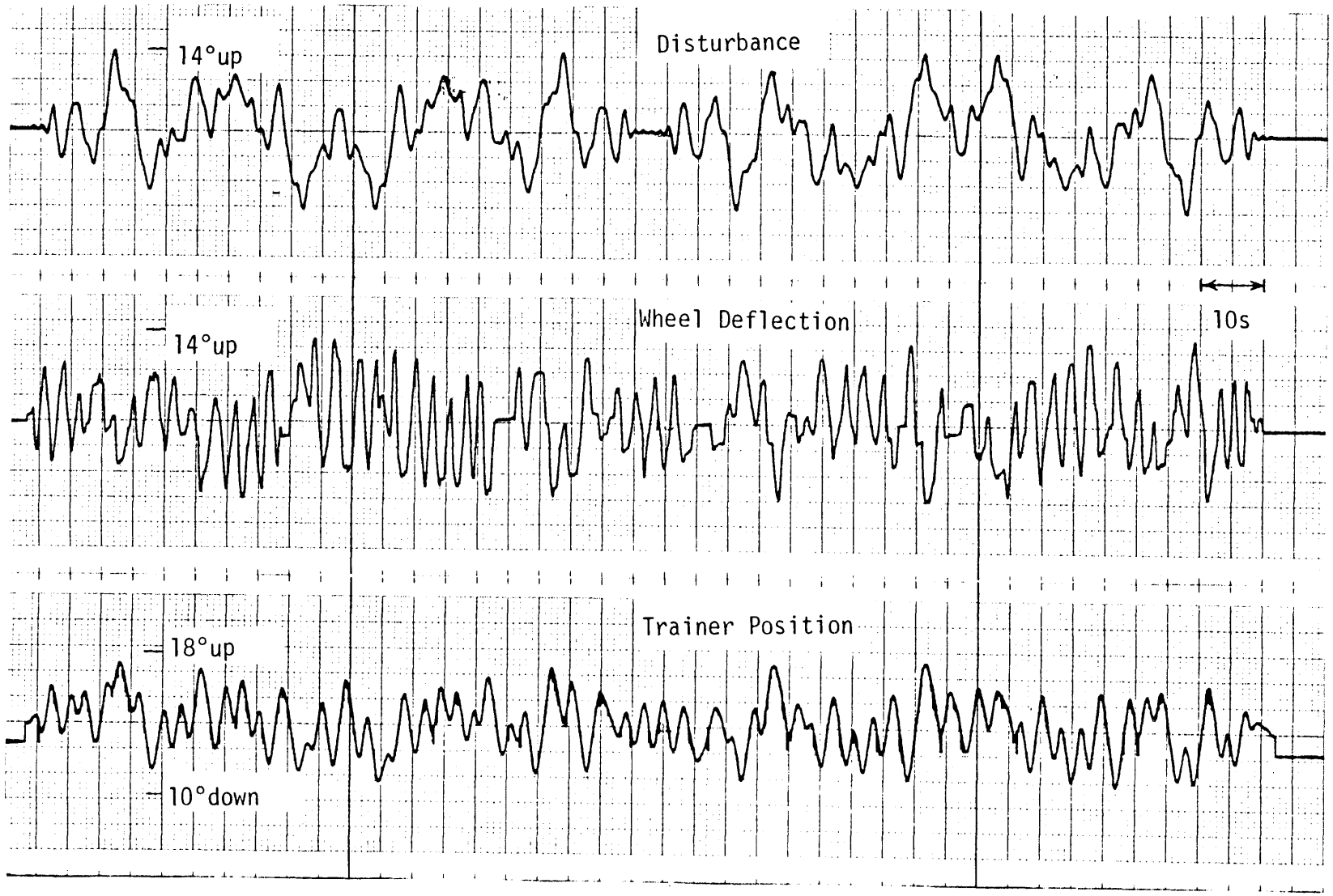

Figure 2.6: Constant velocity (8°/s downward) visual field (CVD) in pitch experiment

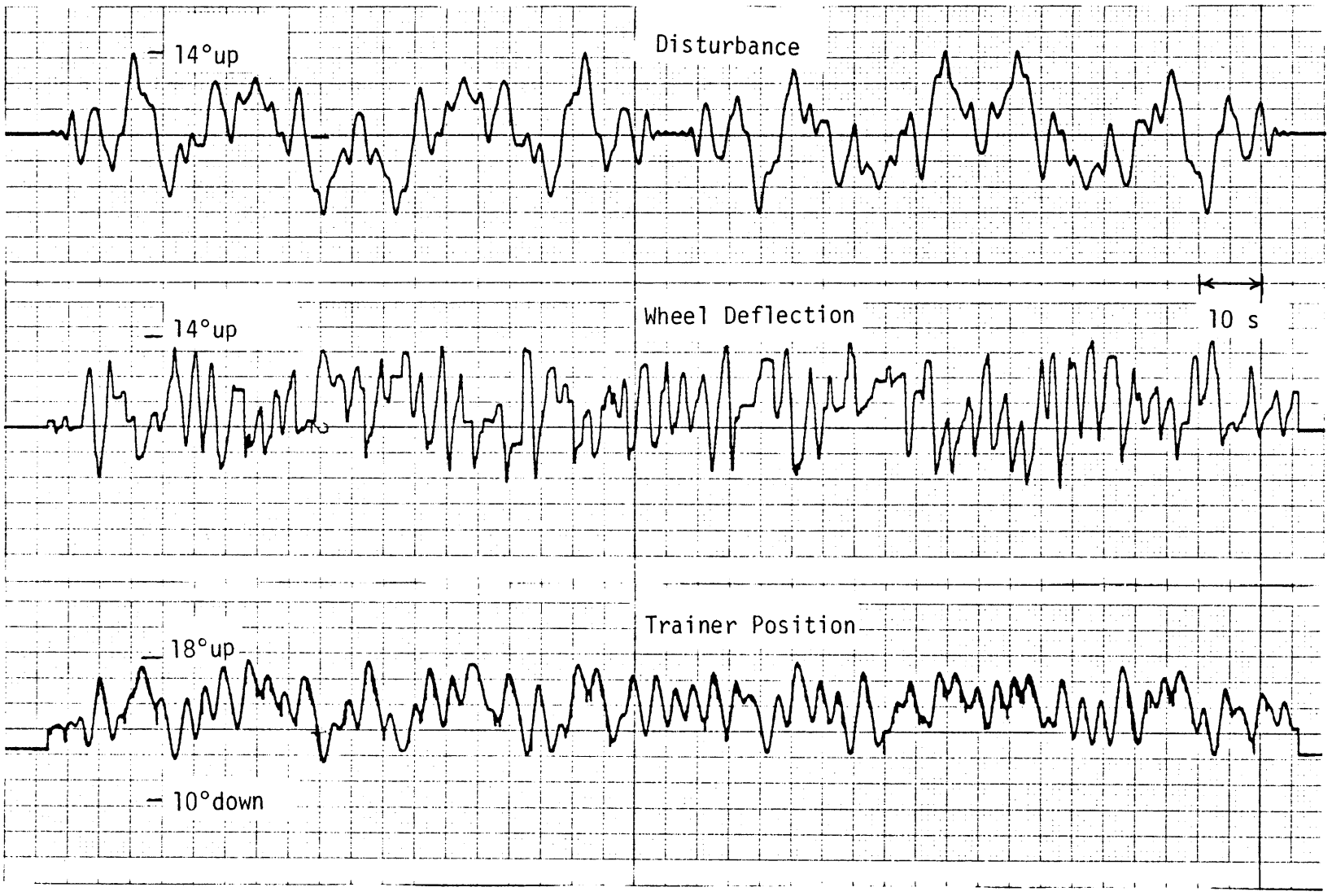

Figure 2.7: Constant velocity (8°/s upward) visual field (CVU) in pitch experiment

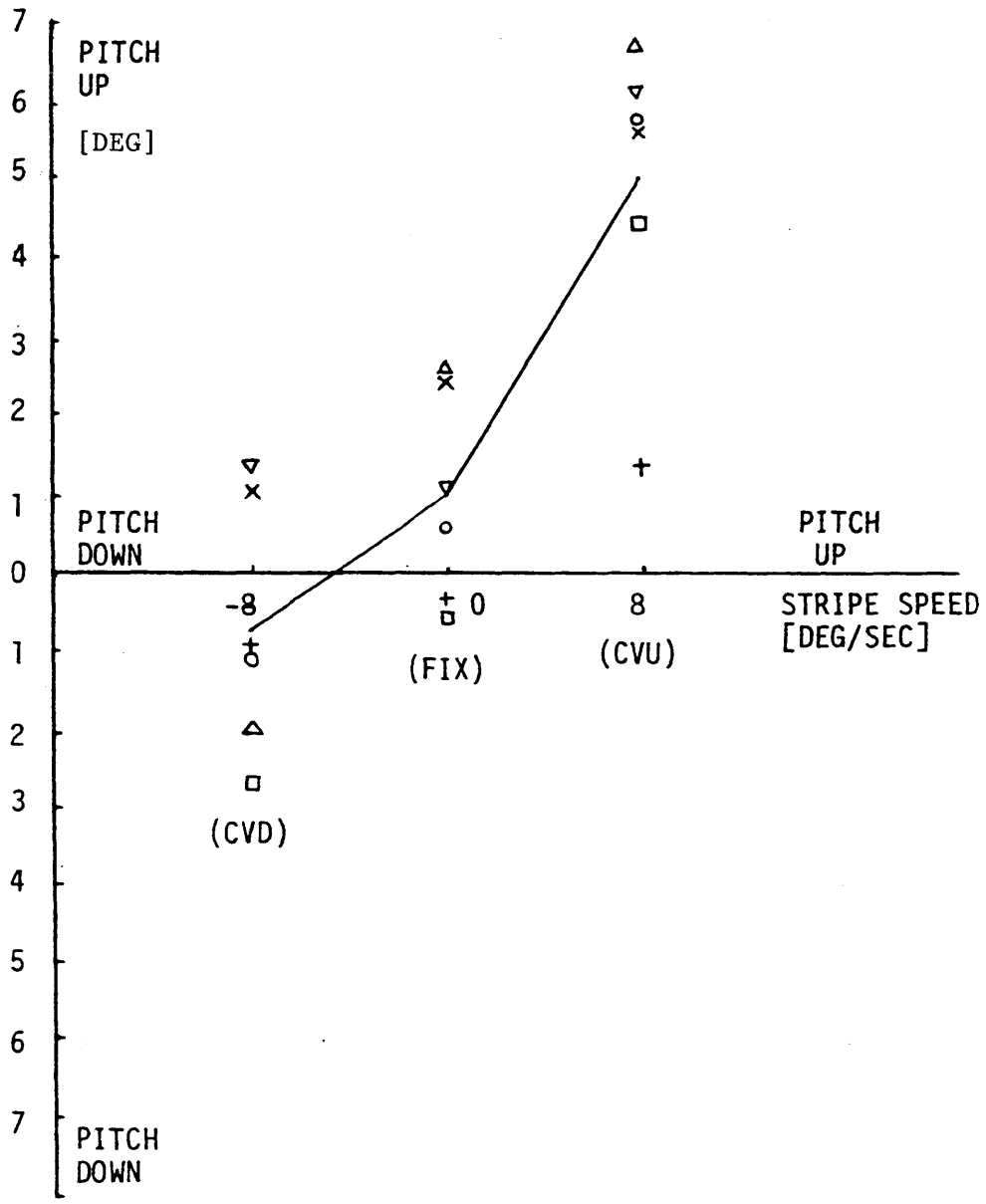

Figure 2.8: Averaged trainer pitch tilt angle induced by pitching visual stimulus. Individual subject data and median lines.

trainer position in CVD (average = -0.72°, σ = 1.63°) is comparable to that in CON and FIX. For the same stripe speed, five out of the six subjects showed this marked asymmetry in pitch, stripes moving upward producing a stronger response than stripes moving downward.

2.4.2 Frequency Response

The overall loop model of the position nulling task has already been given in Figure 2.1. For each visual presentation, the operator transfer function can be solved for in terms of two loop inputs, the disturbance d and the remnant n, and the two measurable loop outputs, trainer position and wheel deflection . It was shown that if the operator's remnant is small with respect to the disturbance signal injected into the loop, then the subject's describing function can be defined by the following (Zacharias, 1977):

$$CE(s) = -\lambda(f_i)/\theta(f_i) \qquad (2.2)$$

where we are working with Fourier transforms evaluated at $f = f_i$, where f_i is one particular frequency contained in the disturbance input. As described in Section 2.2.2.4, the disturbance signal used is composed of a sum of 12 different frequencies, spanning the spectrum of interest. Thus, for each visual field presentation, the describing function can be derived

after Fourier transformation of the wheel deflection and trainer position signals.

Both the wheel and trainer signals are sampled at 20.4 Hz for 200.7 seconds. To obtain the Fourier transforms of both signals, a digital program written for the PDP-11 was used to reduce each signal from 4096 samples to 1024 samples, i.e. pick up one sample out of every four samples, and then calculated each signal's amplitude and phase with a standard FFT algorithm (Brigham and Morrow, 1967). The sample length was chosen to match the 200.7 second period of the disturbance input and the sample rate was chosen as a compromise between constraints imposed by program buffer size and the desire to have a high sample rate with respect to the highest frequency of interest (approximately 1 Hz). The remnant noise is nearly flat through the whole frequency spectrum.

Program output was a teletype listing of all frequency components detected in each signal, specifying amplitude and phase. For each signal, if the amplitude at one particular frequency contained in the disturbance input is below the average of the amplitude of the four neighboring frequencies, the data at that frequency were deleted because they caused an extra large or small gain of the describing function. Further calculation of gain and phase according to (2.2) was then performed at each frequency contained in the disturbance signal. The data were then used to generate Bode plots for individual subject describing functions. After calculation of all the data, the amplitude ratio data for each visual presentation were obtained, first by averaging the data of two trials for each subject

and then by pooling individual subject data across the six subject test population. The results are shown in Figures 2.9 through 2.12. A lag-lead function is used to fit the data and is plotted as the solid curve in each figure. It should be recognized that thhe choice of this model form was motivated primarily by curve-fit considerations, and this simple form can also represent the characteristics of the frequency response as shown in Figure 2.18. The particular parameter values displayed in each figure were obtained from a non-linear regression program which provides the least- squares parameter fit to the amplitude ratio data (BMDP-79, P3R; Dixon, 1979). Shown in Figures 2.13 through 2.16 are the phase data associated with the four visual presentations, again obtained by pooling across the six subject test population. After averaging each subject's phase data, the lag-lead transfer function cascaded with a dead time delay was plotted. The value of the dead time constant was calculated from the figure, while holding fixed the other parameters gained from the previous computation.

2.4.3 Correlations Between Trainer and Wheel Signals

The correlation coefficient of the trainer position (θ) and the wheel deflection (λ) can be calculated as follows:

$$\rho_{\theta\lambda} = \frac{\frac{1}{N}\sum_{i=1}^{N}(\theta_i - \bar{\theta})(\lambda_i - \bar{\lambda})}{\left[\frac{1}{N}\sum_{i=1}^{N}(\theta_i - \bar{\theta})^2\right]^{1/2}\left[\frac{1}{N}\sum_{i=1}^{N}(\lambda_i - \bar{\lambda})^2\right]^{1/2}} \qquad (2.3)$$

where $\bar{\theta} = \frac{1}{N} \sum_{i=1}^{N} \theta_i$ is the average value of the trainer position

$\bar{\lambda} = \frac{1}{N} \sum_{i=1}^{N} \lambda_i$ is the average value of the wheel deflection

and N = 1024.

The values of $\rho_{\theta\lambda}$ for each subject in different visual fields are shown in the first column (labelled C/TL) of Table 2.1. The negative value is caused by the nulling task - when the trainer pitches down (negative), the subject will rotate the wheel upward (positive). Because the pitch axis of the trainer is about 1 meter below the subject's head, the otolith organ is stimulated by two kinds of linear acceleration during the pitch motion as shown in Figure 2.17, with:

R = 1 m, the distance from the subject's head to the pitch axis

θ = trainer pitch axis in degrees

g = force of gravity (9.8 m/s^2)

For small excursions of the pitch angle, θ is small and $g\cos\theta$ will be much larger than $R(d\theta/dt)^2$. So the vertical linear acceleration, F_V, is approximately equal to g and will produce a very small stimulation to the otolith organs. On the other hand, $Rd\theta^2/dt^2$ is comparable to $g\sin\theta$ and the horizontal linear acceleration, F_H, will be an effective stimulation to the otolith organs. As a result, the true body angle θ' which will stimulate the otolith organ can be derived from the trainer position.

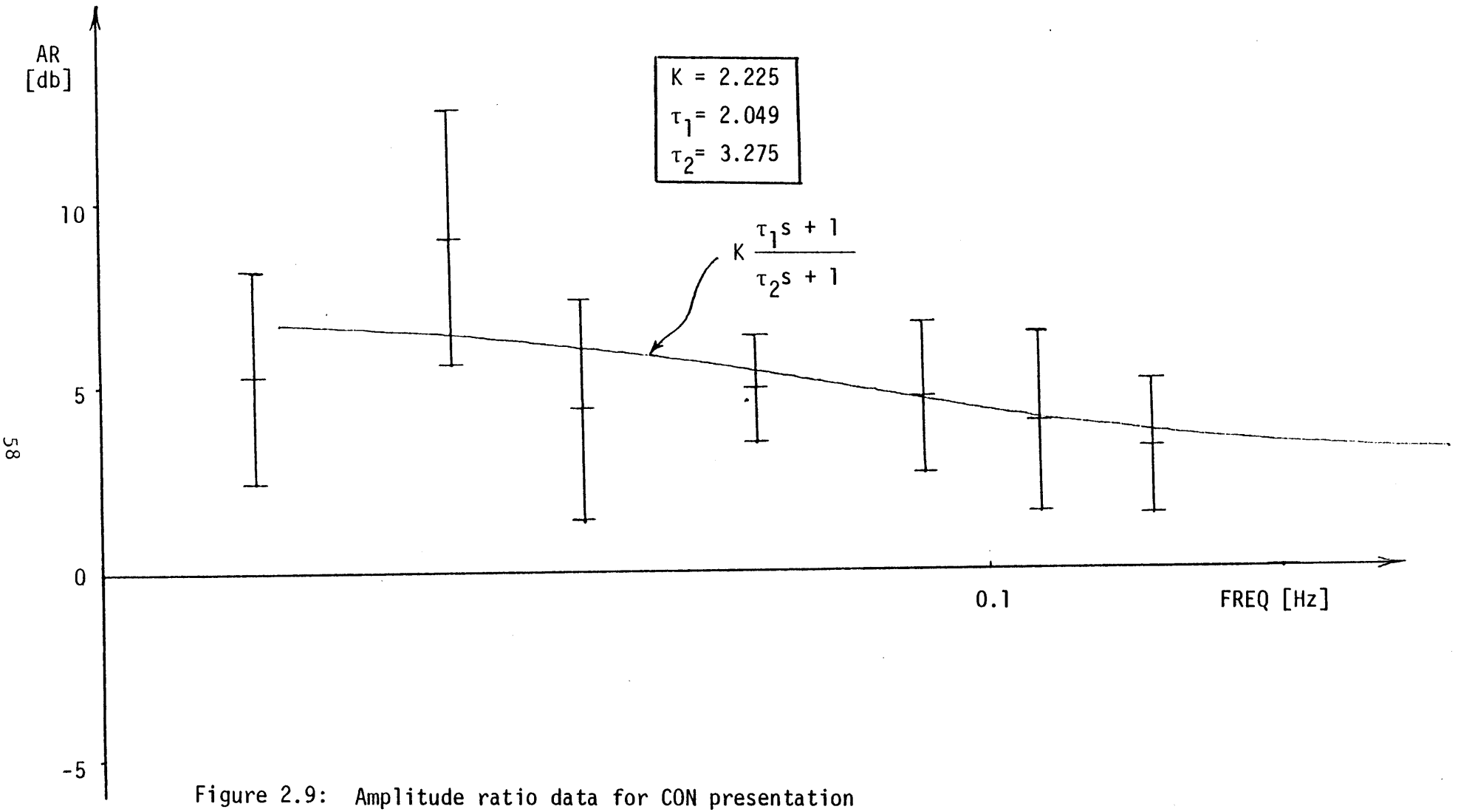

Figure 2.9: Amplitude ratio data for CON presentation

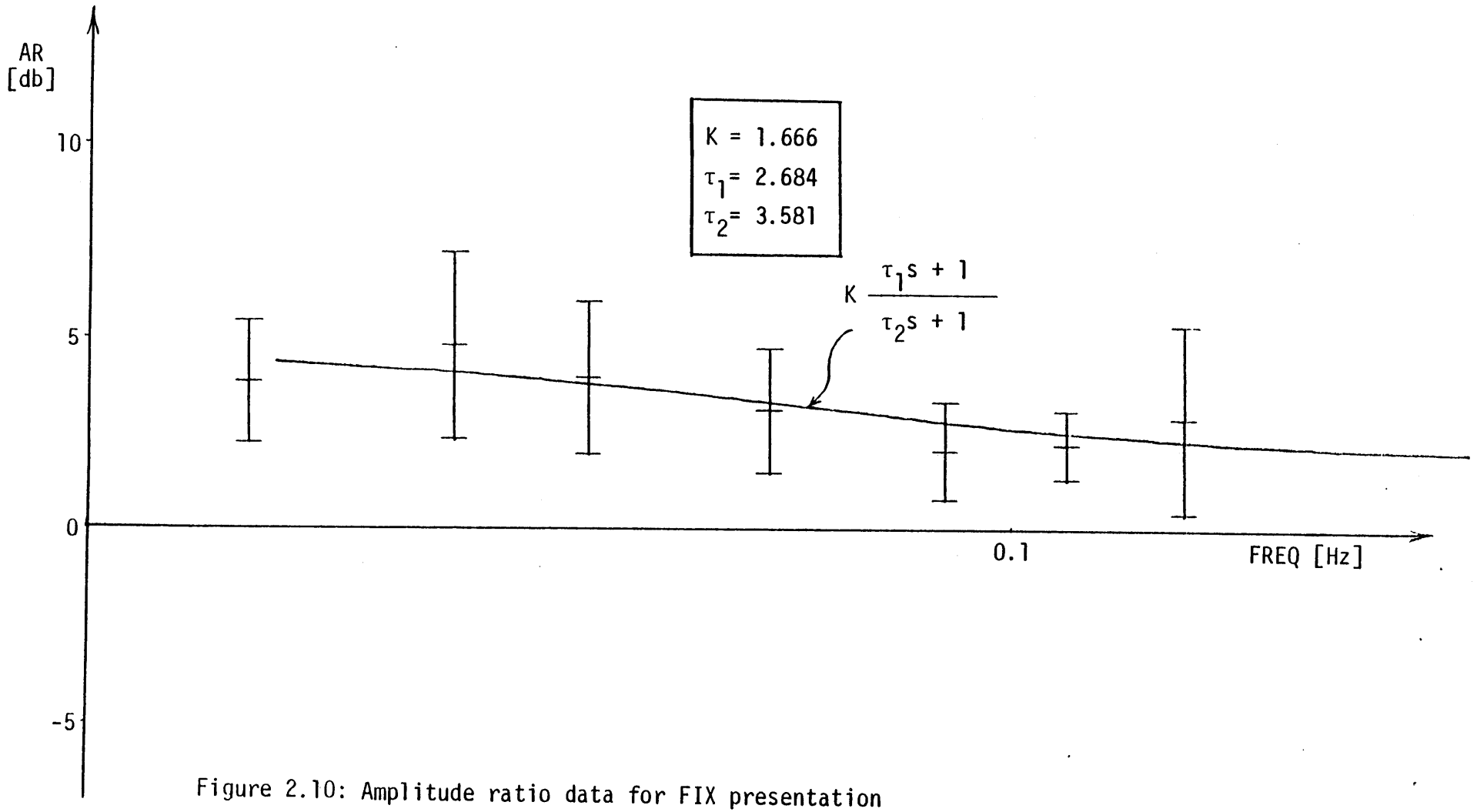

Figure 2.10: Amplitude ratio data for FIX presentation

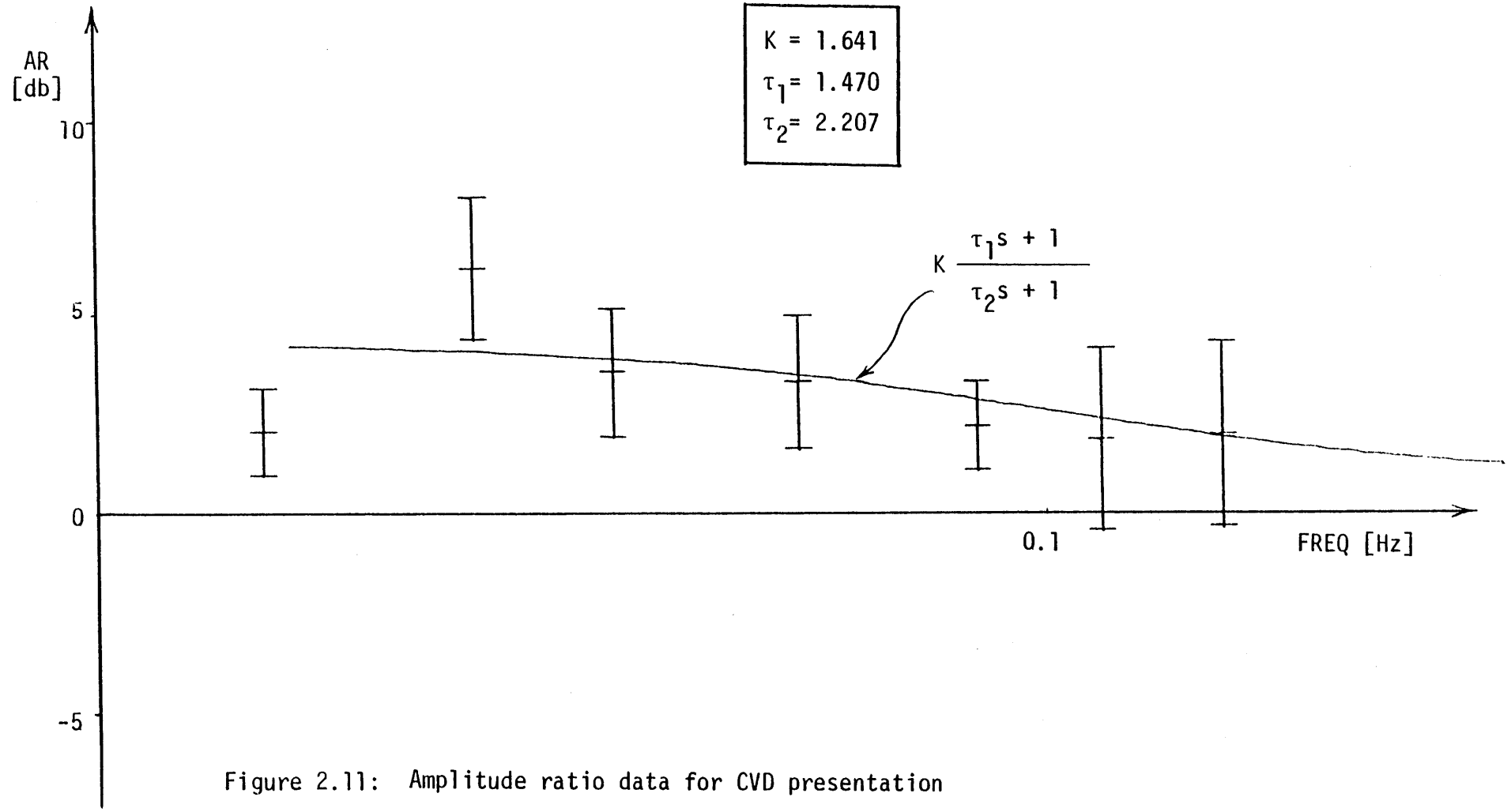

Figure 2.11: Amplitude ratio data for CVD presentation

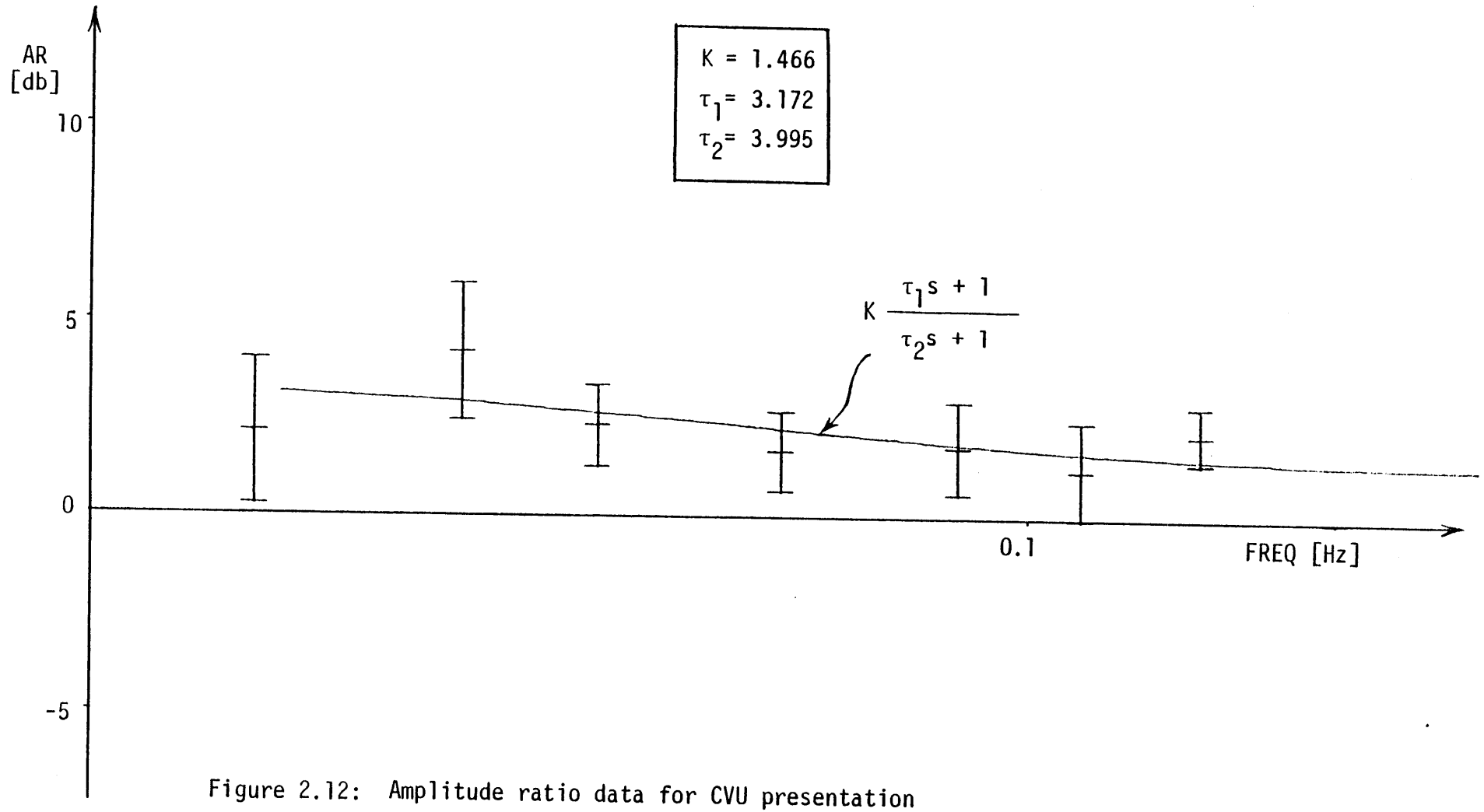

Figure 2.12: Amplitude ratio data for CVU presentation

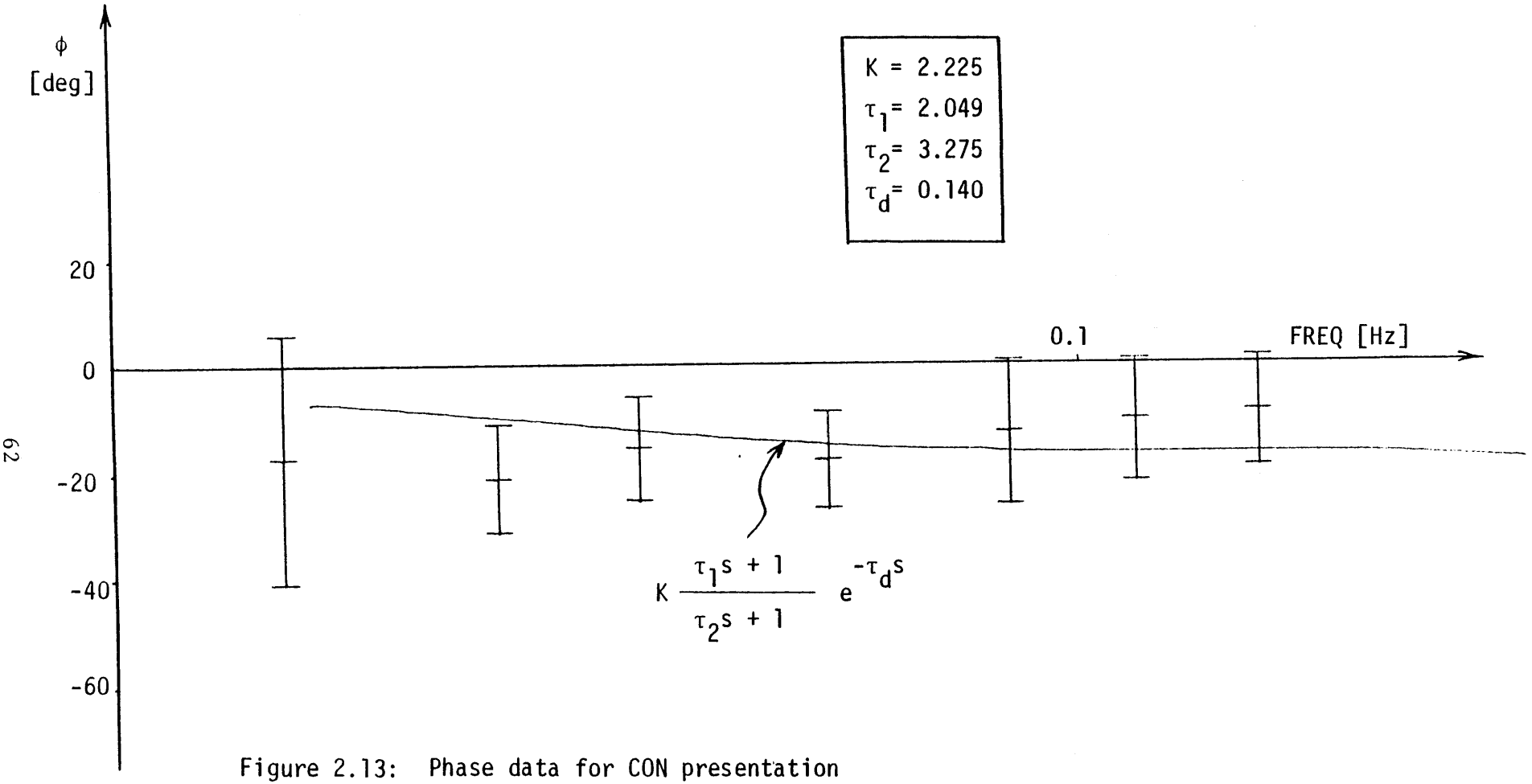

Figure 2.13: Phase data for CON presentation

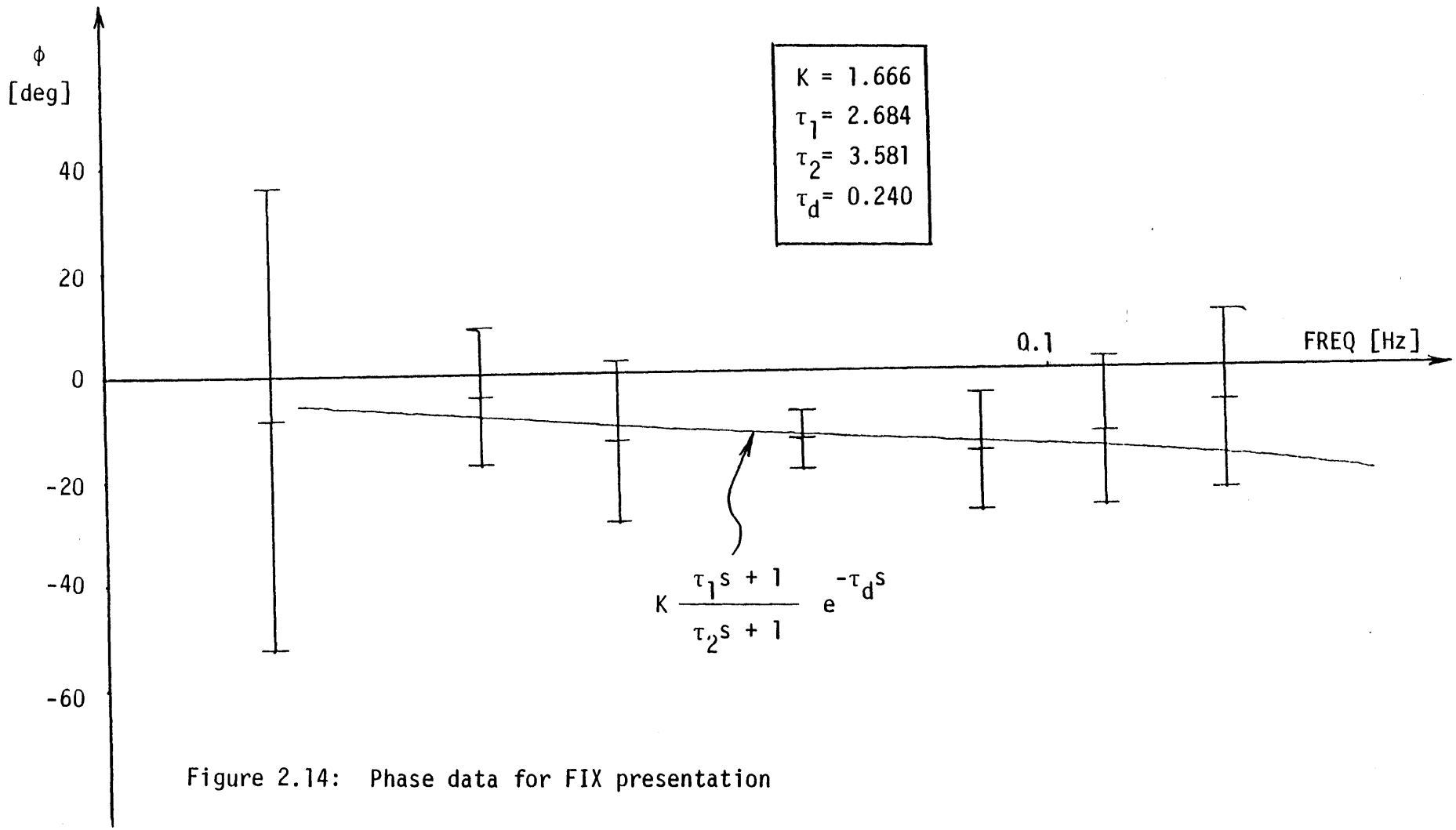

Figure 2.14: Phase data for FIX presentation

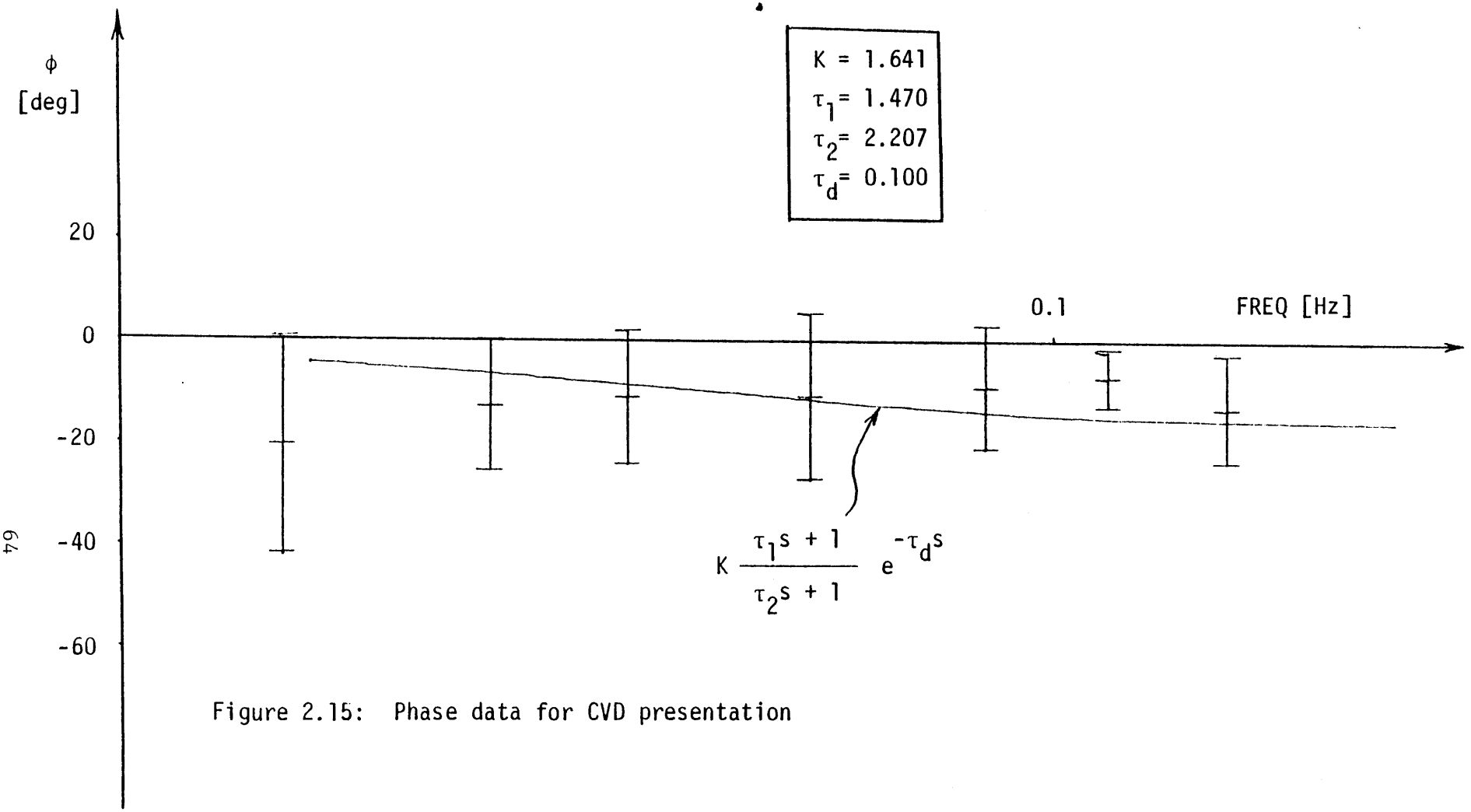

Figure 2.15: Phase data for CVD presentation

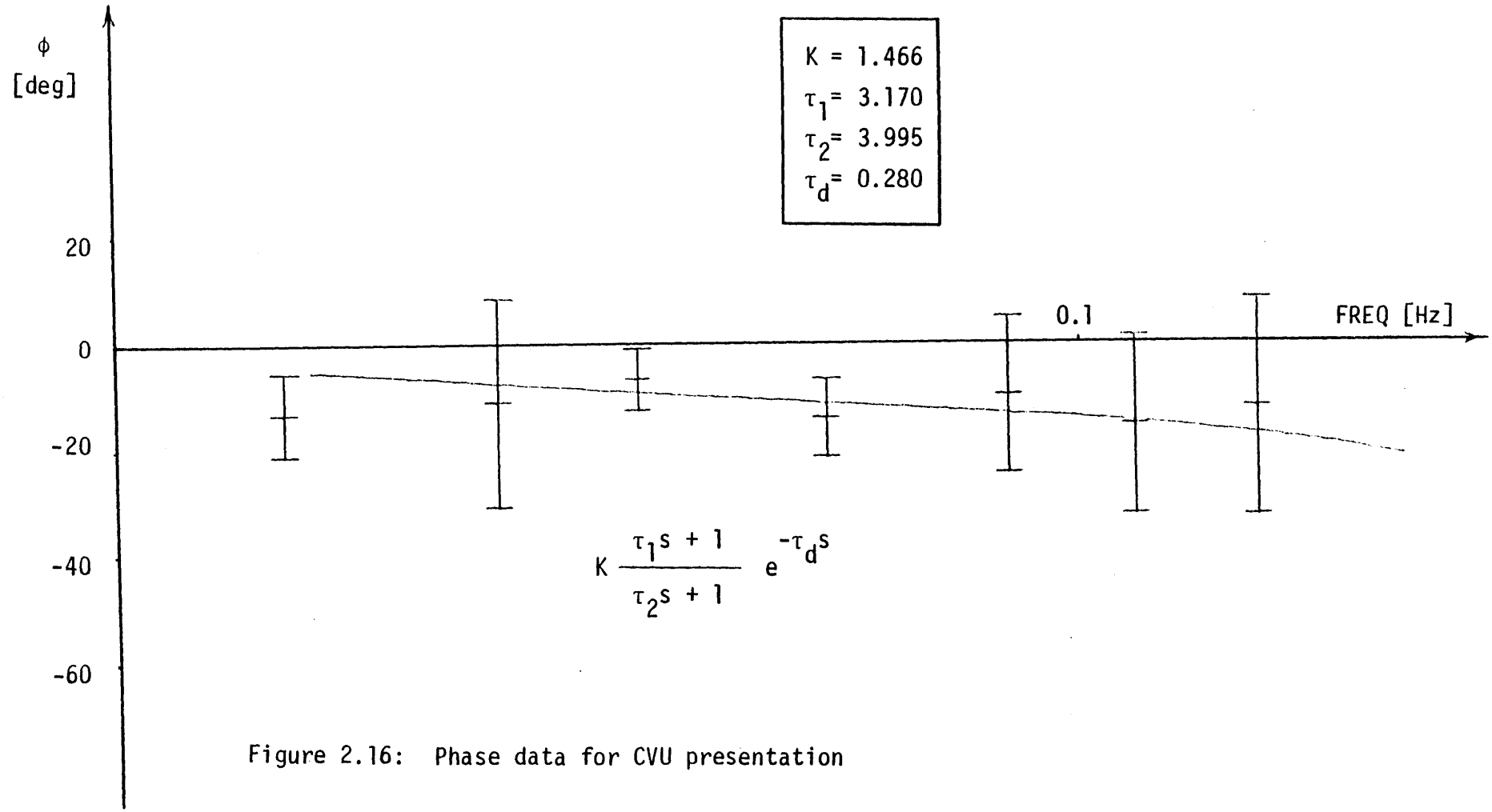

Figure 2.16: Phase data for CVU presentation

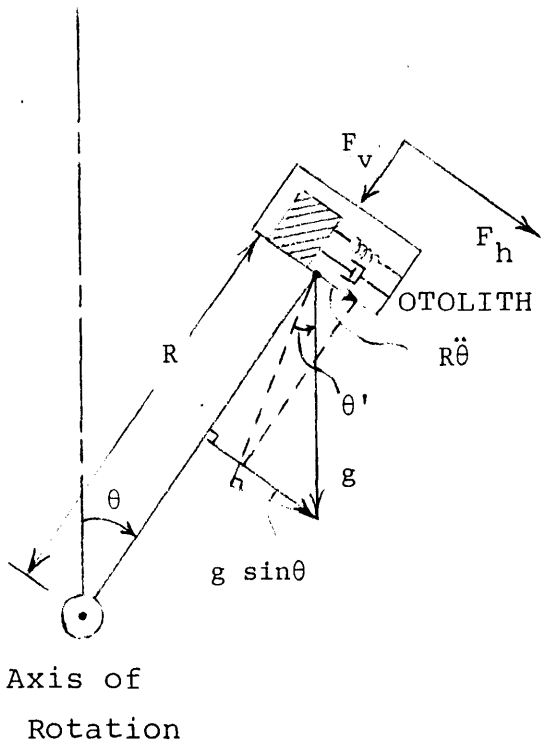

$$F_v = g \cos \theta - R \dot{\theta}^2$$

$$F_h = g \sin \theta - R \ddot{\theta}$$
$$= g \sin \theta'$$

Figure 2.17: Horizontal and vertical forces on the otolith organ

TABLE 2.1 CORRELATION BETWEEN TRAINER AND WHEEL SIGNALS IN PITCH EXPT

SYMBOL C=CORRELATION COEFFICIENT, T=THIETA, L=LAMDA, N=THIETAPRIME
1=LOW FREQUENCY, 2=HIGH FREQUENCY, M=(A-B)/B
AVG=MEAN VALUE, VAR=VARIANCE

DATA	C/TL	C/NL	C/T1L1	C/N1L1	C/T2L2	C/N2L2	M/T1N1	M/T2N2
(I)VISUAL FIELD-----CON								
JENG	-0.843	-0.175	-0.686	-0.715	-0.905	-0.204	0.131	0.984
BOBR	-0.716	-0.113	-0.620	-0.651	-0.812	-0.132	0.105	0.992
KYON	-0.707	-0.146	-0.648	-0.661	-0.783	-0.162	0.081	0.985
TYNG	-0.833	-0.182	-0.785	-0.788	-0.872	-0.218	0.102	0.974
YAMM	-0.797	-0.156	-0.715	-0.725	-0.856	-0.179	0.095	0.984
JOHN	-0.867	-0.360	-0.707	-0.748	-0.909	-0.410	0.140	0.908
AVG	-0.794	-0.189	-0.694	-0.715	-0.856	-0.218	0.109	0.971
VAR	0.068	0.087	0.058	0.052	0.051	0.099	0.022	0.031
(II)VISUAL FIELD----FIX								
JENG	-0.813	-0.133	-0.564	-0.601	-0.925	-0.161	0.118	0.990
BOBR	-0.746	-0.100	-0.677	-0.704	-0.810	-0.116	0.108	0.994
KYON	-0.640	-0.107	-0.522	-0.542	-0.787	-0.129	0.083	0.992
TYNG	-0.702	-0.198	-0.624	-0.634	-0.784	-0.245	0.091	0.955
YAMM	-0.693	-0.171	-0.550	-0.571	-0.869	-0.203	0.076	0.979
JOHN	-0.682	-0.309	-0.385	-0.415	-0.863	-0.365	0.077	0.924
AVG	-0.713	-0.170	-0.554	-0.578	-0.840	-0.203	0.092	0.972
VAR	0.060	0.078	0.100	0.097	0.056	0.093	0.017	0.028
(III)VISUAL FIELD---CVD								
JENG	-0.711	-0.146	-0.383	-0.424	-0.904	-0.185	0.101	0.985
BOBR	-0.653	-0.104	-0.560	-0.590	-0.750	-0.122	0.098	0.992
KYON	-0.806	-0.138	-0.800	-0.808	-0.840	-0.153	0.091	0.989
TYNG	-0.754	-0.234	-0.672	-0.685	-0.820	-0.282	0.099	0.944
YAMM	-0.586	-0.164	-0.386	-0.407	-0.828	-0.218	0.073	0.972
JOHN	-0.649	-0.319	-0.594	-0.617	-0.874	-0.352	0.075	0.930
AVG	-0.693	-0.184	-0.566	-0.589	-0.836	-0.219	0.090	0.969
VAR	0.080	0.079	0.163	0.154	0.053	0.086	0.012	0.026
(IV)VISUAL FIELD----CVU								
JENG	-0.594	-0.109	-0.087	-0.132	-0.876	-0.152	0.095	0.991
BOBR	-0.476	-0.065	-0.105	-0.145	-0.740	-0.091	0.085	0.997
KYON	-0.789	-0.101	-0.712	-0.724	-0.850	-0.113	0.086	0.996
TYNG	-0.564	-0.158	-0.295	-0.333	-0.825	-0.220	0.079	0.970
YAMM	-0.650	-0.138	-0.435	-0.463	-0.873	-0.173	0.077	0.986
JOHN	-0.777	-0.337	-0.455	-0.509	-0.902	-0.389	0.119	0.918
AVG	-0.642	-0.151	-0.348	-0.384	-0.844	-0.190	0.090	0.976
VAR	0.123	0.096	0.237	0.228	0.057	0.108	0.015	0.030

After we derive θ' from θ, the correlation coefficient between θ' and θ for each visual field presentation can be calculated and is shown in the second column (labelled C/NL) of Table 2.1. It is obvious that $\rho_{\theta\lambda}$ is significantly higher than $\rho_{\theta'\lambda}$. We will discuss this in more detail in Section 2.5.3.

2.5 Discussion

2.5.1 Pitch Vection

Pitch vection is an illusion induced by a rotating visual field whose spin axis is perpendicular to the saggital plane. Just like circular-vection, the induced pitch motion is opposite to the direction of pattern motion. However, in contrast to circularvection, subjects experience only limited displacement despite a continuous sensation of self motion. The constraint on displacement may be caused by the inputs from the otoliths and somatosensory graviceptors, which are in conflict with the visual effect.

As reported by Young et al. (1975), there is an induced pitch tilt illusion which is similar to roll vection in terms of its dependence on stimulus speed and head position. It differs, however, in that there exists a marked directional asymmetry: for the same stimulus speed, the pitch down sensation is stronger than the pitch up sensation (Young and Oman, 1974). No corresponding left-right asymmetry is seen in the population responses in the roll vection experiments (Huang, 1979; Young et al., 1975). In our experiments, the results confirmed the findings mentioned

above. Even with our limited visual field, a constant stripe speed pitching upward produced significant pitch vection downward, and resulted in a marked compensatory upward tilt of the trainer. An interesting further experiment might be to see if this asymmetry holds true for larger populations, especially trained pilots, whose experience with pitch upward is more extensive than the general population.

Chu (1976) examined some of the characteristics of vertical linear-vection which was elicited through projection of vertically moving uniformly spaced horizontal stripes onto the side windows of the LINK trainer. The result showed that the visually induced downward moving sensation was stronger than the sensation of upward motion. In this experiment, although the side windows were covered with black cloth and the stripes were only moving on the front window, the results still suggest a stronger downward moving sensation, inducing a remarked upward tilt of the trainer. However, no subject reported the existence of linear-vection from the motion cues presented in this experiment.

Young et al. (1975) also studied visually induced pitch sensation with the head in various orientations and noted that the asymmetry of the pitch sensitivity appears fixed with respect to the head, rather than with the direction of "down", since in the head inverted position, the induced pitch-forward (up) was significantly larger than the induced pitch-backward (down). This finding suggested a visual origin for the pitch sensitivity asymmetry. Due to the predominance of forward locomotion in man, this asymmetry may be caused by an asymmetry in the visual system

which is adapted to downward motion of the "seen" environment.

A similar asymmetry is observed in vertical nystagmus. Unlike horizontal nystagmus which is usually equally strong in either direction in normal subjects, there are differences between upward and downward optokinetic nystagmus (OKN) and vestibular nystagmus in a number of species (Collins et al., 1970; Evinger and Fuchs, 1978; Money and Scott, 1962; Pasik et al., 1971; Takahashi and Igarashi, 1977). Maximum velocities of upward OKN are generally lower than those of horizontal or downward OKN, and decay time constants of upward nystagmus after velocity steps are shorter (Takahashi and Igarashi, 1977; Takahashi et al., 1978; Matsuo et al., 1979). Upward optokinetic after-nystagmus (OKAN) is frequently absent, indicating that there is little or no velocity storage for upward nystagmus (Matsuo et al., 1979). These differences may largely depend on differences in storage capabilities of the central mechanism that produces them, as the different semicircular canal responses are symmetrical (Goldberg and Fernandez, 1971b).

Another asymmetry is observed for postural reactions to linear motion of visual scenes (Lestienne et al., 1977). The results showed that the tendency to fall backward is considerably stronger than the tendency to fall forward.

This last postural asymmetry is consistent with our results, for which the directional asymmetry in pitch vection did effect the performance of the position nulling task during a constant field rotation and resulted in a marked compensatory upward tilt of the trainer.

2.5.2 Simplified Parametric Model

The major findings of Section 2.4.2 may be summarized in a schematic fashion as shown in Figure 2.18, which shows the amplitude ratio asymptotes for the four visual field treatments. As we expect, the visual field motion provides low frequency information driving the subjective sensation up to about 0.06 Hz. The high frequency gain $K\tau_1/\tau_2$ is close together among these four presentations, also supporting the indifference to visual inputs when the vestibular signal contains high frequency components. Figure 2.19 shows the model parameter mean values and their variance for CON, FIX, CVD and CVU presentations. There is a significant ($p < 0.005$, t-test) gain drop from the CON to the FIX (or CVD) presentation. In the CON presentation, a horizontal line in the lab can be seen through the front window of the trainer and the distance between this line and the bottom edge of the front window can be used as a reference to estimate the degree of tilt of the trainer. In this case, the visual field motion exactly confirms the vestibular sensation in stabilizing the trainer, and the laboratory also provides a much richer field information as compared to the black and white stripe pattern used in other visual presentation. However, in the FIX presentation, the visual field does not provide any information about horizontal position and pitch angular rotation to confirm the signals from the otoliths and semicircular canals respectively. This visual-vestibular conflict produces a significantly lower gain in the FIX presentation. The gain drop from the FIX to the CVU presentation is barely significant ($p < 0.05$). With higher conflicting visual-vestibular signals, the subjects are unable to use higher gain at

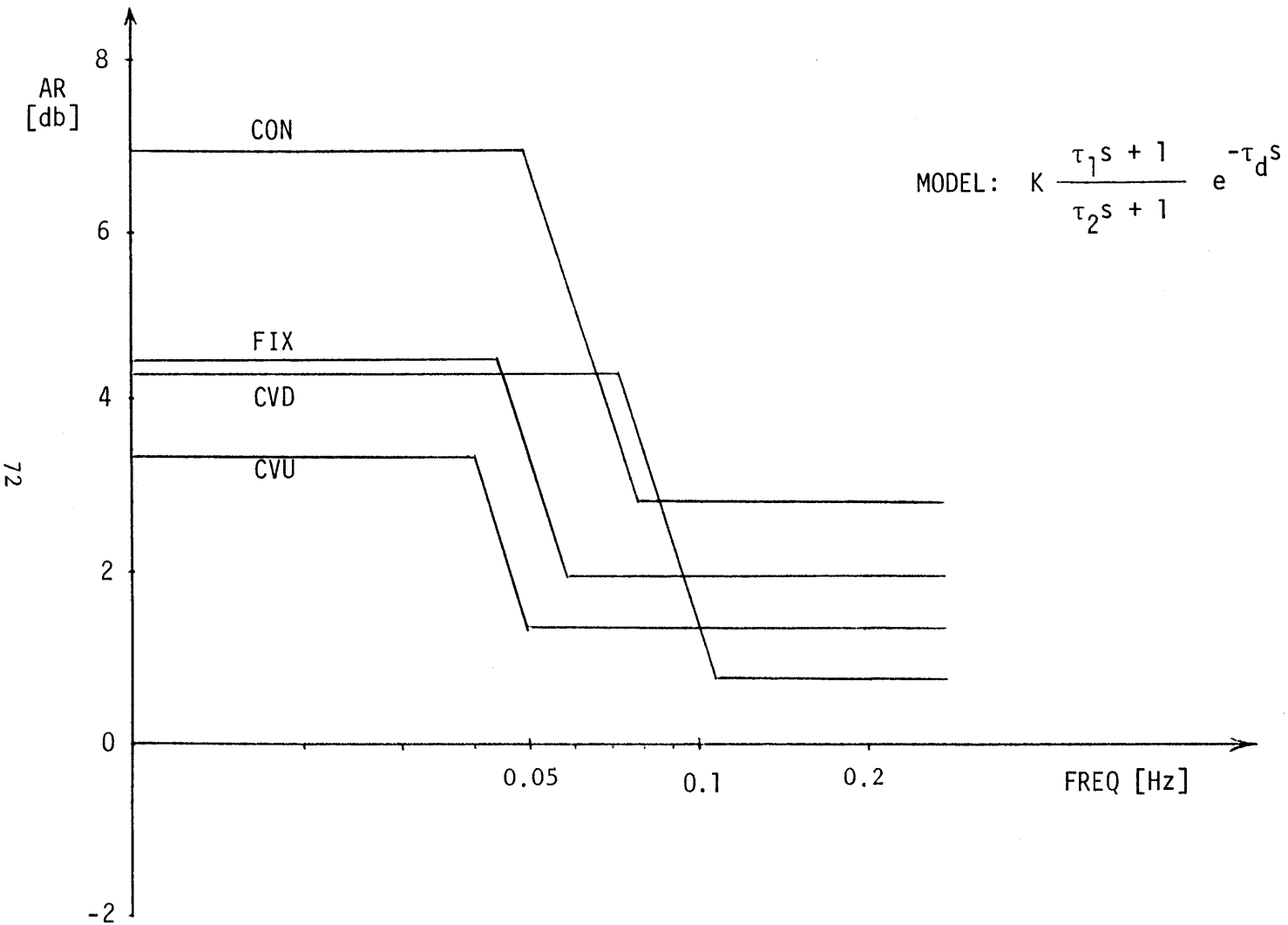

Figure 2.18: Amplitude ratio asymptotes for the CON, FIX, CVD and CVU presentations in pitch experiment

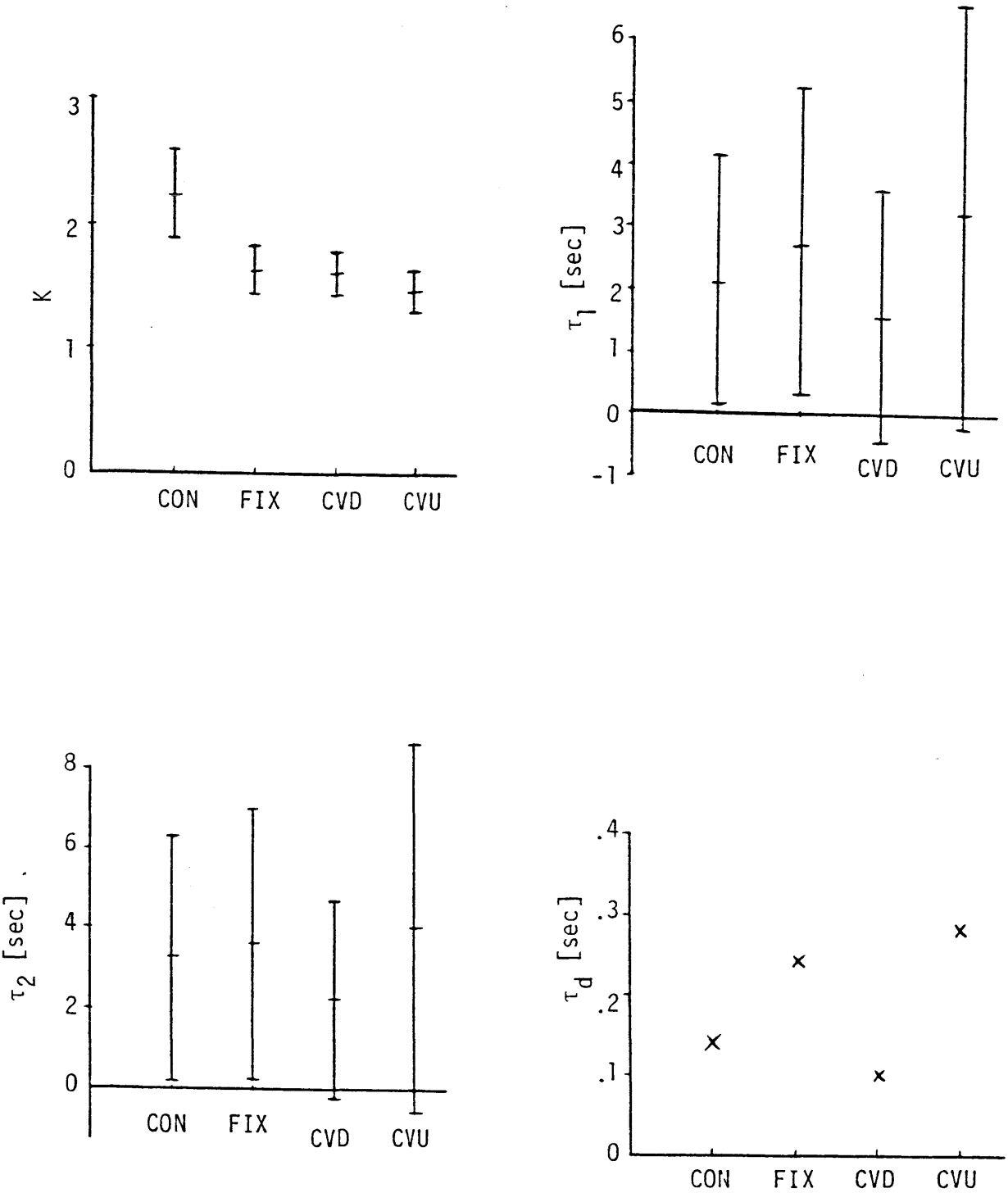

Figure 2.19: Parameter dependence on visual field type

low frequencies.

The lead-time constant τ_1 and lag-time constant τ_2 are both comparable among different presentations. It can also be noted that for the FIX among different presentations. It can also be noted that for the FIX presentation, there is significantly ($p < 0.005$) lower gain in the pitch as compared in the roll (Huang, 1979). This is probably caused by a higher threshold during the pitch rotation. Clark (1967) reviewed two studies - one concerned with pitch rotation (Sadoff et al., 1955) and one with roll (Meiry, 1965). The former reported threshold values of 5.3 to 8.2 $°/s^2$ for pitch away from the vertical, while a pilot was operating a Link trainer flight simulator. The latter reported a threshold value of approximately 0.5 $°/s^2$ for roll about earth-vertical (with the subject face down in a yawing vehicle). Clark and Stewart (1968) also studied thresholds about all three axes by suitably changing the body position so that rotation was always about earth vertical. The results showed that the pitch threshold is barely significantly ($p \simeq 0.05$) greater than the roll and yaw thresholds. Hosman and van der Vaart (1978) investigated pitch and roll tilt motion thresholds using sinusoidal waveforms. By starting with a very low amplitude fixed-frequency sinusoidal acceleration, they were able to measure the amplitude (which is called upper threshold) for detection onset by gradually increasing the amplitude. After the subject detected the acceleration, the amplitude was decreased until the subject was no longer able to follow the oscillation, thus providing the lower threshold. At the low frequency of 0.6 rad/s, the results showed that the upper (average = 0.29 $°/s^2$, σ = 0.12 $°/s^2$) and

lower (average = 0.16 °/^{2}, σ = 0.09 °/s^2) thresholds in pitch are barely significantly ($p \simeq 0.05$) greater than the upper (average = 0.18 °/s^2, σ = 0.05 °/s^2) and lower (average = 0.06 °/s^2, σ = 0.05 °/s^2) thresholds in roll, respectively. After adjusting the data to arrive at an equivalent acceleration step threshold, they found the thresholds to be remarkably below those found in the literature. This may becaused by the predictability of a sinusoidal stimulus. The influence of central processing is also evidenced (Hosman and van der Vaart, 1978) by the higher thresholds found if subjects are required to perform an additional mental task. These thresholds are comparable in roll and pitch with a frequency of 4.94 rad/s. This value was used as a threshold unit in the design of moving flight simulator washout systems by Sivan et al. (1982). As a result, for the FIX presentation, a lower gain was found in the low frequency range in pitch as compared to roll.

2.5.3 Correlation between Trainer and Wheel Signals

2.5.3.1 Canal-Otolith Interaction

It is well known that motion cues aid human operator responses at high frequency in compensatory tracking tasks. The extent of otolith contributions to motion sensation was studied by Dinsdale (1968). In his thesis, he concluded that the addition of otolith stimulation to semicircular canal stimulation allowed the human operator to increase his gain and phase lead over the middle and high frequency range ($\geq$ 1 rad/s). In

Section 2.4.3, we show that the correlation coefficient of θ (trainer position, input signal to the semicircular canals) and λ (wheel deflection) is significantly higher than the correlation coefficient of θ' (calculated input signal to the otolith organ) and λ. In order to see the difference more clearly, we pass θ, θ', and λ through a digital filter (break frequency = 1 rad/sec) and divide each signal into a low-frequency part (labelled 1 in Table 2.1) and a high-frequency part (labelled 2 in Table 2.1). We obtain

$$\begin{aligned} \theta(t) &= \theta_1(t) + \theta_2(t) \\ \theta'(t) &= \theta'_1(t) + \theta'_2(t) \\ \lambda(t) &= \lambda_1(t) + \lambda_2(t) \end{aligned} \tag{2.4}$$

then we calculate $\rho_{\theta_1\lambda_1}\rho_{\theta'_1\lambda_1}\rho_{\theta_2\lambda_2}\rho_{\theta'_2\lambda_2}$. The results are shown in Table 2.1 (from column 3 to column 6, respectively). It is clear that for each subject in each visual field, $\rho_{\theta_1\lambda_1}$ is quite the same as $\rho_{\theta'_1\lambda_1}$ in this low frequency range, but $\rho_{\theta_2\lambda_2}$ is significantly larger than $\rho_{\theta'_2\lambda_2}$ in the high frequency range. In advance, we compare θ_1 and θ'_1 by using the following formula:

$$D_{\theta_1\theta'_1} = \frac{\text{Norm}(\theta'_1-\theta_1)}{\text{Norm}\ \theta_1} = \frac{\{\sum_{i=1}^{N}[(\theta'_{1i} - \bar{\theta}'_1) - (\theta_{1i} - \bar{\theta}_1)]^2\}^{1/2}}{[\sum_{i=1}^{N}(\theta_{1i} - \bar{\theta}_1)^2]^{1/2}} \tag{2.5}$$

where

$$\bar{\theta}'_1 = \frac{1}{N}\sum_{i=1}^{N}\theta'_{1i} \qquad \bar{\theta}_1 = \frac{1}{N}\sum_{i=1}^{N}\theta_{1i}$$

θ_{1i} is one of the 1024 samples of the low frequency part of θ and N = 1024.

The values of $D_{\theta_1\theta_1'}$ and $D_{\theta_2\theta_2'}$ are shown in the last two columns of Table 2.1. Because $D_{\theta_1\theta_1'}$ is quite near zero, θ_1 is similar to θ_1'. In fact, this is expected from the formula we used to derive θ':

$$g \sin\theta' = g \sin\theta - R\, d\theta^2 / dt^2$$

At low frequencies, the last term on the right hand side is much smaller than the first term, so $\theta_1' \approx \theta_1$ and $\rho_{\theta_1'\lambda_1} \approx \rho_{\theta_1\lambda_1}$. Because $D_{\theta_2\theta_2'}$ is larger than zero (in fact this is caused by Norm θ_2' > Norm θ_2), we get the result that $\rho_{\theta_2\lambda_2}$ is different than $\rho_{\theta_2'\lambda_2}$. Next we can use the following equations to check our previous result:

$$\begin{aligned}\rho_{\theta'\lambda}\,(\text{Norm }\theta')(\text{Norm }\lambda) = {} & \rho_{\theta_1'\lambda_1}(\text{Norm }\theta_1')(\text{Norm }\lambda_1) + \\ & \rho_{\theta_2'\lambda_2}(\text{Norm }\theta_2')(\text{Norm }\lambda_2) + \rho_{\theta_1'\lambda_2}(\text{Norm }\theta_1')(\text{Norm }\lambda_2) \\ & + \rho_{\theta_2'\lambda_1}(\text{Norm }\theta_2')(\text{Norm }\lambda_1)\end{aligned} \tag{2.6}$$

With $\rho_{\theta_1'\lambda_2}=0$, $\rho_{\theta_2'\lambda_1}=0$, we can derive

$$\rho_{\theta'\lambda} = \rho_{\theta_1'\lambda_1}\frac{(\text{Norm }\theta_1')(\text{Norm }\lambda_1)}{(\text{Norm }\theta')(\text{Norm }\lambda)} + \rho_{\theta_2'\lambda_2}\frac{(\text{Norm }\theta_2')(\text{Norm }\lambda_2)}{(\text{Norm }\theta')(\text{Norm }\lambda)} \tag{2.7}$$

Because Norm θ_1' < Norm θ_2', Norm λ_1 and Norm λ_2 are comparable, $\rho_{\theta_2'\lambda_2}$ is much more weighted than $\rho_{\theta_1'\lambda_2}$ and a lower value of $\rho_{\theta_2'\lambda_2}$ will result in a lower value of $\rho_{\theta'\lambda}$. As a result, at the low frequency range, because both $\rho_{\theta_1\lambda_1}$ and $\rho_{\theta_1'\lambda_1}$ are high, the stimulation is quite well estimated by both the semicircular canals and otoliths and produces a good estimation

of pitch sensation. But at the high frequency range, $\rho_{\theta_2\lambda_2}$ is significantly higher than $\rho_{\theta_2'\lambda_2}$, the stimulation is mainly processed through the semicircular canals rather than the otoliths. The results are expected from the dynamic model of the semicircular canals and otolith system:

semicircular canals (in pitch): (Melvill Jones, 1964)

$$\frac{\hat{\omega}}{\omega} = \frac{5.3s}{(5.3s+1)(0.1s+1)} \qquad (2.8)$$

otolith system: (Young and Meiry, 1968)

$$\frac{\hat{a}}{f} = \frac{0.4s(13.2s+1)}{(5.33s+1)(0.66s+1)} \qquad (2.9)$$

where $\hat{\omega},\omega$: input and perceived angular velocity
f: lateral specific force
a: perceived tilt angle or lateral acceleration

In the high frequency range ($f \geq 1.5$ rad/s), the Bode diagram shows that the semicircular canals still pass the signal from 0 db up to 10 rad/s, but that the otolith organ will pass the signal with -20 db/dec fall off.

Next, we will compare the correlation values found in the pitch and roll experiment (Huang, 1979) for each visual field. In the roll experiment, the correlation between trainer roll position and wheel deflection can be derived using the same experimental approach and analysis techniques. The results are shown in Table 2.2. At the low frequency range, the correlation values shown in column 3 (or column 4) in Table 2.1 and Table 2.2 are comparable for the CON (or FIX, or constant rotating stripe) presentation. However, at the high frequency range, the correlation

TABLE 2.2 CORRELATION BETWEEN TRAINER AND WHEEL SIGNALS IN ROLL EXPT

SYMBOL C=CORRELATION COEFFICIENT,P=PHI,L=LAMDA,N=PHIPRIME
1=LOW FREQUENCY PART,2=HIGH FREQUENCY PART,M=(A-B)/B
AVG=MEAN VALUE,VAR=VARIANCE

DATA	C/PL	C/NL	C/P1L1	C/N1L1	C/P2L2	C/N2L2	M/P1N1	M/P2N2
(I)VISUAL FIELD-----CON								
BILL	-0.798	-0.380	-0.797	-0.792	-0.811	-0.402	0.090	2.555
ANTH	-0.812	-0.430	-0.804	-0.799	-0.868	-0.459	0.068	2.047
TYNG	-0.556	-0.265	-0.562	-0.558	-0.635	-0.319	0.119	2.715
ROGE	-0.662	-0.384	-0.679	-0.671	-0.733	-0.331	0.081	2.480
JENG	-0.630	-0.322	-0.586	-0.583	-0.691	-0.375	0.105	2.435
KERY	-0.762	-0.545	-0.734	-0.731	-0.836	-0.604	0.080	1.426
WIFE	-0.627	-0.446	-0.626	-0.624	-0.651	-0.481	0.089	1.445
YAMM	-0.368	-0.335	-0.368	-0.374	-0.520	-0.395	0.071	1.304
AVG	-0.652	-0.388	-0.645	-0.642	-0.718	-0.421	0.088	2.051
VAR	0.146	0.086	0.144	0.141	0.117	0.093	0.017	0.578
(II)VISUAL FIELD----FIX								
BILL	-0.753	-0.381	-0.745	-0.736	-0.794	-0.429	0.093	2.339
ANTH	-0.634	-0.357	-0.594	-0.595	-0.782	-0.419	0.062	2.092
TYNG	-0.583	-0.312	-0.551	-0.551	-0.628	-0.347	0.092	2.424
ROGE	-0.728	-0.422	-0.722	-0.718	-0.746	-0.448	0.078	2.197
JENG	-0.541	-0.305	-0.458	-0.459	-0.662	-0.387	0.095	2.204
KERY	-0.694	-0.493	-0.621	-0.626	-0.839	-0.563	0.066	2.273
WIFE	-0.408	-0.335	-0.356	-0.361	-0.630	-0.422	0.077	1.323
YAMM	-0.311	-0.281	-0.199	-0.210	-0.566	-0.429	0.066	1.335
AVG	-0.582	-0.361	-0.531	-0.532	-0.706	-0.431	0.079	2.023
VAR	0.156	0.070	0.186	0.180	0.097	0.062	0.013	0.440
(III)VISUAL FIELD---CVT								
BILL	-0.727	-0.366	-0.733	-0.728	-0.775	-0.406	0.086	2.489
ANTH	-0.676	-0.361	-0.656	-0.654	-0.736	-0.393	0.066	2.199
TYNG	-0.511	-0.282	-0.471	-0.474	-0.562	-0.315	0.098	2.385
ROGE	-0.600	-0.352	-0.578	-0.573	-0.360	-0.190	0.057	1.221
JENG	-0.547	-0.289	-0.447	-0.453	-0.705	-0.360	0.083	2.606
KERY	-0.689	-0.490	-0.616	-0.620	-0.855	-0.587	0.070	1.592
WIFE	-0.156	-0.180	-0.316	-0.313	-0.370	-0.330	0.091	1.251
YAMM	-0.030	-0.034	-0.199	-0.187	-0.313	-0.251	0.056	1.375
AVG	-0.492	-0.294	-0.502	-0.500	-0.585	-0.354	0.076	1.890
VAR	0.259	0.137	0.180	0.182	0.213	0.118	0.016	0.588
(IV)VISUAL FIELD----CNB								
BILL	-0.671	-0.338	-0.636	-0.629	-0.739	-0.403	0.096	2.305
ANTH	-0.314	-0.201	-0.232	-0.239	-0.571	-0.313	0.058	2.218
TYNG	-0.075	-0.078	-0.097	-0.114	-0.240	-0.103	0.072	2.259
ROGE	-0.533	-0.344	-0.487	-0.390	-0.618	-0.393	0.075	2.074
JENG	-0.458	-0.179	-0.367	-0.374	-0.600	-0.336	0.069	2.442
KERY	-0.493	-0.370	-0.387	-0.395	-0.831	-0.568	0.077	2.065
WIFE	-0.126	-0.117	-0.057	-0.061	-0.132	-0.127	0.082	1.517
YAMM	-0.160	-0.177	-0.041	-0.051	-0.419	-0.339	0.057	1.283
AVG	-0.354	-0.226	-0.288	-0.282	-0.519	-0.323	0.073	2.020
VAR	0.218	0.111	0.217	0.202	0.240	0.151	0.013	0.407

values shown in column 5 in Table 2.1 are significantly ($p < 0.01$) higher than those in Table 2.2 for each visual field condition, and the correlation values shown in column 6 in Table 2.1 are significantly higher than those in Table 2.2 for each visual field. This suggests that with the head in the erect position, the subject tends to rely more on the semicircular canals in pitch as compared to roll in the high frequency range.

2.5.3.2 Dependence on the Visual Field

In this section, we would like to see what the effect of the visual field is on the correlation values we derived in the pitch axis. In Table 2.1, the third and fourth columns (labelled C/T1L1 and C/N1L1) show that in the low frequency range, there is a significant ($p < 0.05$) correlation value drop from the CON presentation to the FIX (or CVD) presentation, and there is another significant ($p < 0.05$) correlation value drop from the FIX (or CVD) presentation to the CVU presentation. As we expect from the results we found in Section 2.5.2, the counterrotating visual field does produce the highest correlation value which corresponds with the highest gain shown in the low frequency domain. However, in the high frequency range, the fifth and sixth columns (labelled C/T2L2 and C/N2L2) shown in Table 2.1 show that the correlation values among different visual presentations are comparable. Again this suggests that the subjective high frequency dynamics are relatively unaffected by visual field motion as we found in Section 2.5.2.

2.6 Conclusions

Human control performance in the closed-loop task of nulling perceived tilt angles about the pitch axis was studied. Four types of visual motion cues were presented on the front window of the trainer. Time histories of subject response showed that the subjects would bias the trainer in the direction of field rotation, and that this bias was much stronger for pitch backwards than for pitch forward. This may be caused by the directional asymmetry in pitch vection. Describing function data, relating subject compensatory response to actual trainer pitch angle, is shown to be usefully described by a simple lag-lead transfer function with cascaded dead time, whose parameters varied for the different visual fields used during the nulling task. With confirming visual cues, a high gain was found at low frequency, which drops significantly when the visual field is either held stationary or moving at a constant velocity. Finally, by calculating the correlation between trainer position and wheel deflection, both stimulation of the semicircular canals and otoliths showed a high correlation with subjective response in the low frequency range (< 1 rad/s). However, the high frequency stimulation is mainly processed through the semicircular canals as compared with the otolith organ. On the other hand, the results suggested that the subject tends to rely less on the otolith organs in pitch as compared to the roll case.

CHAPTER III

THE LINEAR VISUAL DISPLAY SYSTEM

In the previous chapter, we treated the visual influence on flight simulator stabilization during angular rotation. It is interesting to apply this same approach to study flight simulator stabilization during linear motion. In the Center for Space Research at MIT, Lichtenberg (1979) constructed the "MIT Sled", which is a rail mounted linear acceleration cart. The apparatus as it existed at the time of his experiments is described in his dissertation. The sled was then modified by Loo (1980) and Arrott (1982). In order to study visual-vestibular interaction during flight simulator stimulation, a visual display system had to be designed and constructed based on the specifications of the MIT sled. This chapter describes how the display system was designed and what its specifications are. Section 3.1 first briefly describes the MIT sled specifications and then discusses the design criteria for the display system. Section 3.2 provides a detailed description of the specific assembly of the visual display system. Finally, Section 3.3 summarizes the design and overall specifications of the visual display system.

3.1 General Design

This section discusses the design criteria for the display system. Different types of display systems were considered and compared, and these will be discussed. This section also includes a discussion of what equip-

ment was available for use, as well as what had to be designed, in order to build the complete system.

3.1.1 Sled Specifications

A linear acceleration sled was designed and constructed by Lichtenberg (1979). The specifications are described briefly as follows:

Weight: cart, 100 lbs; subject, up to 200 lbs.

Track length: 21 feet

Motion profiles: step acceleration -- up to 1.0 g; sinusoidal acceleration -- 0.02 to 1.0 Hz up to 1.0 g amplitude.

Vibration: During measurement phases, the superimposed vibration level was limited to the range from 9.3×10^{-4} g (0.5 Hz) to 4.3×10^{-1} g (30 Hz). The settling time was less than 250 msec and the overshoot less than 10 percent.

Dynamics: Bode plot analysis shows that over a 0.3 to 1.0 Hz range, the amplitude ratio was flat to within 1.5 dB. The phase data shows a maximum of 19° of phase lag at 1.0 Hz. The system reached a resonance peak near 5.0 Hz.

Mode of motion: The seat is independent of the cart and can be positioned to allow x, y, or z-axis acceleration. The y-axis (lateral, left-right) position can be accomplished with the subject upright or on his back.

3.1.2 Types of Display Systems

The object of the display system is to provide a wide angle visual field moving linearly with a velocity controlled by the experimenter. It should permit use in the x, y and z-axes. Many types of display systems were considered:

Helmet: The Integrated Helmet and Display Sight System (IHADSS) (USAF, 1977) is usually used in pilot training. It is composed of three functional subsystems: the helmet mounted sight, the helmet mounted display, and an integrated helmet unit. Although there is no problem in constructing this type of display system, the visual display is generated mainly in the central part of the visual field (40° horizontally and 30° vertically). Because peripheral vision is so important in motion sensation generation, this type of display system was not appropriate.

Curtain type: A wide loop of cloth could be stretched tight in front of the subject. This loop of cloth would be fixed by aluminum poles to the acceleration cart itself. If the curtain had a length of 5 feet, a height of 4 feet, and were placed 2 feet in front of the subject, the visual angle would be 140° horizontally and 90° vertically. The required maximum speed of the cloth would have to be greater than the maximum speed of the cart (17 ft/s). This would make it difficult to find a suitable motor to rotate the whole curtain at such a high speed. A very heavy motor on the cart would also degrade the performance of the sled.

Fiber optics: A high intensity visual image generated by a CRT or projector could be transmitted by fiber optics and projected in front of the subject by reflection through small mirrors. However, if the fiber optics wires were bent, they would have different path lengths and thus would generate an image which would be out of phase. This phase difference is probably not sensed by the subject.

Projector system: One type of projector display was designed by Murphy (1972) and was then revised and used on the GAT-1 trainer. This display system consists of a slide projector, mirrors and a translucent screen and could be modified for use on the sled. The visual display image would be generated by using a film drive mechanism and a film strip, and the pattern of the image could be easily changed. By reflecting the image through two mirrors at a large distance, a wide field image can be obtained with good quality. This system was chosen as the best alternative for use on the sled.

3.2 The Visual Display System

3.2.1 Specific Assembly

The visual display system was designed for use in the y-axis. It can be modified for use in the x and z directions. A Kodak Carousel 600 projector with an f3.5 lens was the basic element of this system. It was found to have optics which were sufficient for meeting the image size requirements, so they were left in tact.

The initial design is shown in Figure 3.1. This involved projecting the image onto a screen which is mounted in front of the subject. The projector is mounted on the back of the seat with a small mirror over the seat and a long mirror is hung on the wall at a distance far enough away that the image would cover the entire translucent screen. A film drive mechanism was designed so that the projected image on the screen can be moved linearly in the y axis. The speed of the motion had to be continuously variable in a range from 0 to 5.36 m/s (which is the maximum speed of the cart). The translucent screen is back-lighted and is long enough to provide a wide visual display (120° horizontally and 53° vertically). The parts mentioned above are all mounted on the cart in such a way that the small vibration noise of the cart will not be transmitted to the seat through these parts.

The slide changing mechanism of the projector was removed to give more room for the film. The projector was then mounted on a frame which is fixed vertically on the cart. The space between the lens and the projection lamp was increased so that the lamp will not be overheated.

A film drive mechanism was attached to the side of the projector's frame. It consists of four guide shafts (1 inch in diameter) set in roller bearings and supported by aluminum bars to form the outline of a rectangle. The film which goes around this mechanism is a standard 35 mm film strip (developed without being exposed) with the desired pattern draw or taped on it (we are currently using a 1/16" wide black and white

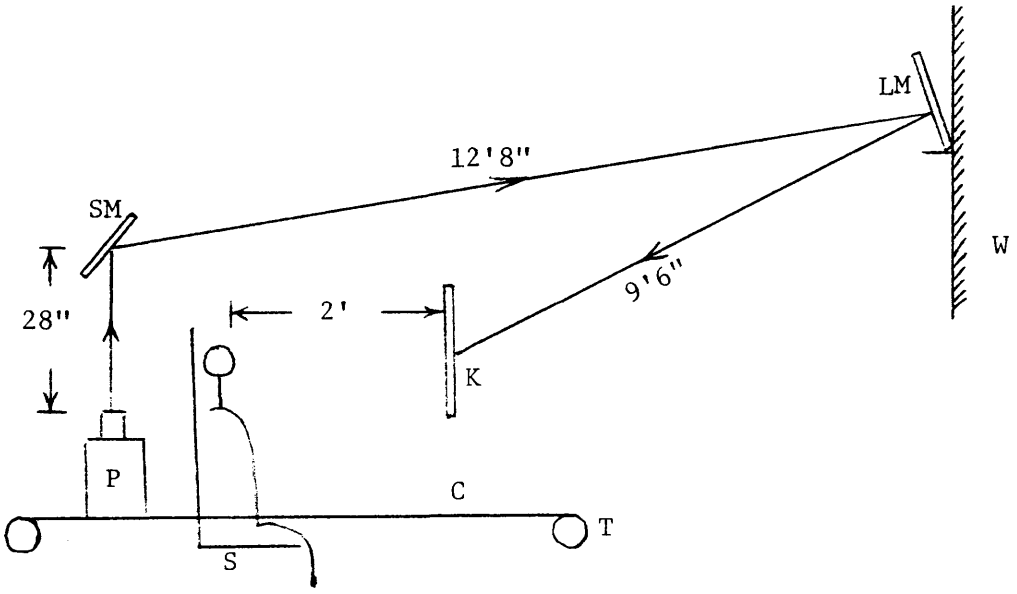

C:	Cart (4.74' x 2')	K:	Backlighted translucent screen (7' x 2')
LM:	Long mirror (25' x 2.5')	P:	Slide projector
S:	Seat	SM:	Small mirror (15" x 15")
T:	Track	W:	Wall

Figure 3.1: Side view of the visual display system.

stripes). The film runs around the outside of the guide shafts, passing down through the projector in the slot where the slide is normally placed, and out through a slot cut in the bottom casing of the projector. The film is spliced together to form a 32 to 34 inch continuous loop. The lower rear shaft has a 35 mm sprocket attached to it which drives the film. This shaft extends outside the rectangular outline and is connected through an anti-backlash worm wheel to the shaft of a dc motor (Torque Systems MT3310-002DE) which is also fixed to the projector's frame. The anti-backlash worm wheel was used to reduce the speed of the motor (ratio 45:1) and to provide a zero phase lag when the direction of rotation is reversed. A controller and dc power supply (Torque Systems, C0401-001) were mounted on the ground. The gain of the controller can be adjusted so that the maximum speed of the image on the screen will be 5.36 m/s which is the maximum speed of the cart. Instead of mounting the projector frame directly on top of the seat, it is mounted to the back of the seat so that the entire system will be more stable and the path of the projected light will be longer.

The overhanging small mirror (15" x 15"), which is mounted 28" above the projector, is used to reflect the projected image to the long mirror which is hung on the wall. The angle that the mirror makes with the incoming light can be varied from 0 to 360 degrees. Its position left and right relative to the projector is adjustable.

The translucent screen (7' by 2') consists of a thin back-lighted screen (Polacoat Flex screen) sandwiched between two pieces of transparent

plexiglass. It is fixed on the cart and placed 2' in front of the subject. The projected image is 120° horizontally and 53° vertically. The visual angle of the subject can be limited to this range by means of an adjustable goggles. The image should be sufficient to generate a powerful visual cue. A black and white vertical stripe pattern was selected for the image. By using a projection zoom lens, the size of the stripe on the screen can be varied from 1.5" to 6". If the subject fixates on a point level with his eyes, the spatial frequency will vary from 0.004 to 0.14 cycles per degree at the fovea to 0.16 to 0.56 cycles per degree at 60° from the fovea. Patterns with spatial frequencies in this range are quite effective in generating linearvection (Lestienne et al., 1977). The pattern is quite uniform so that relative positional cues are unlikely and a powerful velocity cue will be provided.

3.2.2 Dynamics

The Bode plot analysis of the visual system was derived from the sine wave velocity command (peak velocity 3.1 m/sec) and the recorded tachometer signal of the motor. Figure 3.2 shows the Bode plot as a function of frequency from 0.015 to 1.46 Hz. The amplitude ratio is flat to within 0.5 dB and the phase data shows a maximum of 17° of phase lag at 1.0 Hz.

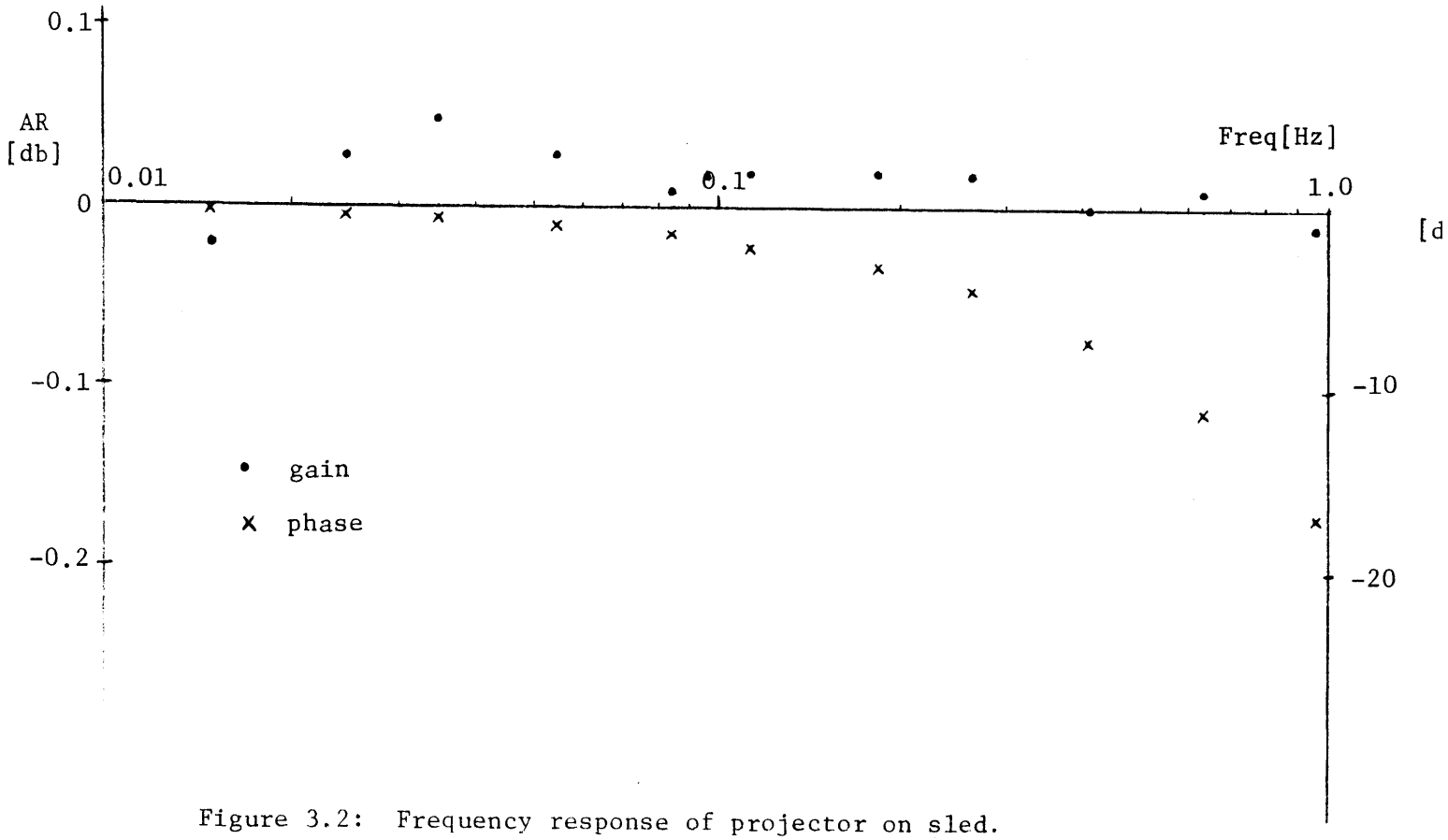

Figure 3.2: Frequency response of projector on sled.

3.3 Summary

Different types of display systems were considered for use on the MIT sled. The type of projector display accompanied with a set of reflecting mirrors was chosen and constructed in order to provide a linear visual field motion which is coupled or uncoupled to the sled motion. This display system was tested and the specifications are summarized as follows:

Type of motion: linear horizontal motion in the y axis.

Field of view: 120° horizontally and 53° vertically.

Speed: 0 to 5.36 m/s (500°/s).

Pattern: black and white stripe pattern (the width of the stripe on the screen can be varied from 1.5" to 6" by using the zoom lens).

Spatial frequency: 0.04 to 0.14 cycles per degree at the center and 0.16 to 0.56 cycles per degree at 60° from the fovea.

Weight: 65 lbs for all parts mounted on the cart.

Dynamics: Bode plot analysis shows that the amplitude ratio is flat up to 1.46 Hz and the phase data shows a maximum phase lag of 17° at 1 Hz.

Servo: The servo is driven by computer generated commands of velocity.

CHAPTER IV

VISUAL FIELD INFLUENCE ON MANUAL LATERAL STABILIZATION

The basic objective of this chapter is to develop a quantitative functional model of motion sensation dependence on combined visual and vestibular motion cues during the lateral motion. In particular, first we wish to propose a human operator describing function which adequately models the subject's dynamic behavior observed during a closed loop nulling task on lateral stabilization. A dynamic model of the otolith organ will be derived after investigating the control strategy that the subject used in the nulling task. Then the modelling effort will be extended to an investigation of dynamic response to a wider variety of visual motion cues. Specifically, we wish to study how the subject will respond to combined cue stimulation, in a situation in which both visual and vestibular cues contain wide bandwidth information resulting in a subjective sensation of lateral motion. Finally, we explore the extent of field dependence of the subjects who participated in this experiment.

This chapter is organized into seven sections. Section 4.1 describes the general experimental approach utilizing the pseudo-random time-varying inputs and based on the closed-loop velocity nulling task, the measurement technique used in Chapter II. Section 4.2 then presents a detailed description of the experimental apparatus and protocol used, while Section

4.3 shows the describing function of the human operator with different visual motion cue stimuli. Section 4.4 demonstrates how the estimator model can be derived by an independent measure of human operator dynamics. Section 4.5 shows an extended effort to perform an experiment with time-varying visual stimuli in order to develop a human operator dual-input describing function which adequately models a subject's sensation in response to combined cue stimulation. Section 4.6 describes a study on the field dependence of the subjects which used two psychological tests - the rod and frame test and the embedded figures test. Finally, Section 4.7 summarizes the results.

4.1 Experimental Approach

The method used in Chapter II was based on measurements made on the position nulling behavior of subjects presented with simultaneous visual and vestibular motion cues. The same approach will be used here. In order to provide lateral motion, the MIT sled with its velocity-servo will be used. The subject is required to null the lateral velocity of the sled on which he is seated, using a velocity control which commands the sled drive. The velocity nulling task requires that the subject match his sensation, mainly derived from visual and vestibular motion cues, with the sensation of standing still. A pseudo-random disturbance signal is added to the sled drive, so that the disturbance compensation must be performed throughout the course of the run. The overall block diagram of the experiment is given in Figure 4.1. During the lateral motion, the estimator shown in the diagram of the subject involves the otolith organ only.

Since we are currently interested in subjective response to low-frequency visual motion cues, some of the candidates for a test stimulus are similar to those we used in the pitch experiment, i.e. a linear countermotion visual field, a field fixed with respect to the subject, and a constant velocity field motion. However, we are also interested in providing a visual field in darkness. Huang and Young (1981) showed that the sensation of yaw rotation with a fixed visual field is different from that in the dark. It would be interesting to extend this investigation to linear motion sensation.

These choices motivate the visual field stimuli, illustrated in the block diagram, labelled as follows:

(1) CON (countermotion): A countermotion field, which moves right with respect to the subject when the sled moves left, and which has the same speed as the sled.

(2) FIX (fixed): A field fixed with respect to the subject.

(3) DK (dark): Subject in the dark with eyes open.

(4) CV (constant velocity): A field moving at a constant velocity of 5°/s to either direction with respect to the subject, independent of actual sled velocity.

By measuring subject responses during the nulling task, in particular his control of sled velocity and wheel deflection, the differences due to operation in these four visual field environments were compared. How

field type could be correlated with subject response to infer a functional model of low-frequency parallel channel processing was studied. For now, we will describe some of the details of the experiments.

4.2 Experimental Description

This section gives a description of the hardware implementing the loop of Figure 4.1 and the procedure used in the experimental runs.

4.2.1 Experimental Apparatus

4.2.1.1 MIT Sled

The "MIT sled" is a rail mounted linear acceleration cart designed and built by Lichtenberg (1979). The sled was then modified by Loo (1980) and Arrott (1982). The apparatus, as it existed at the time of this experiment, is described in detail by Arrott (1982). However, it is worthwhile to provide a short description here.

The various parts of the sled consist of the drive mechanism, guide rails, seat, head fixation device, and data recording apparatus. The seat, which is independent of the cart, is positioned to allow y-axis (lateral, left-right) motion. The drive system is a commercially available DC permanent magnet motor and pulse width modulation (PWM) controller. The motor drives the cart through a direct drive, cable and winch drum system. The control of the motor is accomplished through a PDP 11/34 computer which acquires the position, velocity and acceleration of

the cart and selects various control logic algorithms. The motor uses tachometer feedback for accuracy and stability, and the input to the controller is a velocity command. The figure specifications of the sled are summarized briefly in Section 3.2.1.

In the experiment, the subject is secured in the seat with a four-point aircraft-type lap belt and shoulder harness and an additional chest strap to reduce left-right movement. In addition, stiff foam blocks are wedged between the subject's shoulder and the seat frame to further reduce torso motion. The head is supported with a foam rubber insert within a hard case. It completely encases the head up to the frontal plane of the face. The head support is adjustable vertically and has an aluminum plate on each side which holds the earphones and provides additional lateral support when they are pushed tightly against the foam.

4.2.1.2 Projector System and Goggles

During CON, FIX, and CV presentations, the visual motion cue is provided to the subject via a projector system (described in Chapter III). When the subject is seated in the sled, looking forward, the screen subtends approximately 120° horizontally and 53° vertically. Alternating black and white vertical stripes subtend angles of approximately 4.7° each. A small red dot is on the screen at eye level, so that the subject can focus on it during the run. The motion of the stripes was controlled by the PDP 11/34 through the small motor and controller. The input to the controller is a velocity command. The software was revised to provide and

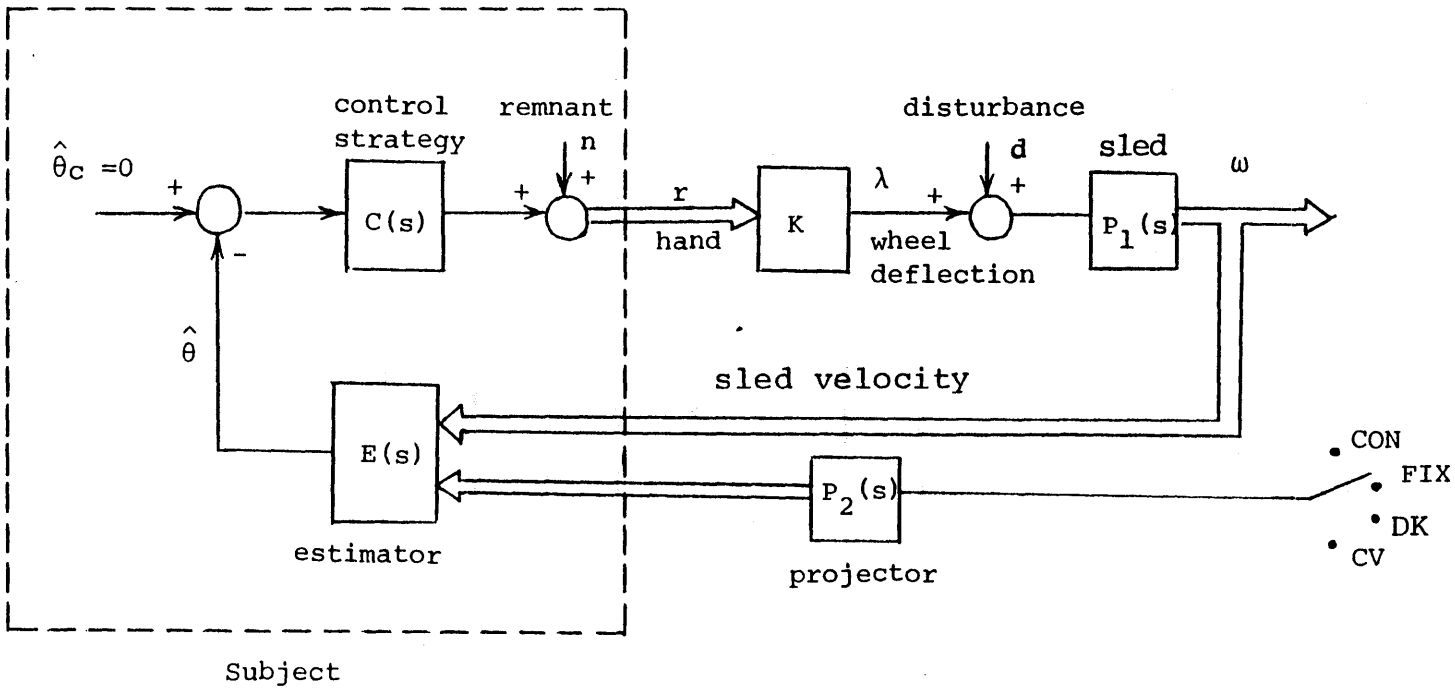

Figure 4.1: Closed-loop velocity nulling task in the sled experiment

record the cart and visual signals at the same time, as is shown in Appendix A. The visual and cart command signals could be uncorrelated or correlated with any desired coefficient. It is appropriate to note that the projector drive dynamics are faster than the response dynamics noted in the previous chapter, so that the field motion faithfully follows sled motion when the countermotion mode is utilized.

A pair of ski goggles were modified to be worn by the subject so that only the full display screen could be seen. The size of the window on the goggles could be adjusted to fit individual subjects. The field of view is 120° horizontally and 53° vertically.

4.2.1.3 Control Wheel

A thumb wheel (diameter 3", 1/8" thick) is used as a control wheel for nulling the sled lateral motion. This wheel is mounted directly in front of the subject so that the subject can easily rotate it (the axis of the wheel lies in the x-axis). The wheel is not spring loaded and can be moved on the top smoothly in the left-right direction without providing tactile cues concerning the center, left or right position. The center position of the wheel provides zero commanded velocity to the sled. Full excursion of the control wheel (mechanical stops limit the wheel deflection to 130° in either direction) would result in a 0.8 m/s sled velocity with a direction corresponding to the direction of the control wheel.

4.2.1.4 Disturbance

As shown in Figure 4.1, the sled will be driven by a pseudo-random (sum of sines) disturbance. In order to provide a spectrum containing low frequency range stimulation (below 0.04 Hz), a long duration profile is desired (about 200 s). In Table 4.1, a sum-of-25-sines profile was designed where the frequency spectrum varies from 0.016 Hz to 1.08 Hz. The sampling time increment and duration of profile were also chosen to provide 1024 12 sampling points for the entire run, so that the recorded data can be filtered and the fast Fourier transform could be used to analyze the data later. The sled motion was mainly restricted by a limited length of track (4 m) and an allowable maximum acceleration (0.41 g). The disturbance amplitude was chosen by passing an equal velocity amplitude through a shaping filter to approximate a smooth power spectral density function of the following form:

$$\Phi_{dd} = \left| \left(\frac{P}{(s + a)^n} \right) \right|^2_{s=j\omega} \tag{4.0}$$

where n is the order of the filter, a is the pole and p is the scaling factor. These parameters and the successive phase angle were tuned to generate a signal which had the allowed maximum acceleration signal, 100 percent usage of the track, and also provided a larger RMS value for the velocity signal. The parameters shown in Table 4.1 are for the case with n = 1, a = 0.31 Hz and a successive phase angle of 247°. Each spectral component listed is a prime multiple of a base frequency of 1/184.32 Hz, so that the signal is periodic with a period of 184.32 seconds. The time history is shown in Figure 4.2.

SUM OF SINES PROFILE

1. DURATION OF PROFILE: 184.32 SEC

PARAMETERS OF SINUSOIDS:

2. NUMBER OF SINUSOIDS: 25
3. FUNDAMENTAL FREQUENCY: 0.0054 HZ
4. EQUAL AMPLITUDE DOMAIN: 0 (-1,P;0,V;+1,A)
5. SUCCESSIVE PHASE ANGLE: 247. DEG

PARAMETERS OF SHAPING FUNCTION:

6. ORDER OF FILTER: 2
7. POLE: 0.28 HZ

PHYSICAL CONSTRAINTS:

8. LENGTH OF TRACK 3.60 M
9. ALLOWED ACCELERATION 0.41 G
10. TIME INCREMENT: 0.015 SEC

RESULTING IN THE SUM OF SINUSOIDS:

FREQ [HZ]	AMP [M/S]	ACCEL AMP [G]	PHASE [DEG]
0.016	0.08	0.001	0.
0.027	0.09	0.002	247.
0.038	0.11	0.003	134.
0.060	0.11	0.004	21.
0.071	0.10	0.005	268.
0.092	0.10	0.006	156.
0.103	0.10	0.006	43.
0.125	0.12	0.009	290.
0.157	0.10	0.010	177.
0.168	0.09	0.010	64.
0.201	0.10	0.012	311.
0.222	0.07	0.010	198.
0.233	0.06	0.010	85.
0.255	0.08	0.013	332.
0.288	0.08	0.015	220.
0.331	0.08	0.018	107.
0.396	0.07	0.018	355.
0.450	0.06	0.019	242.
0.548	0.05	0.019	130.
0.613	0.04	0.018	17.
0.743	0.04	0.017	265.
0.808	0.02	0.013	153.
0.884	0.02	0.013	40.
0.982	0.02	0.013	288.
1.080	0.02	0.012	176.

MAXIMUM ACCELERATION IN SIGNAL: 0.140 G
PERCENT USAGE OF TRACK: 100.00%
STARTING POSITION: 0.00

Table 4.1: Disturbance used for single input sled experiment

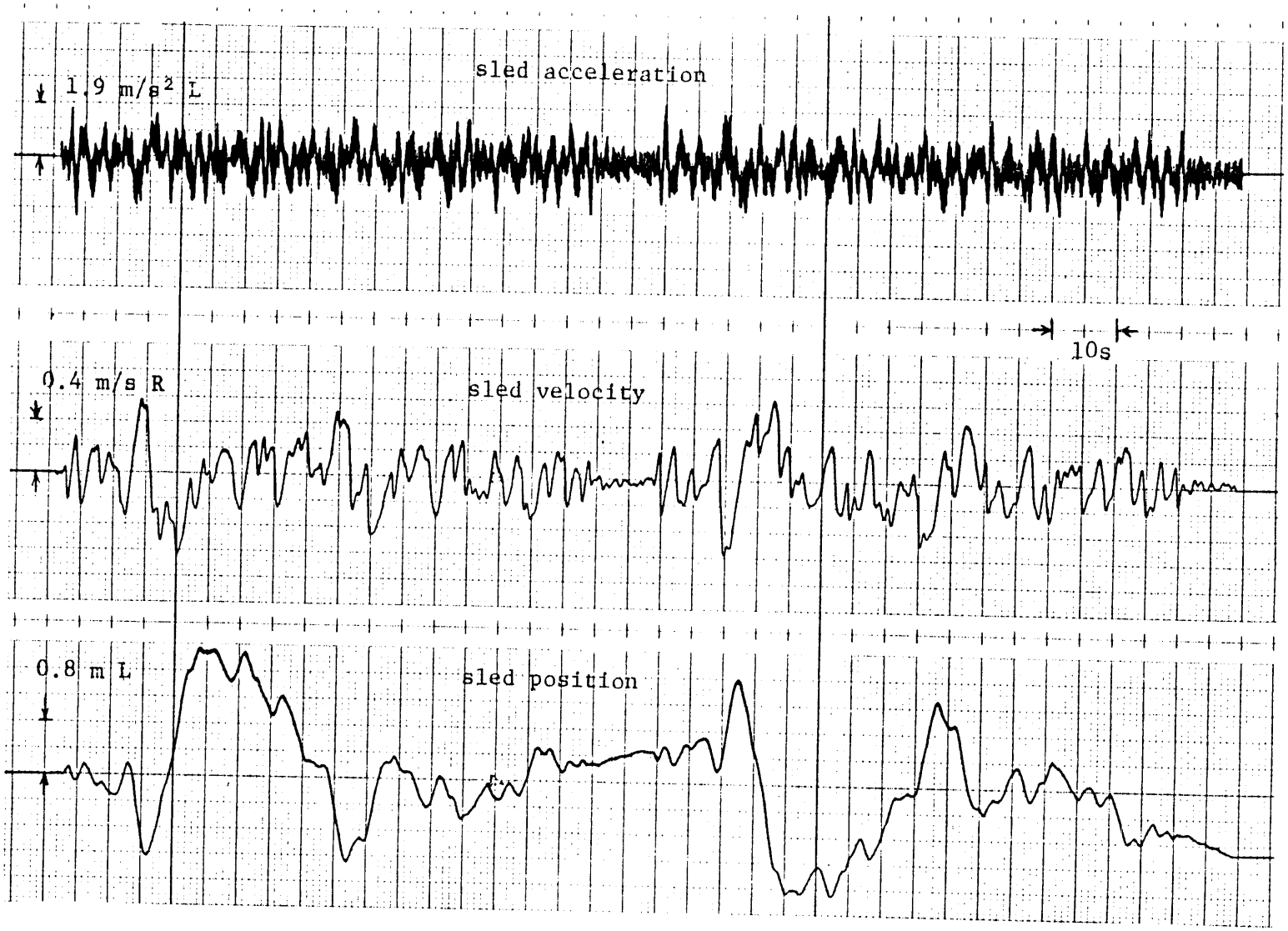

Figure 4.2: Disturbance used for single input sled experiment

4.2.1.5 CART Program

An interactive FORTRAN program, CART, was written by Arrott (1982) and modified to accommodate the visual display system. This program first generates the disturbance and then stores it in a motion profile. During the real time operation of an experiment, the disturbance profile is retrieved and summed with the filtered subject's wheel signal (Figure 4.1) to generate velocity commands for the analog controller; this program then records and stores the physical and physiological signals of interest. In addition, the program uses position and velocity feedback to provide a safety interlock. Since the analog controller does not compensate for drifts in the sled position, a drift compensation algorithm using position feedback was developed and incorporated into the program (Loo, 1980). The program operates interactively with the experimenter, permitting him to alter operating parameters during the course of an experiment. Alternatively, complete protocols can be established prior to the experiment. A listing of the CART program is provided by Arrott (1983).

4.2.1.6 Supplementary Equipment

Additional equipment used in the experiment included a white noise generator and a four channel strip chart recorder to record the basic variables of the closed-loop task: disturbance input, sled velocity, sled position and subject wheel deflection. In addition, a headphone is provided for audio cue elimination during a run, by means of white noise from the white noise generator.

4.2.2 Experimental Procedure

Eleven subjects participated in the experiment, eight males and three females, aged 22 to 30, in normal health with normal vision and having no known vestibular dysfunction. All subjects were asked to sign an informed consent statement which provides a brief description of the experiment to be performed (shown in Appendix C). Each subject was instructed to use the velocity-nulling method to keep the sled as motionless as possible, by concentrating on his own sensation of motion and by providing the appropriate compensatory control wheel deflections. Before the experiment, with the control wheel disabled, the disturbance signal was injected into the sled so that the subject, first standing outside the sled, and then seated inside (with outside lab view), could obtain some estimate of the amplitude and frequency content of the signal he would be asked to null. The subject was seated in the sled, the safety belt tightened, and the head restraint adjusted to fit his head. Then, without a disturbance input, the subject was asked to move the thumb wheel to drive the sled so that he could see how well the wheel controlled the sled. During this time, the white noise was provided through the headphone and the volume was adjusted to a comfortable level for the subject, which assured that th motor sounds from the sled were inaudible. Finally, the subjects entered a practice session to access their performance and decide whether or not to continue the experiment.

Because we are particularly interested in the dominance of the visual cues in the low frequency range, a successful run which can last a fairly

long time without hitting the end of the track is necessary. For CON presentation, since the visual field motion exactly confirms the vestibular sensation, we would expect the subject to finish the entire run (184.32 seconds) without difficulty. On the other hand, in the CV presentation, the existence of linearvection may make it impossible to finish the run without encountering the end of the track. For DK presentation, the task may be harder than in the FIX presentation as we learned from the yaw experiment (Young and Huang, 1981). So the DK presentation is chosen to be used in the practice session, not only because it is hard enough to provide practice, but also due to ease of preparation.

In the practice session, the subject was first given a run with his eyes viewing in the lab. Then the subject was instructed to close his eyes as long as possible while performing the same task in the run. If he felt that he might hit the end of the track, he was allowed to open his eyes at once and then make the correction. Once the subject could perform the task over half of the run, a further experiment with different visual presentations was performed. Five subjects, all males, successfully continued on the following experiments. It may be implied that the perception of spatial orientation of these subjects was mainly based on their body sensation rather than the surrounding field. A further psychological test was then performed (described in Section 4.6) to investigate the field dependence of all the subjects.

The following experiment included eight runs for each subject with a random order of visual presentations (two runs of each visual field: CON,

FIX, DK and CV). For CON, FIX, and CV presentations, the projector was turned on and the subject wore goggles which were adjusted so that only the full display screen could be seen. For DK presentation, the subject wore another pair of goggles so that no light could be seen, although the subject was instructed to keep his eyes open during the whole run. Between each run, there was at least one minute rest.

At the end of the experiment, each subject was questioned as to whether he may have been consciously using other cues besides motion sensation to null the sled velocity. No subjects felt that any other cues were available for inferring sled motion.

4.3 Results

This section presents four illustrative sample chart histories, one for each visual field type, and will have a further statistical analysis on the performance of the task for different visual field presentations. Then, we will propose a simple human operator describing function which adequately models the subject's dynamic behavior observed during the course of the assigned velocity nulling task. This describing function, as we studied in the pitch experiments, will show how low frequency visual cues dominate low frequency sensation and how they can be used to vary the AC transduction characteristics of the vestibular system. Finally, a further experiment is motivated by the need to derive the describing function of the estimator which represents the otolith organs.

4.3.1 Time Histories of Subject Response

In the time histories of subject response, we are mainly interested in four basic variables of the closed loop task: disturbance input, subject wheel deflection, sled velocity, and sled position. These signals are first recorded and then stored in the digital computer, and then plotted on the strip chart recorder after passing through a digital filter, which is described in the next section, in order to get rid of the spikes in the recorded signal.

Figure 4.3a shows a set of typical histories of the disturbance signal sent to the sled, the subject's compensatory control wheel deflection, the sled velocity and the sled position. Since the visual field is countermotion (CON), that is, stationary in the laboratory, operator performance in this situation results in a well-met task objective with the sled being maintained at zero mean velocity throughout the run. The sled position is maintained within one meter. Similarly, Figure 4.3b illustrates performance in the fixed (FIX) visual field, where the visual field is held stationary with respect to the subject. Although no visual cues were available during the presentation, the subject can still maintain the sled without a velocity or position drift to a fixed direction. In earth-vertical rotation, an unrecognized velocity drift in a preferred direction of the trainer was observed in the FIX presentation (Young and Zacharias, 1981), and the drift rate was below threshold. This may be caused by the imbalance between left and right semicircular paths. However, in lateral motion, the lack of drift in the sled implied that there

was no apparent imbalance between left and right otolith paths. Figure 4.3c shows performance in the dark (DK) visual field. Although no drift is observed, as in the FIX presentation, it is interesting to compare the performance in these two presentations. Finally, Figure 4.3d illustrates performance in the visual field moving with constant velocity (5°/s or 5 cm/s to the left). Note the change of time scale and that the sled velocity signal is unfiltered. With a visual field moving to the left, the subject will have linearvection to the right and this results in a compensatory sled position drift to the left.

Human operator performance for each visual field presentation was evaluated by two key variables: the deviation (or RMS tracking error) of sled velocity and the fraction of total run the subject finished. For each subject, the average values of the deviation of sled velocity and the fraction of total run he performed in each visual field are calculated. The population statistical results of the five subjects are shown in Figure 4.4. As expected, all the subjects finished the whole run in the CON presentation and provided the lowest value of the deviation of the sled velocity. On the other hand, where there is linearvection and conflict between visual and vestibular cues in the CV presentation, only 60 percent of the total run was finished and the highest deviation of sled velocity was found. In the DK presentation, no visual cue is provided. In the FIX presentation, that is, where the visual surround is fixed relative to the subject, one might imply that a "no motion" or null signal, if interpreted as a linear vection input, is provided to cause a conflict with the true motion sensed by the otolith organs and might be

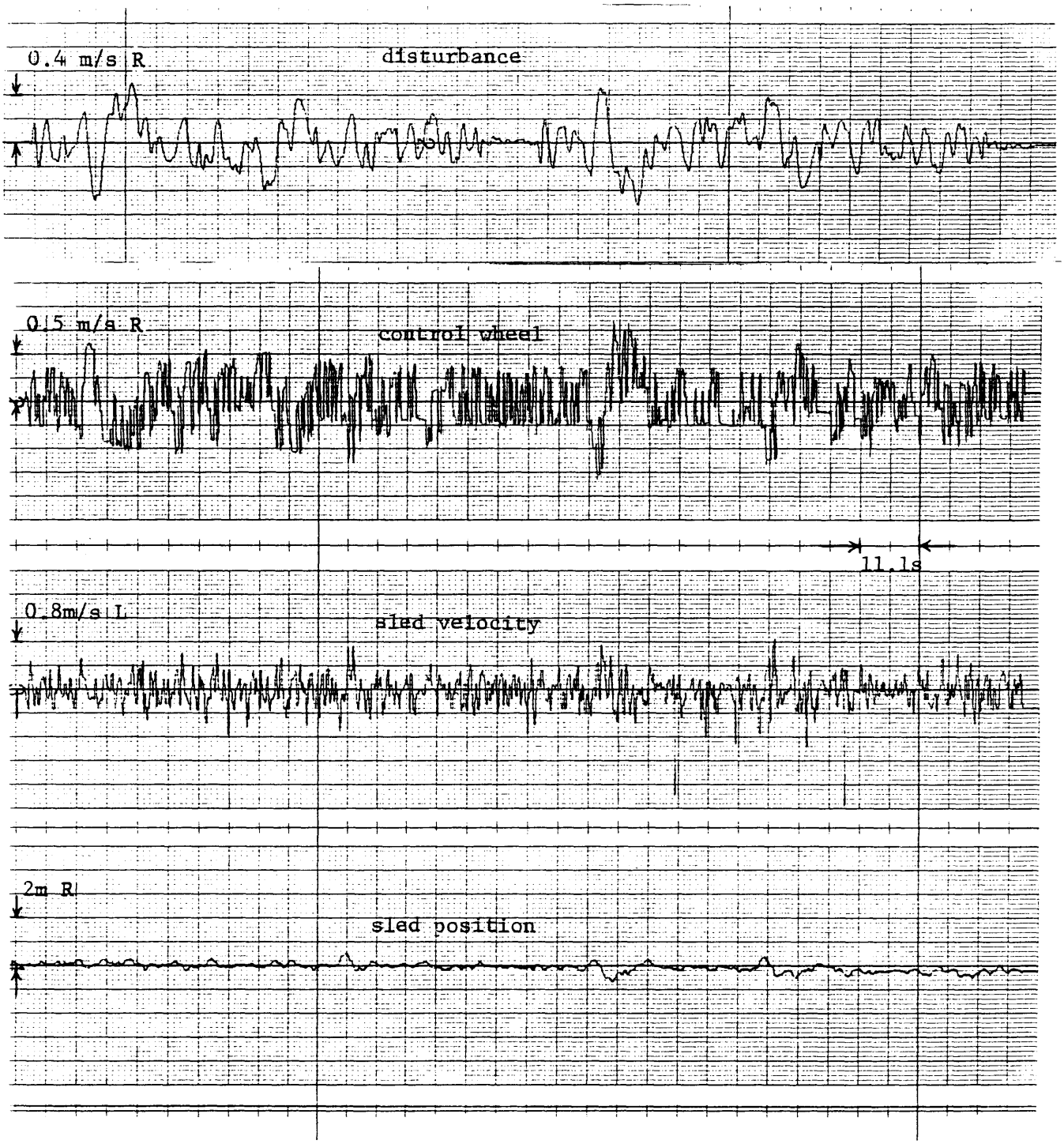

Figure 4.3a: Countermotion visual field (CON) in sled experiment

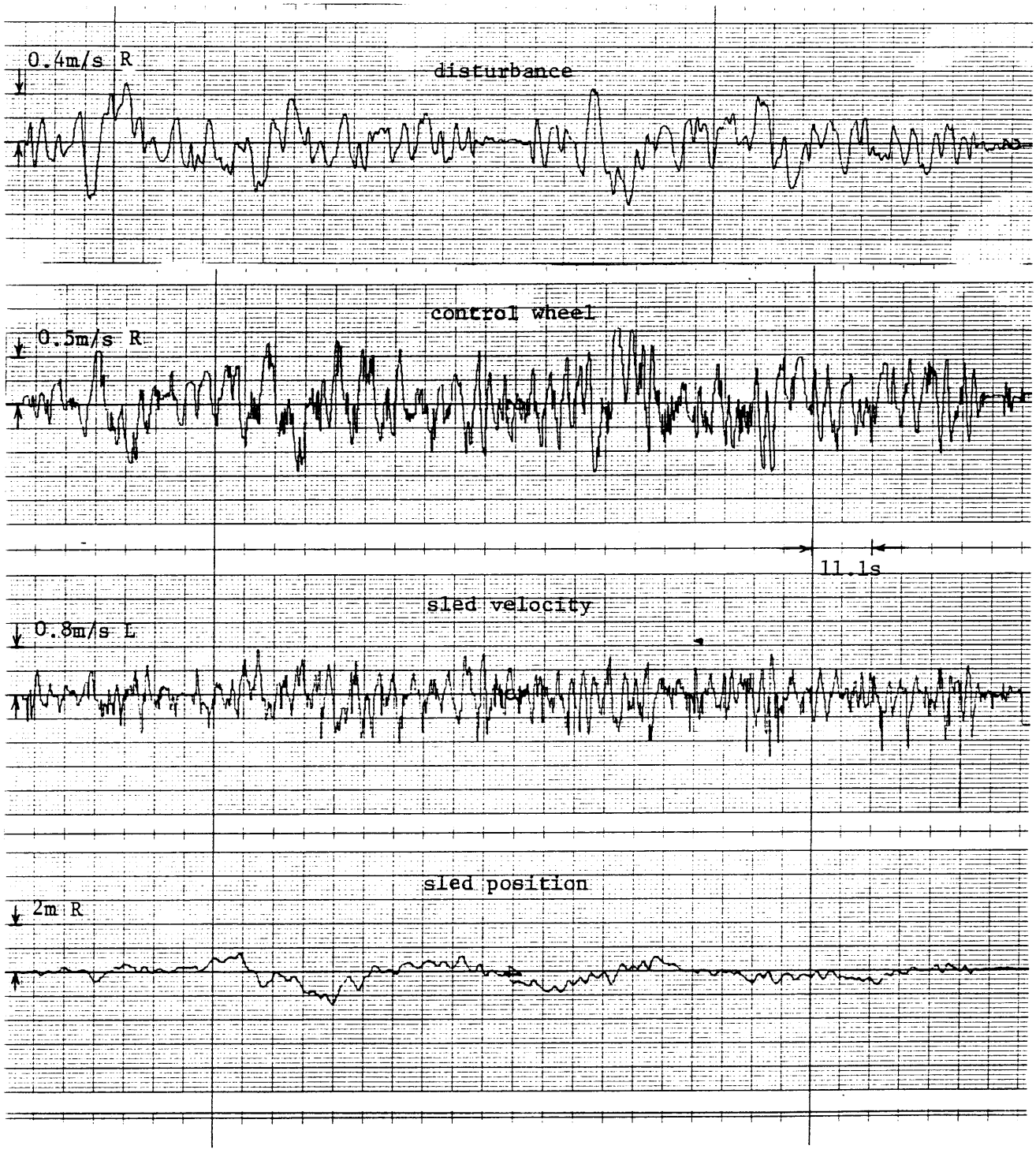

Figure 4.3b: Stationary visual field (FIX) in sled experiment

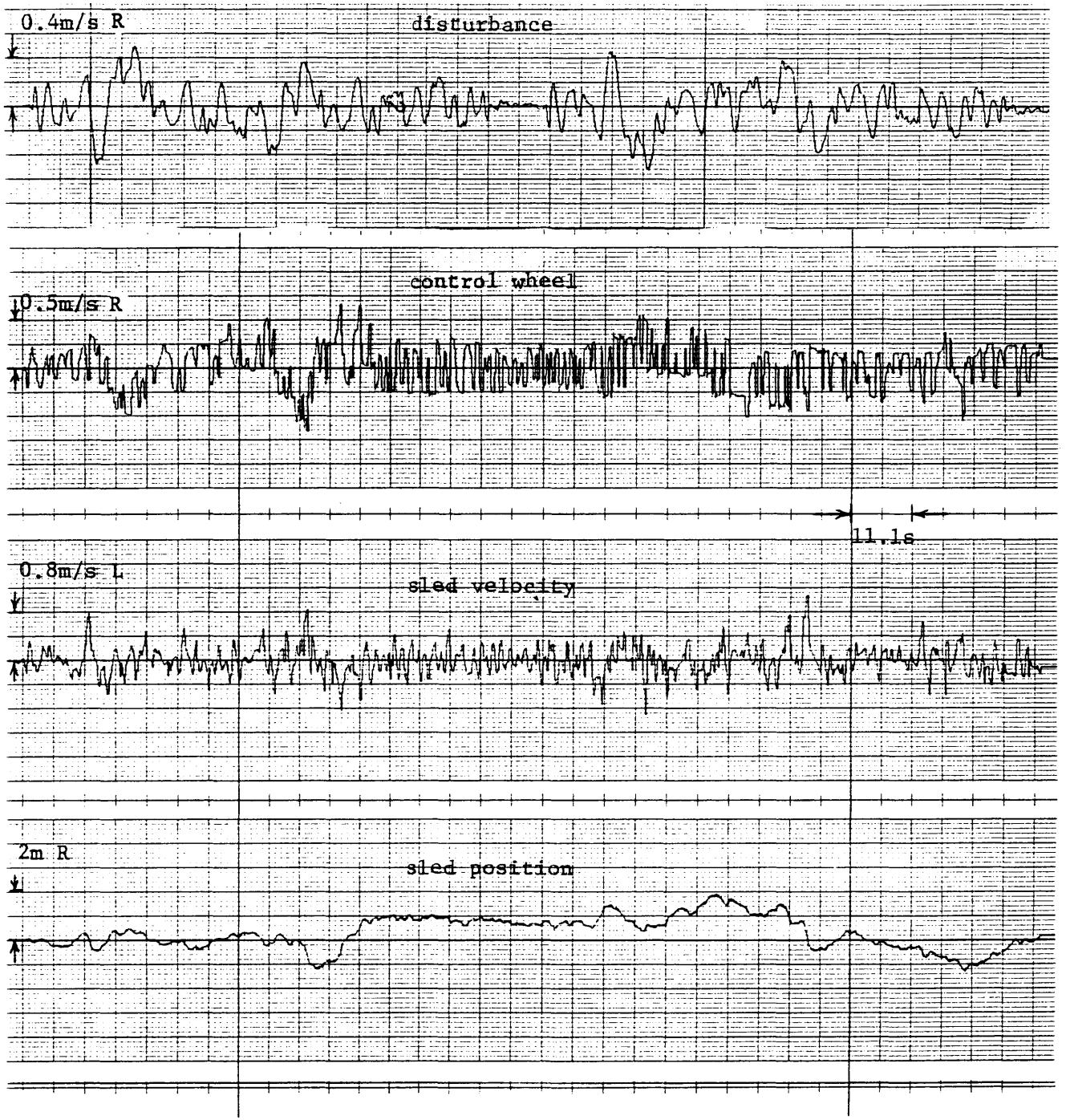

Figure 4.3c: Dark (DK) visual field in sled experiment

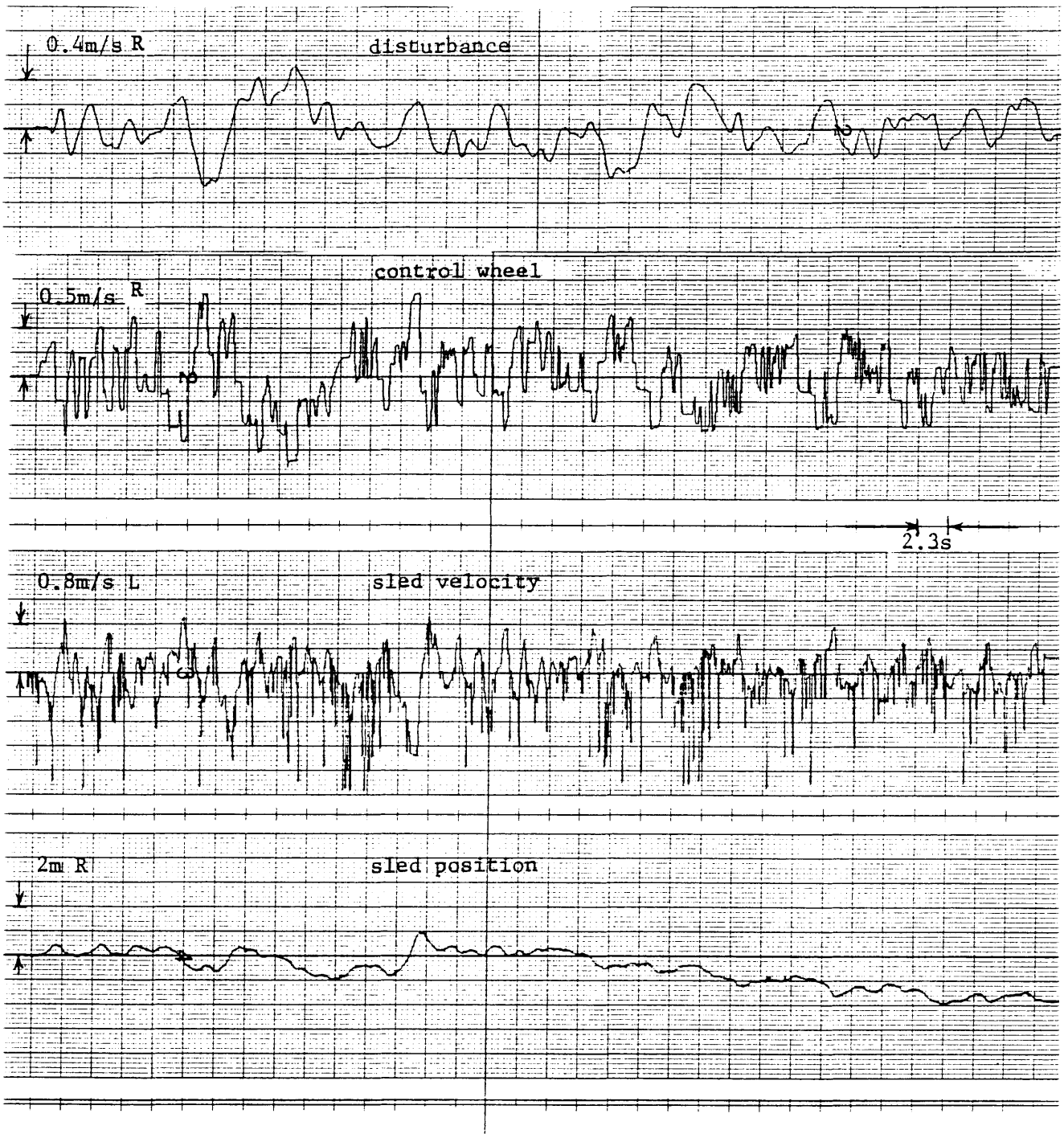

Figure 4.3d: Constant velocity (5°/s L) visual field in sled experiment (Note the change in time scale)

expected to inhibit the motion sensation. Furthermore, vestibular nucleus unit activity was shown by Waespe and Henn (1978) to be inhibited by a fixed visual surround in similar circumstances and compensatory eye movements are suppressed by visual fixation.

However, our results show that most of the subjects could finish the whole run in the FIX presentation and the deviation of sled velocity is lower than that in the DK presentation. This confirmed what we found in the earth-vertical rotation (Huang and Young, 1981). As compared to the DK presentation, the stationary central spot fixed in front of the subject may cause an illusion which is similar to the oculogyral illusion observed in rotation about an earth-vertical axis, and produced a lower threshold in the FIX presentation, although the fixed visual field tends to reduce reliance upon vestibular signals. After the experiment, two subjects mentioned that in the FIX presentation, they felt that the central spot was moving in the same direction as the sled motion.

4.3.2 Frequency Response.

The overall loop model of the velocity nulling task has already been given in Figure 4.1. As shown in section 2.4.2, the operator transfer function can be solved for in terms of the two measurable loop outputs, sled velocity and wheel deflection, if the operator's remnant is small with respect to the disturbance signal injected into the loop. However, each recorded signal (1024 x 12 for a whole run) contains spikes which may raise the noise level in the frequency domain. In order to get

rid of the spikes and to concentrate every signal to 1024 samples for running the FFT, a simple filter was used. For a whole run, this filter will first pick up every 12 samples, calculating the average and the standard deviation of these samples, then rejecting those samples which are above or below two standard deviations, and finally using the average value of the rest of the sample to represent these 12 samples. For a short run, i.e. the subject hit one end of the track before the end of the run, a smaller (less than 12) sample will be picked up and filtered. For each run, the samples which are rejected are about 7 percent for the sled tachometer signals and 4 percent for the wheel deflection signals. Finally, from the two filtered 1024 samples of sled velocity and wheel deflection signals, the describing function can be derived with the standard FFT algorithm and other techniques we described in section 2.4.2. The results are shown in Figures 4.5 through 4.12. A simple lag-lead transfer function with cascaded dead time is also used to fit the data and is plotted as the solid curve in each figure. The particular parameter values (except the dead time constant) displayed in each figure were obtained from a non-linear regression program which provides the least-squares parameter fit to the amplitude ratio data. The value of the dead time constant was used to provide a manual fit to the phase data, while holding fixed the other parameters gained from the previous computation. The discrepancy between the model prediction and the phase data at the low frequency range, may be caused by involving a subjective position nulling instead of velocity nulling. The major findings may be summarized in a schematic fashion as shown in Figure 4.13, which shows the four amplitude

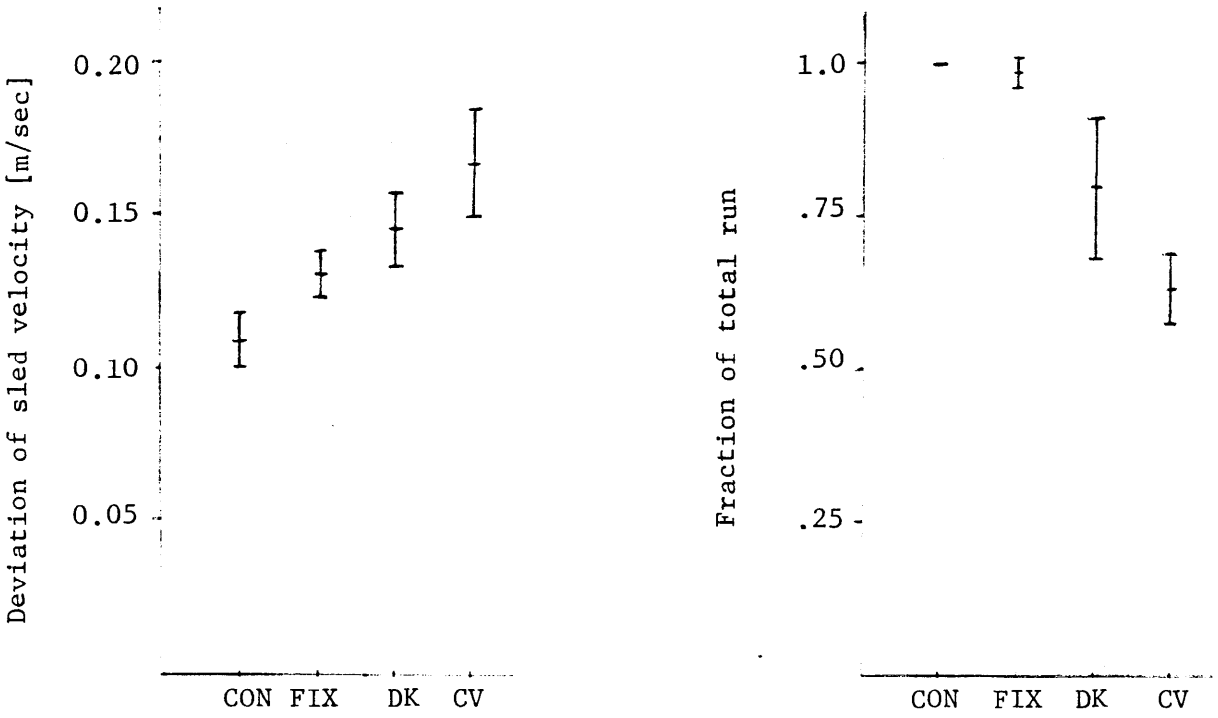

Figure 4.4: Performance of the single input nulling task.

ratio asymptotes, and Figure 4.14, which shows the parameter dependence on the type of visual field cue presented to the subject during the nulling task. The results suggested that the DC gain drops significantly (t-test, $p < 0.05$) when going from a CON presentation to a FIX presentation and from a FIX presentation to a CV presentation. The low freqquency visual cues dominate the low frequency sensation up to about 0.08 Hz. It also showed that the DC gain in a FIX presentation is significantly higher than that in the DK presentation. As we discussed in the last section, since the visual field is fixed relative to the subject, and might imply "no motion" or null signal, it conflicts with the true motion sensed by the otolith organs and might be expected to inhibit the motion sensation. However, the higher gain found here suggests the fixed visual input enhances the sensitivity to self-motion again, and we attribute the enhancement to the sensitive motion detection associated with the relative motion of a fixed foveal spot during subject linear motion.

4.4 Estimator Describing Function

In the previous section, describing function data, relating subject compensatory wheel deflection to actual sled velocity, is shown to be usefully described by a simple lag-lead function with cascaded dead time, whose parameter depend on the type of visual field cue presented to the subject during the nulling task. The object of this section is to derive a linear model for the self-velocity estimator, which is mainly represented by the otolith organs, from the describing function found in the

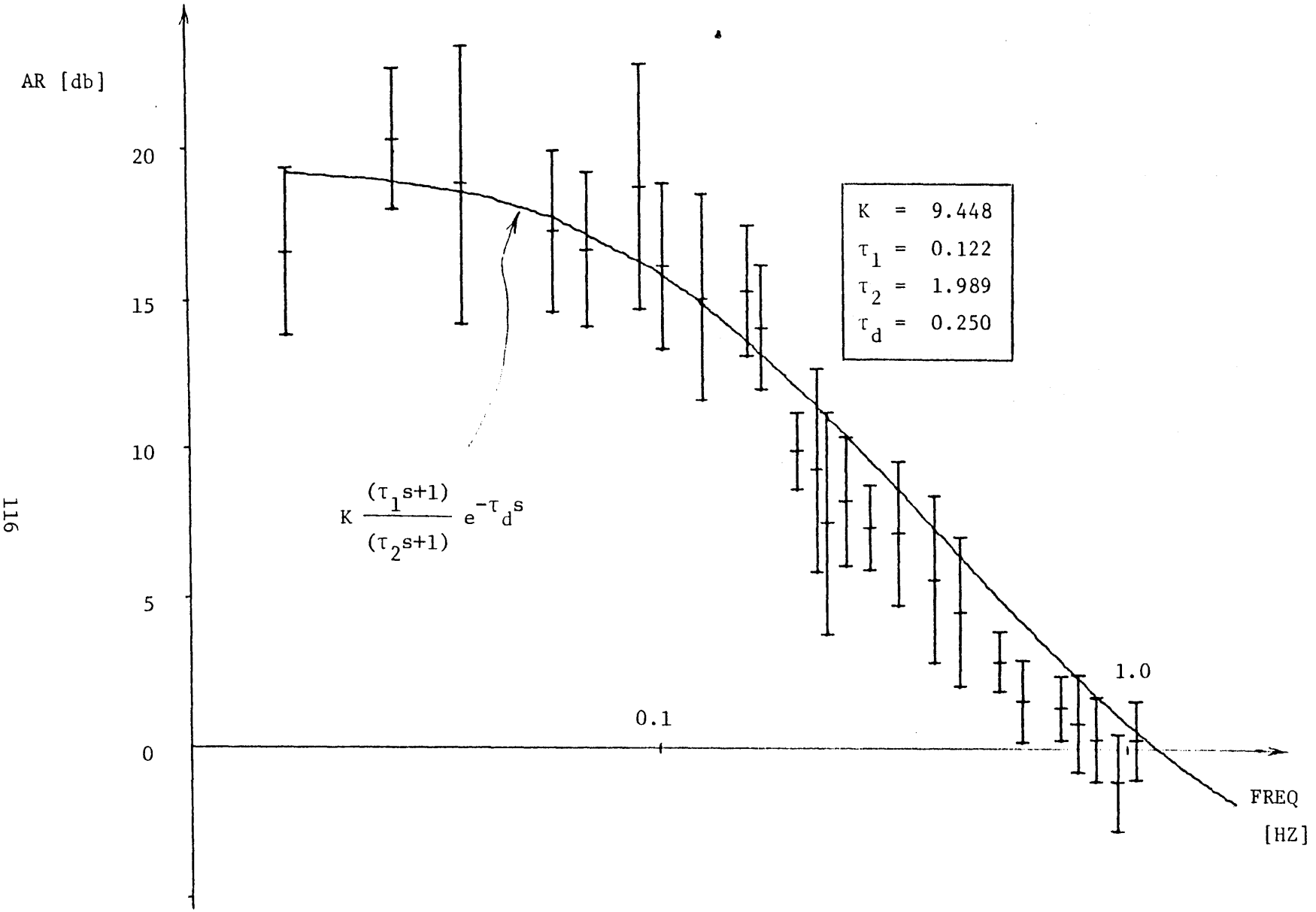

Figure 4.5: Amplitude ratio data for CON presentation

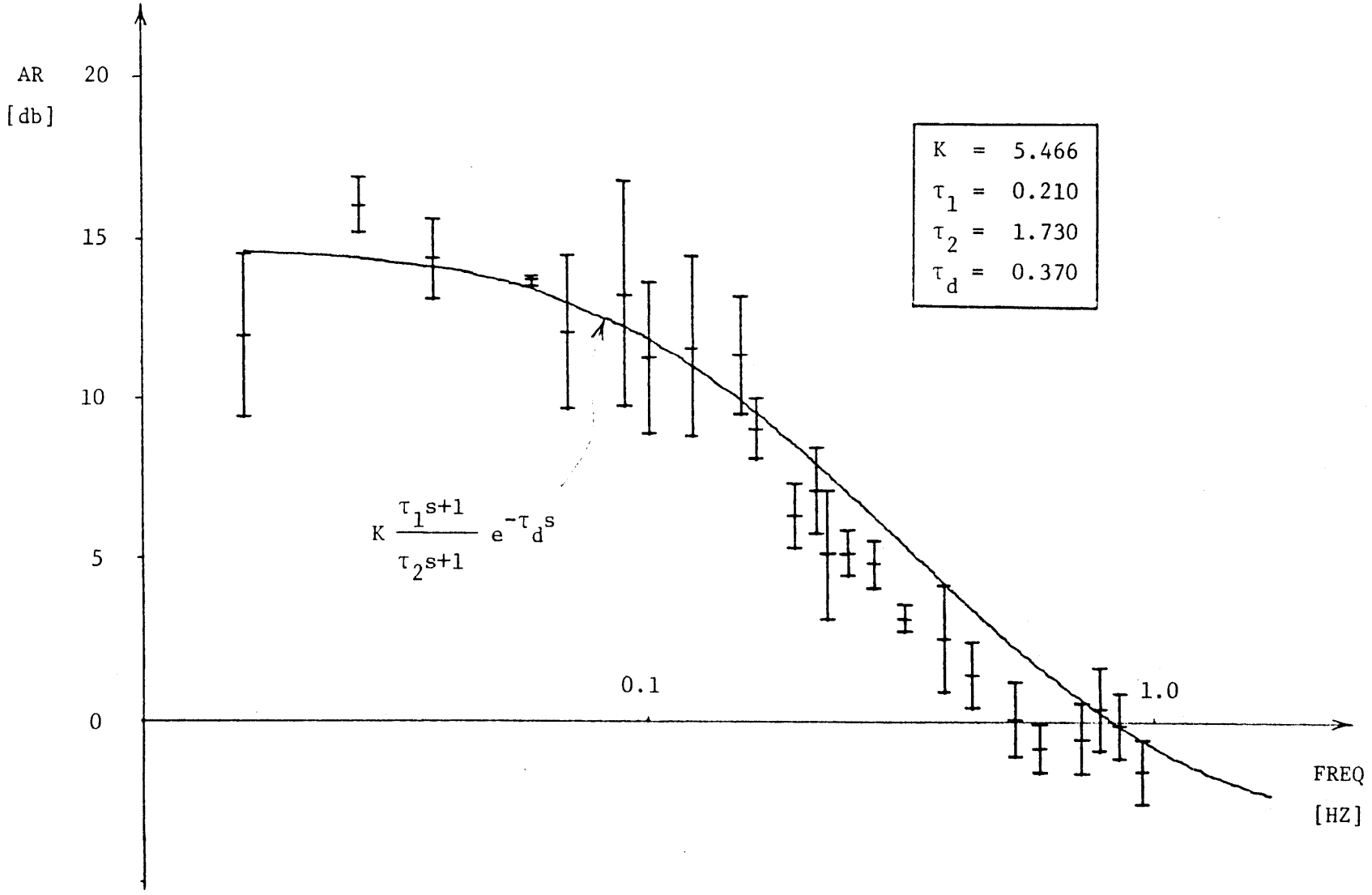

Figure 4.6: Amplitude ratio data for FIX presentation

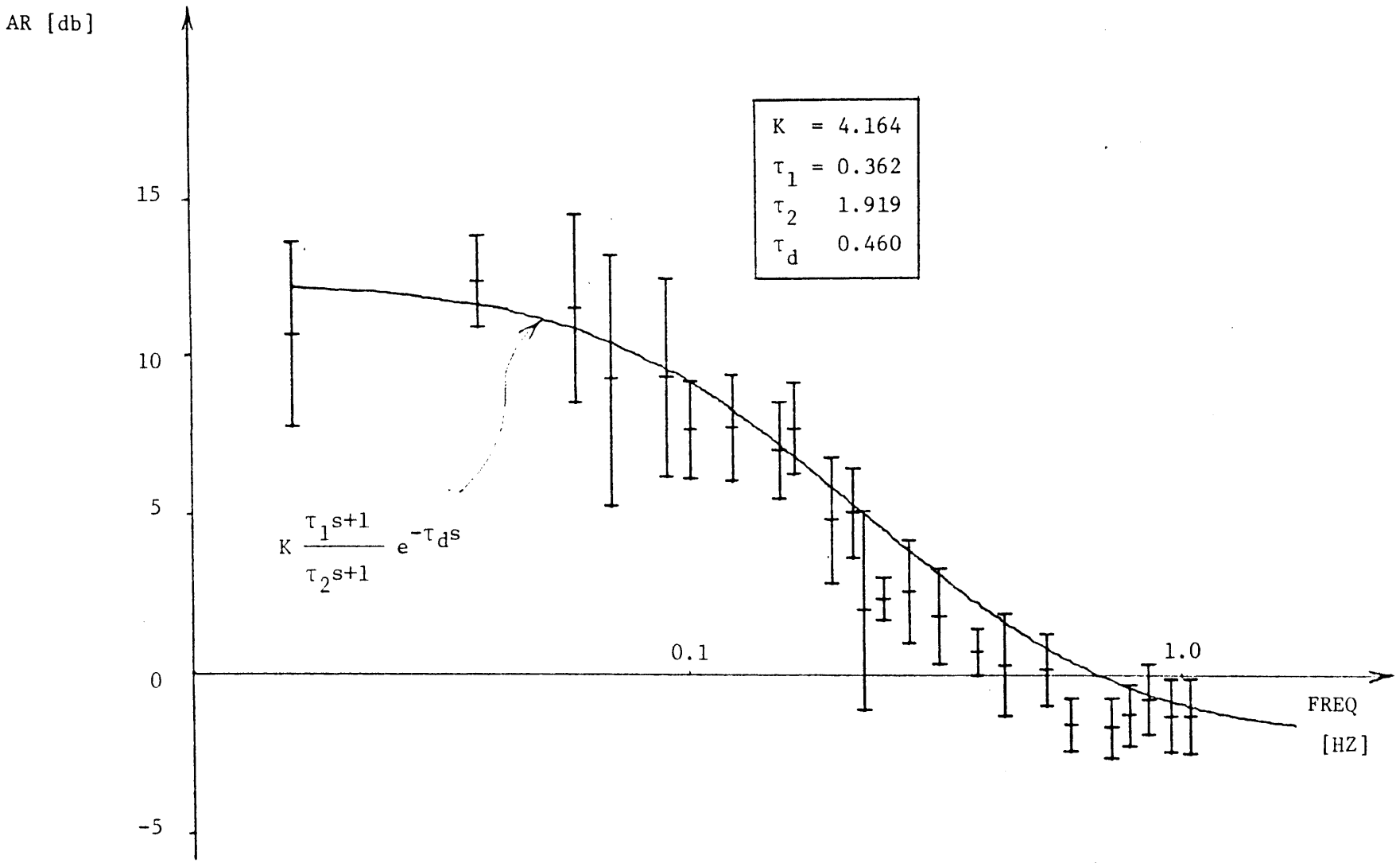

Figure 4.7: Amplitude ratio data for DK presentation

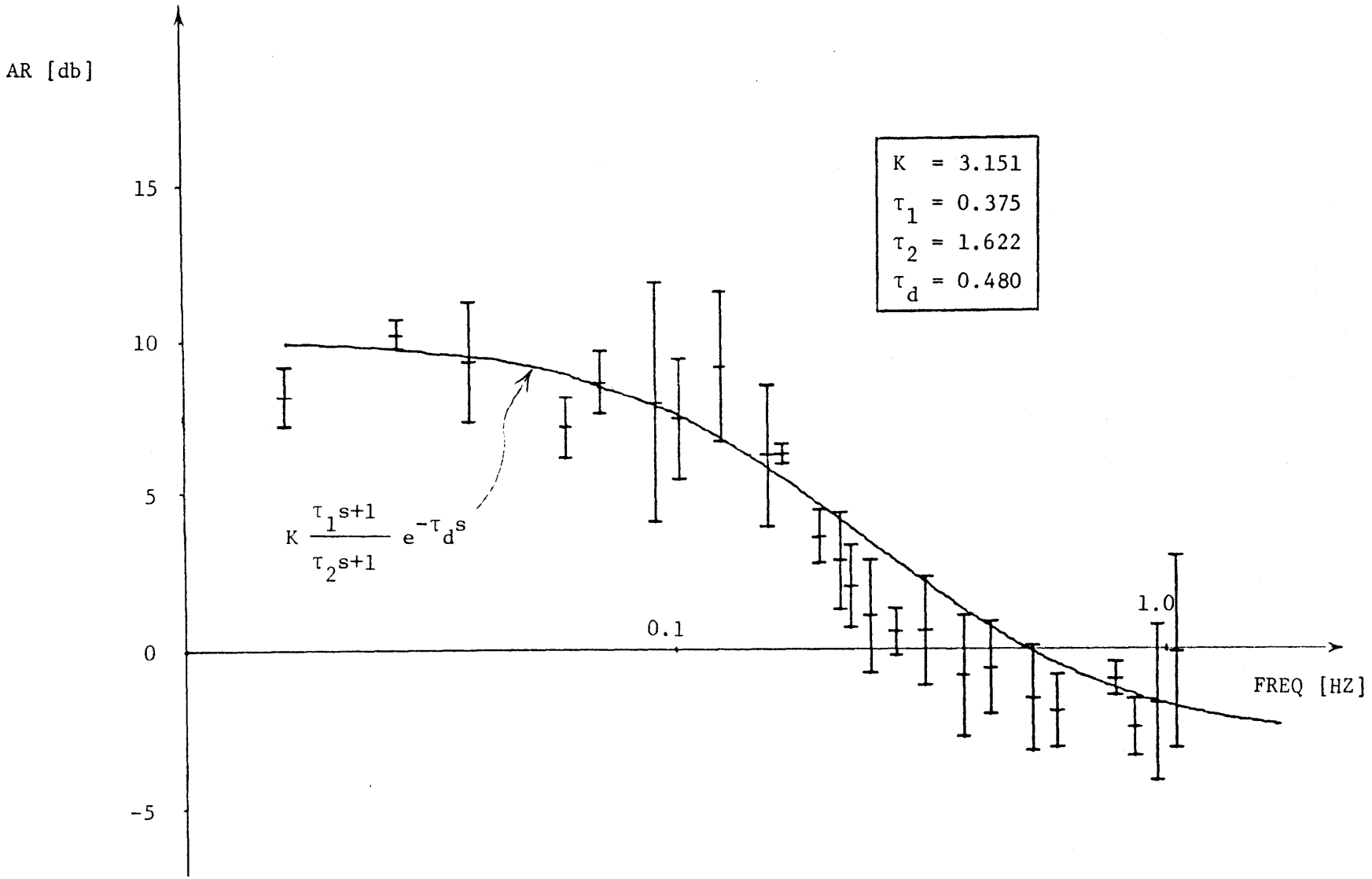

Figure 4.8: Amplitude ratio data for CV presentation

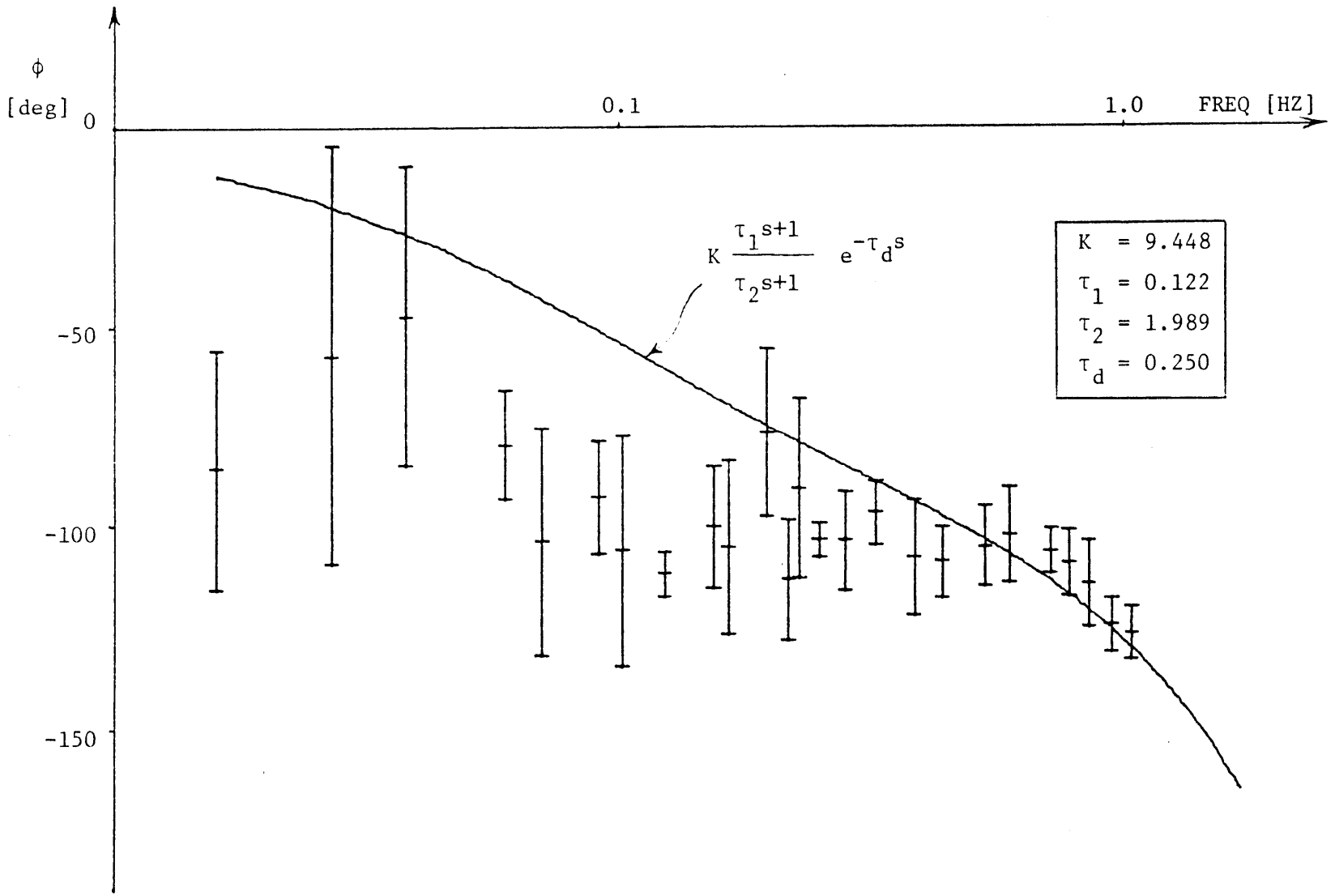

Figure 4.9: Phase data for CON presentation

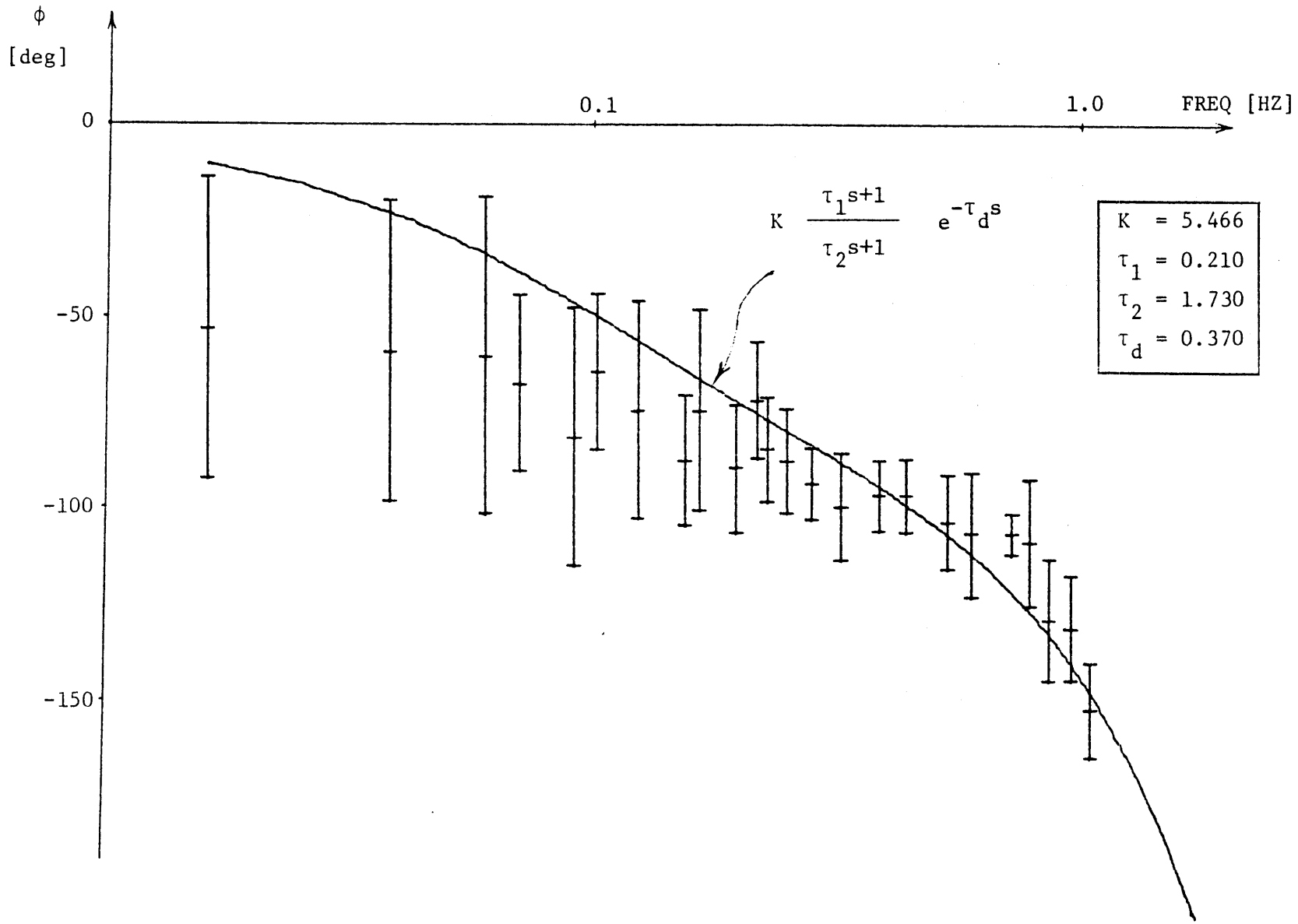

Figure 4.10: Phase data for FIX presentation

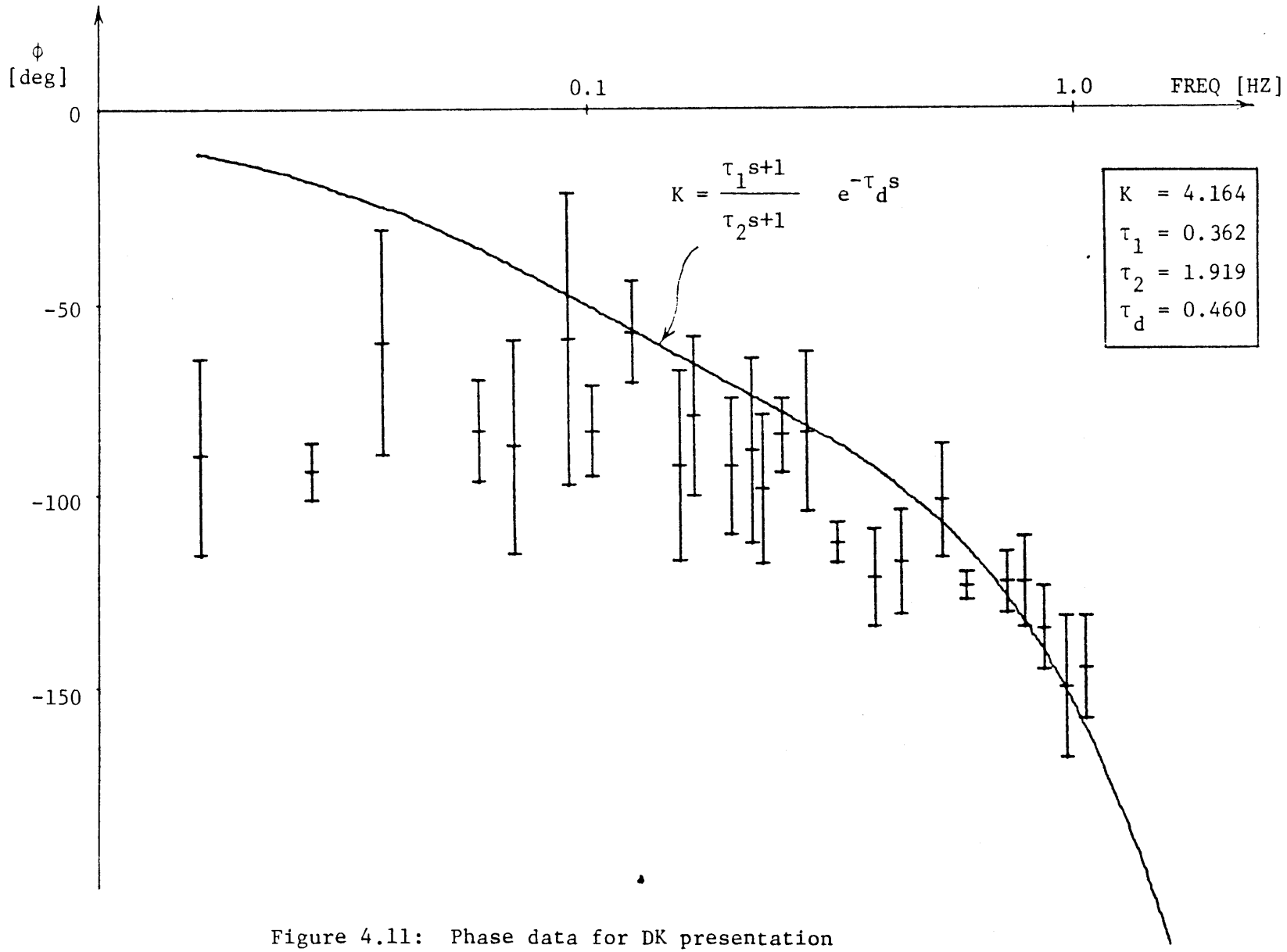

Figure 4.11: Phase data for DK presentation

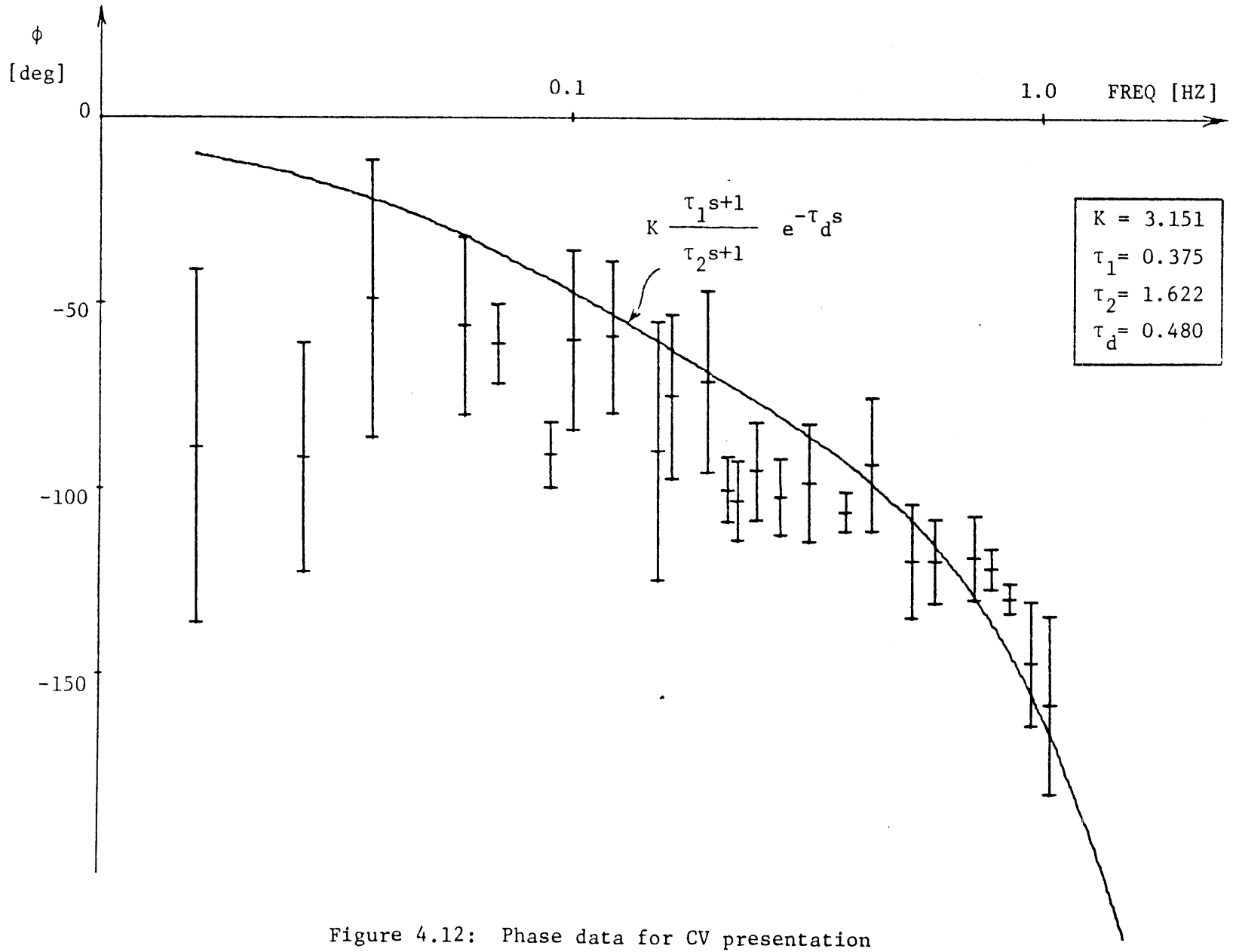

Figure 4.12: Phase data for CV presentation

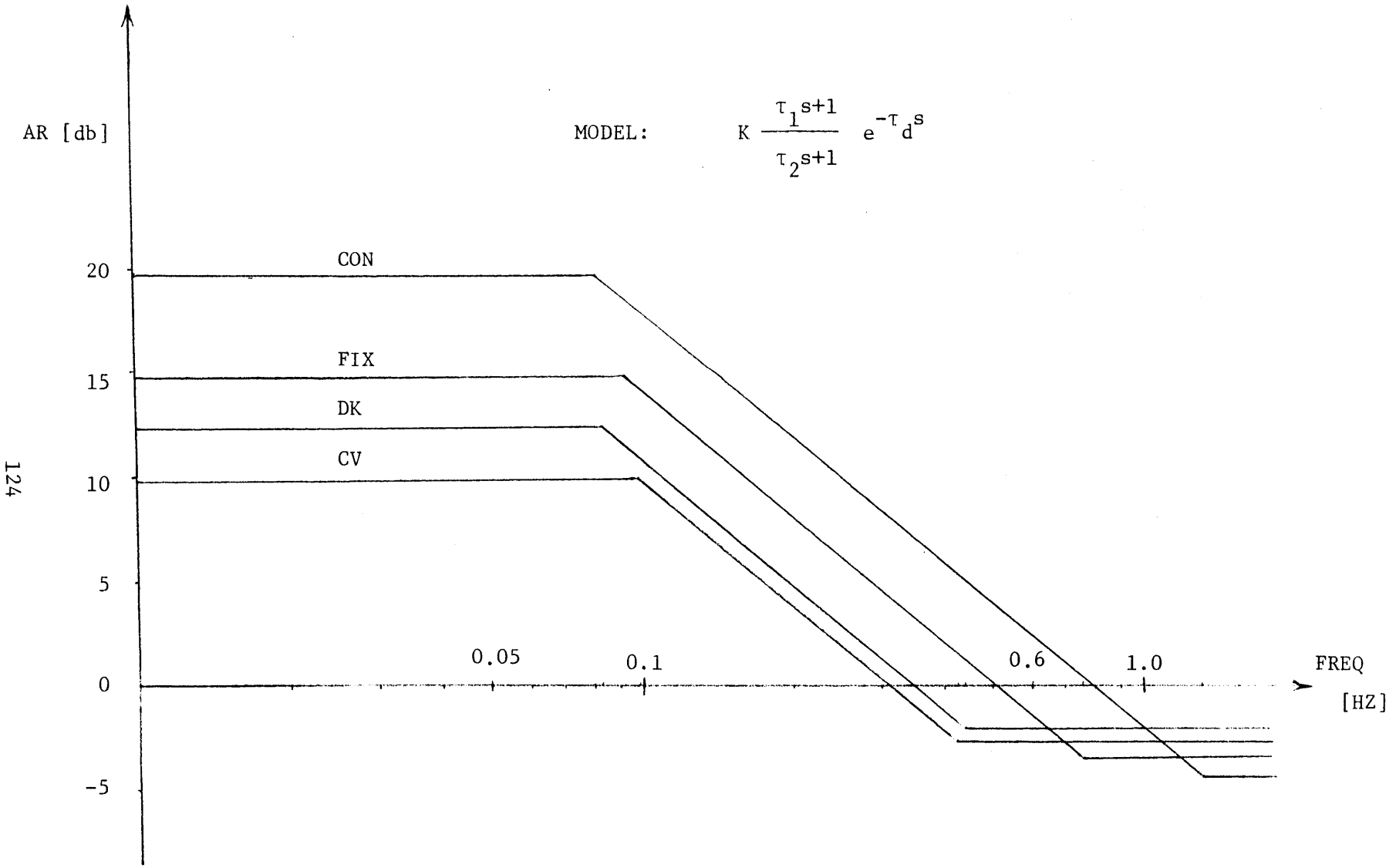

Figure 4.13: Amplitude ratio asymptote for CON, FIX, DK and CV presentations in sled experiment

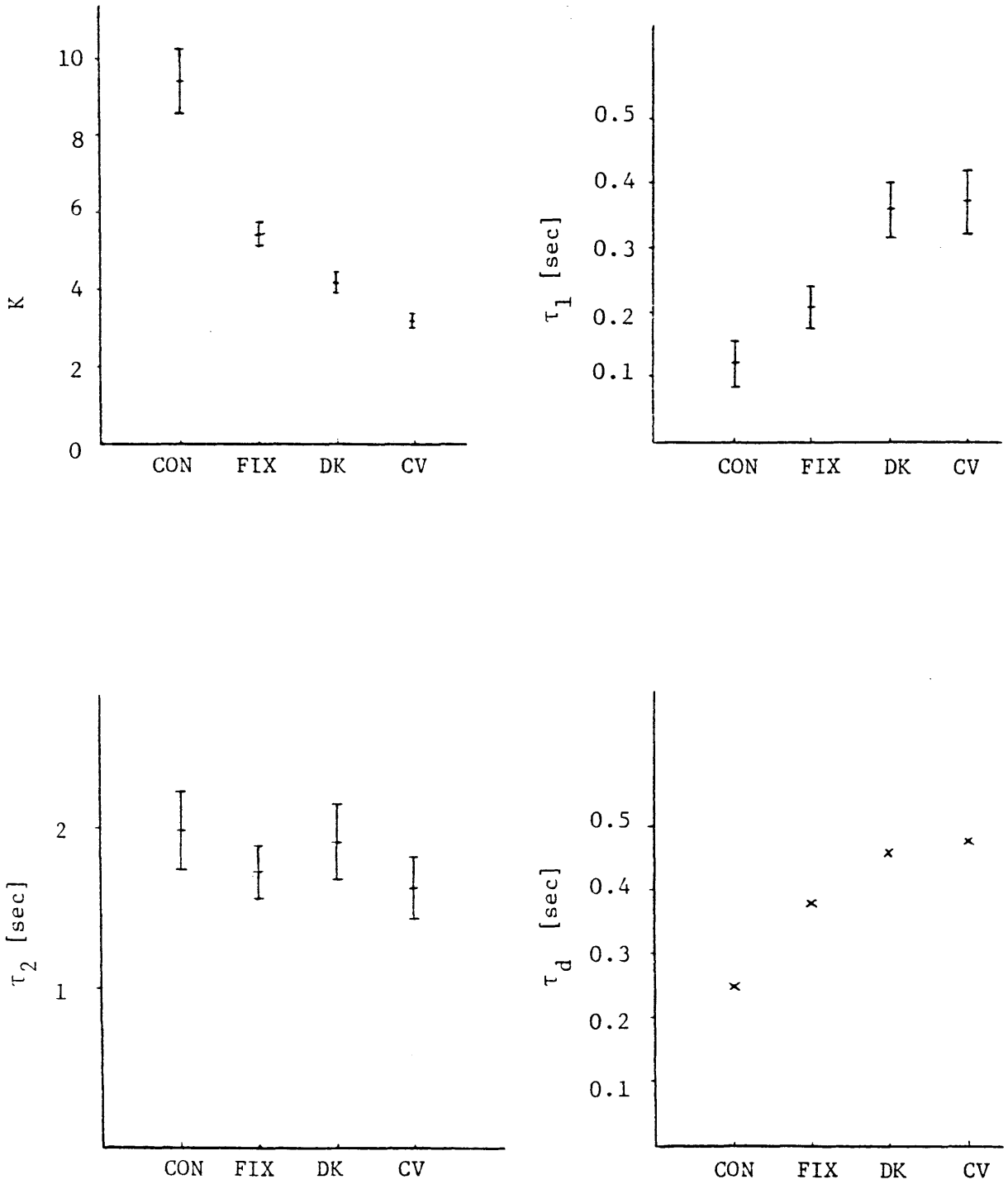

Figure 4.14: Parameter dependence on visual field type in sled experiment

frequency domain. In the FIX presentation, although a stationary visual surround may imply null visual cues, the central fixed spot provided some more sensitive visual cues. Therefore, in order to make sure that only the vestibular estimator was involved in the perception of self-motion, the describing function found in the darkness is chosen for further estimator modelling work.

Although the closed-loop nulling task can avoid the possible pitfalls of using subjective magnitude estimation to measure motion sensation, a drawback is that the tracking or manual control dynamics of the human operator are embedded in the results (Zacharias and Young, 1981). This motivated the design of another experiment aimed at determining the control strategy (Figure 4.1) under conditions functionally similar to those used in the previous experiments, so that its effect could be divided out of the results obtained already.

A brief description of the design of this experiment is given in the next section, which also presents the resulting measured operator control dynamics to be used shortly in deriving the estimator response functions.

4.4.1 Human Operator Dynamics

4.4.1.1 Experimental Design

Zacharias and Young (1981) measured the operator behavior in nulling the horizontal velocity of a projected stripe pattern on the translucent front window of the stationary trainer described in the pitch experiment.

Here, we would also like to measure the operator dynamics for each subject so that we can derive the estimator describing function on an individual-by-individual basis. The same experimental approach was used, although the visual field was changed. Instead of nulling the moving stripes, the subject, seated stationary in front of the sled, was given the task of nulling the sled velocity by using the control wheel to compensate for the disturbance signal injected into the sled.

Figure 4.15 is a block diagram of this nulling task, with the subject represented as a linear operator with remnant. The input disturbance and the plant dynamics are the same as in the previous experiment (Figure 4.1). However, because the subject is seated stationary in the lab, no visually or vestibularly induced sensations of self-motion are generated by this arrangement. It is presumed that the internal visual field velocity estimator is fast with respect to the motion sensation dynamics we were trying to investigate before and hence can be represented by a unity gain. The task of nulling the perceived sled velocity is similar to what we used in the previous experiment, although a different estimator is involved. From the comparison made above, it seems reasonable to assume an identity between the control logic of the two experiments.

4.4.1.2 Experimental Results

The same five subjects participated in this experiment for two full runs. For each run, Fast Fourier Transforms were performed on the sled

velocity and wheel deflection in a manner completely paralleling the input-output analysis used in Section 4.3.2. Figures 4.16a and 4.16b show the five-subject average Bode plots with one-sigma deviations indicated by error bars. Also shown is a least squares fit to the gain data of a simple integrator with lead. The dead time τ_d was calculated from the phase data based on the fitted gain function. The same model (with $K = 1.80$, $\tau = 0.45$), which provided a least squares fit to the data found by Zacharias and Young (1981), is also plotted for comparison. These two curves are comparable in their phase and show a slight shift in amplitude ratio. This small difference may be caused by the different plant dynamics and the visual field involved. In our experiment, a richer visual field was provided, as the subject could see the entire laboratory. In the other case, the subject was seated in the small Link trainer and the visual field was presented only on the front window.

4.4.2 Linear Estimator Calculation

Since the same five subjects participated in both the self-velocity nulling experiment and the visual field velocity-nulling task just described, the estimator describing function can be obtained by adjusting the describing function data found in the dark presentation with the human operator dynamics. Specifically, for each individual, at each test frequency common to the two experiments, the overall describing function gains can be divided by the operator gains and their phases subtracted, to infer the appropriate estimator function gain and phase. The results are shown in Figures 4.17a and 4.17b. At first glance, the data showed that

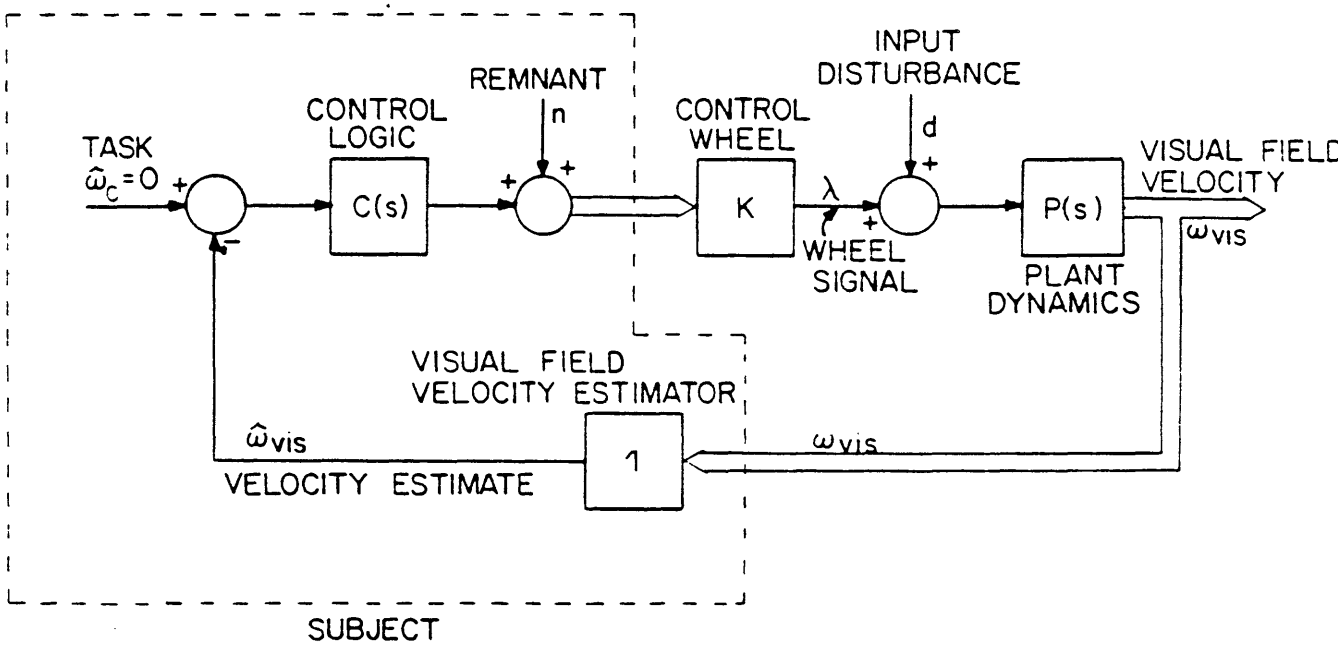

Figure 4.15: Visual field velocity nulling task (from Zacharias and Young (1981)).

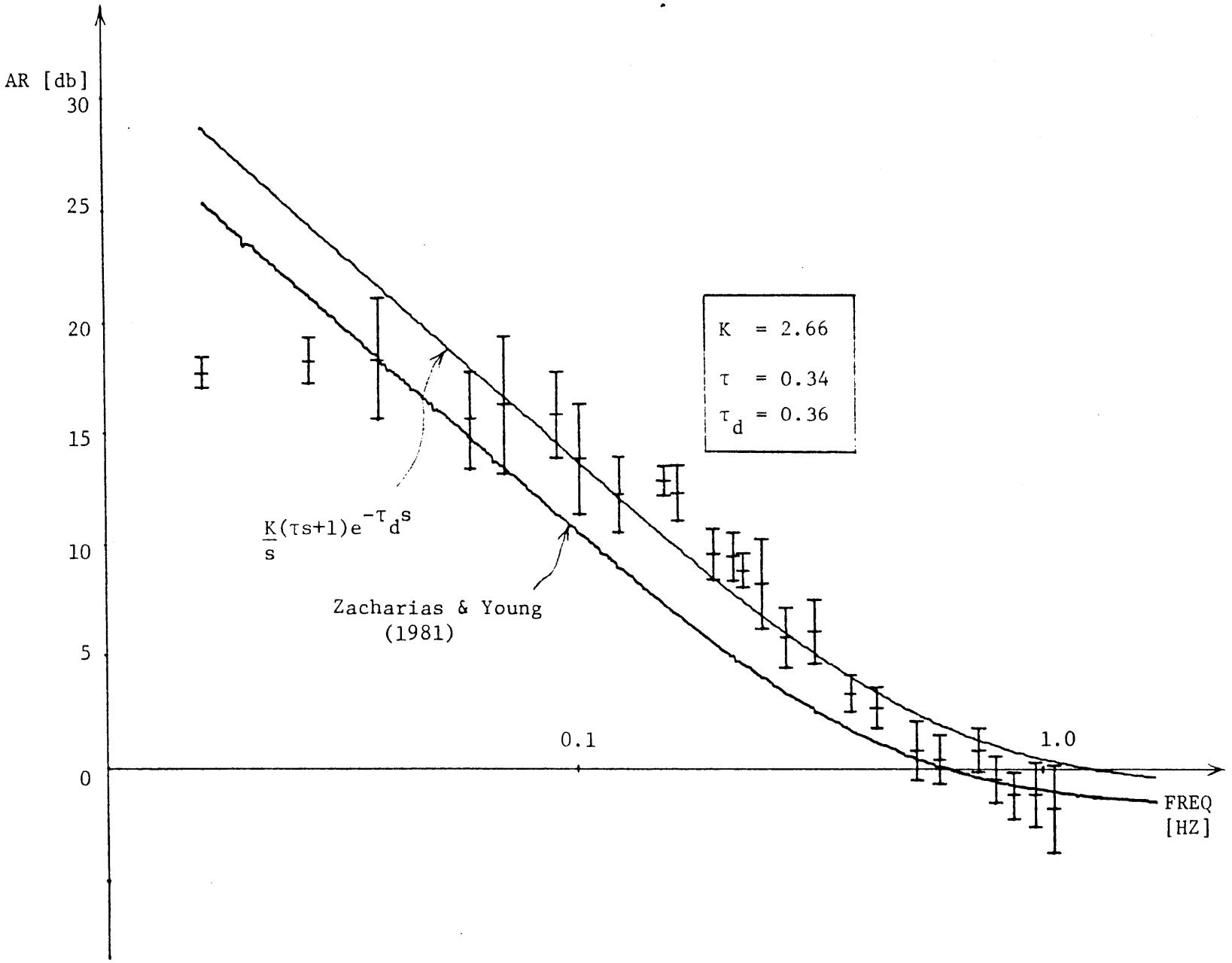

Figure 4.16a: Amplitude ratio data for visual field velocity nulling task

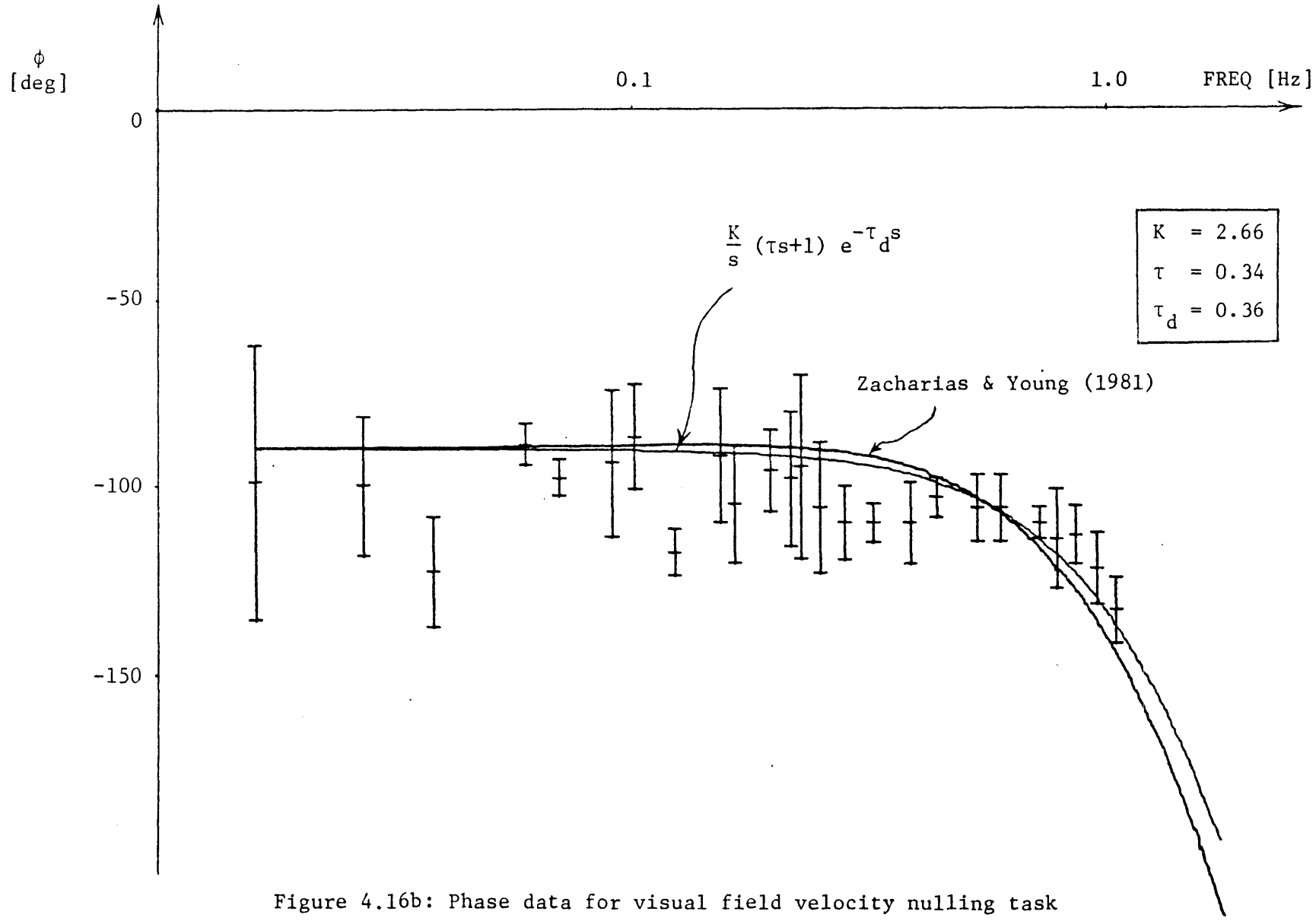

Figure 4.16b: Phase data for visual field velocity nulling task

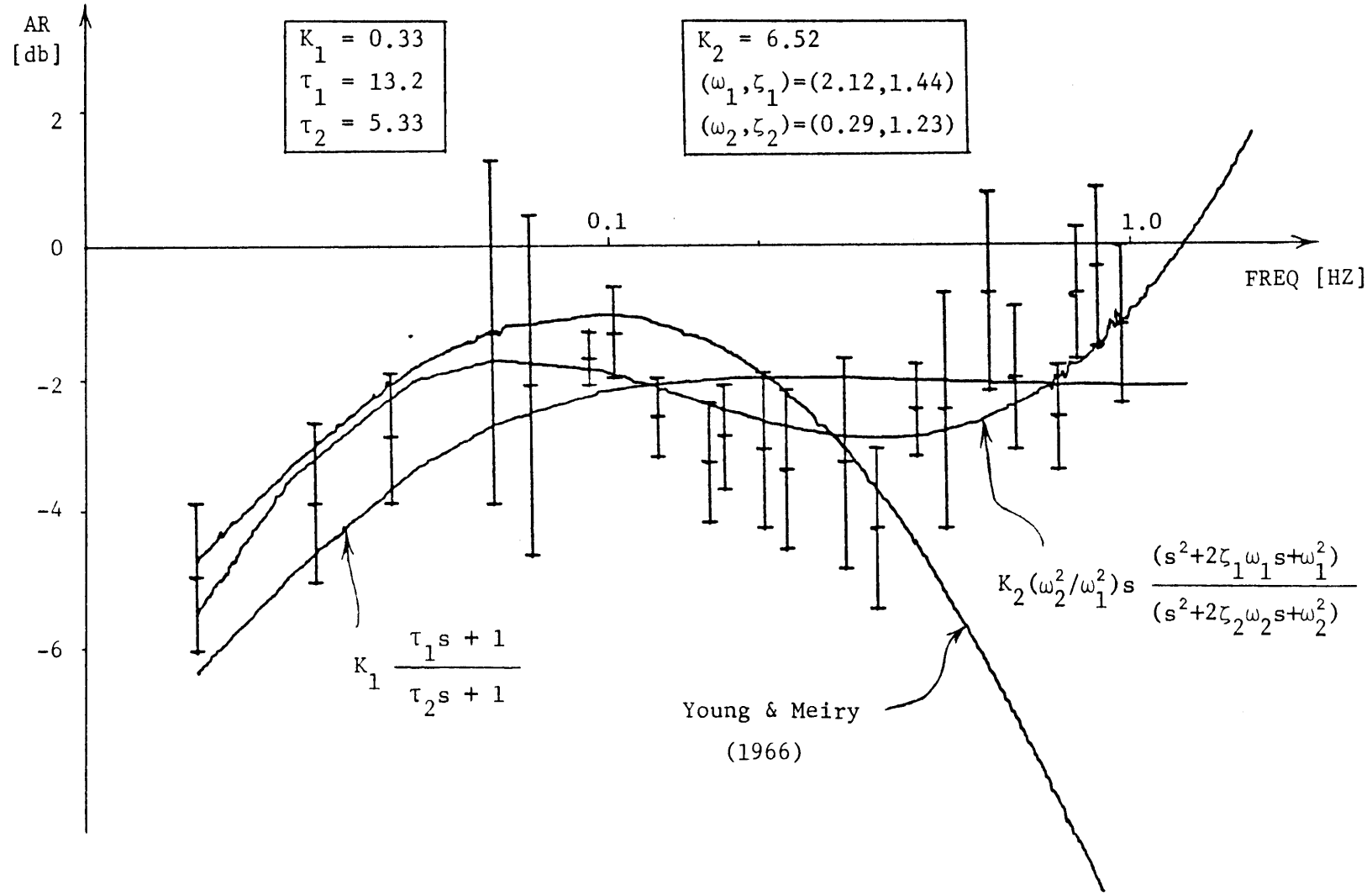

Figure 4.17a: Amplitude ratio data for estimator describing function

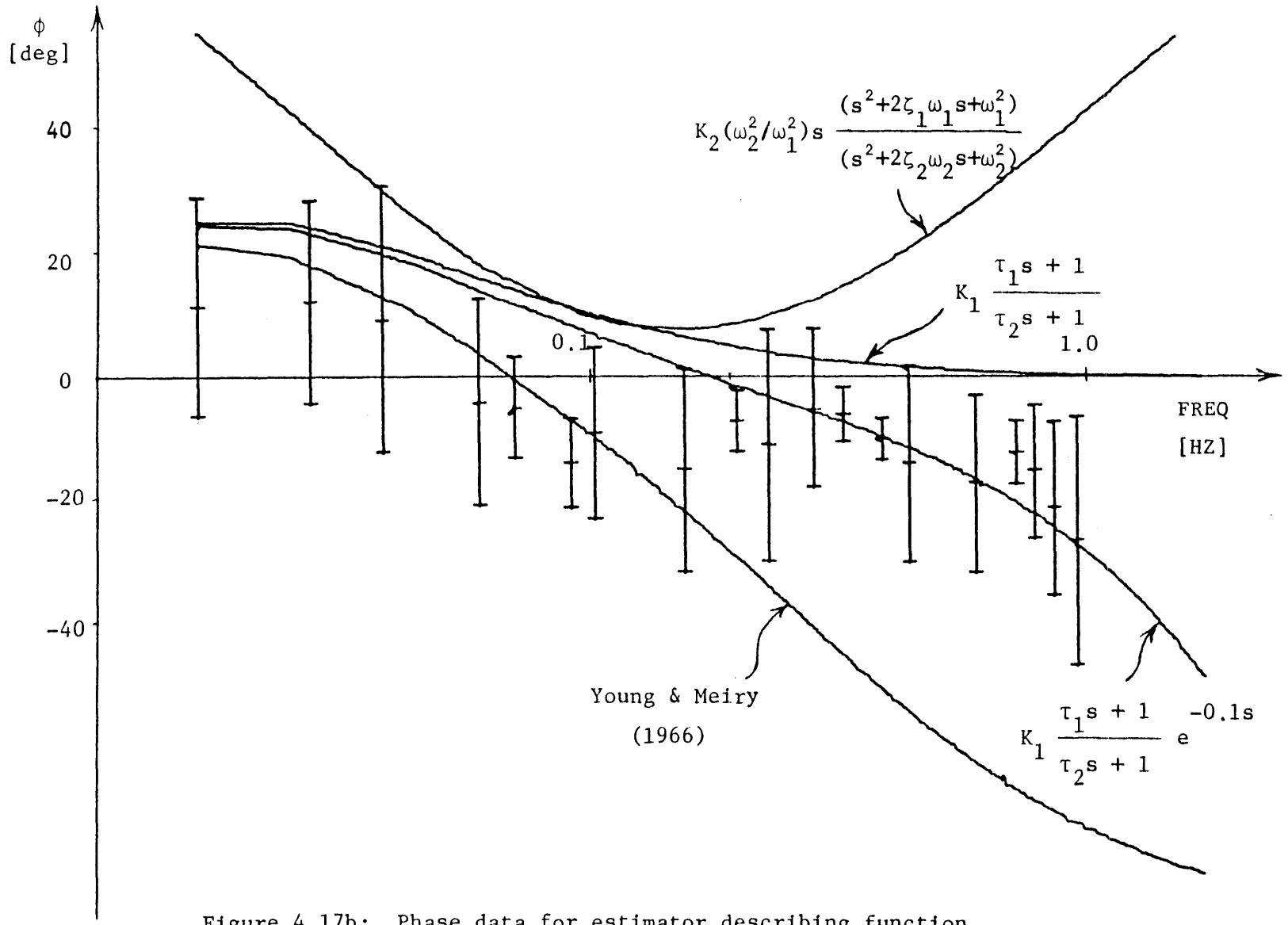

Figure 4.17b: Phase data for estimator describing function

there is a phase lead at low frequencies and a small phase lag at high frequencies. The amplitude ratio showed gain attenuation at the low frequencies and a gain increase at the high frequencies. As discussed in the introduction, a dynamic model of the otolith perception system (Young and Meiry, 1969) is first plotted for comparison:

$$E(s) = \frac{0.4\ (13.2s + 1)}{(5.33s + 1)(0.66s + 1)} \tag{4.1}$$

The model seems to provide a good fit to the data at low frequencies up to about 1 rad/s. However, over the high frequency range, the model predicts about 10 db and 90 degrees of roll-off, which contradicts our data. Because of this discrepancy, the use of other functional linear transfer functions, taking into account how well they fit both the gain and phase data, was considered.

The first transfer function we tried, in order to fit the data for all frequencies, was simply to add a lead term to the Young/Meiry model while allowing the gain to vary:

$$E(s) = K_1 \frac{(13.2s + 1)(\tau s + 1)}{(5.33s + 1)(0.66s + 1)} \tag{4.2}$$

As before, a non-linear regression program was used to generate least-squares parameter estimates. The results showed a lower gain of 0.33 and a lead time constant of 0.63 s, which is very closest one of the poles of the Young/Meiry model and hence resulted in the simplified lead-

lag model shown in Figure 4.17a. The phase data shown in Figure 4.17b suggested that a better fit might be obtained by adding a dead time delay of 0.1 s, which is the difference between the dead time delay shown in the overall describing function in the dark presentation (Figure 4.11) and that shown in the human operator dynamics (Figure 4.16b).

Next, a higher order transfer function was fitted to the amplitude ratio data in an effort to see if a significant reduction in the fit error could be achieved. From Figure 4.17a, a gain attenuation at low frequencies, a gain increase at high frequencies, and a gain decrease at the intermediate frequencies suggests that the fit could be improved by the addition of a low-frequency washout term and a high-frequency lead term to the lag-lead transfer function. The resulting model is:

$$E(s) = K_2\left(\frac{\tau_1 s}{\tau_1 s + 1}\right)\left(\frac{\tau_2 s + 1}{\tau_3 s + 1}\right)(\tau_4 s + 1) \qquad (4.3)$$

Because this fitting function constrained the solution to real poles and zeros, it may result in numerical problems in the search algorithm of the non-linear regression program we used before. To overcome this problem, the transfer function was respecified in a more general format, allowing for complex pole allocation:

$$E(s) = K_2(\omega_2^2/\omega_1^2)\; s\; \frac{(s^2 + 2\xi_1\omega_1\, s + \omega_1^2)}{(s^2 + 2\xi_2\omega_2\, s + \omega_2^2)} \qquad (4.4)$$

The results are also plotted in Figure 4.17a. As compared to the lead-lag model, the RMS residual value is dropped from 3.27 to 2.56, which represents an approximate 20 percent improvement. However, the phase data showed a large mismatch, especially at low frequencies, which cannot be corrected by just adding a dead time delay to the model. Some other transfer function might be used to provide a better fit for both the gain and phase data. However, the simple lead-lag transfer function cascaded with a dead time delay seems to provide a reasonable fit to the data and a good representation of the significance of the data as compared to the Young/Meiry model. As a result, from this model, the estimator data showed good agreement with the Young/Meiry model when a lead term with break frequency around 1.5 rad/s was added. The cause of this lead term is still unclear and needs justification.

4.5 Dual-Input Experiment

The object of this section is to show how the modelling effort in the previous section can be extended to an investigation of the dynamic response to a wider spectrum of visual cues. Based on the same approach used in yaw motion (Zacharias and Young, 1981), a further experiment was performed with time-varying visual stimuli in order to develop a human operator dual-input describing function which adequately models a subject's sensation in response to combined visual and vestibular linear motion cues. A brief experimental description and the results are given in the following sections.

4.5.1 Experimental Design

Figure 4.18 shows a functional block diagram of this experiment, with the same type of schematic model of the human operator introduced earlier. The same sled velocity nulling task was given to the subject. However, his control now determined field velocity as well as sled velocity. Two uncorrelated disturbances with no common frequencies were injected into the sled and projector drives, respectively, requiring constant compensation by the subject. Because simultaneous nulling of both cues becomes an unattainable task objective, the resulting analysis will be based on whichever portion of the cue the subject chooses to null. The sign of the wheel signal is arranged so that left wheel deflection results in left sled motion and a corresponding right field motion. Thus, without a visual field disturbance, the experiment is functionally equivalent to the countermotion (CON) series conducted earlier.

The disturbance signals injected into the sled and projector drive loops are generated by the PDP-11 as before. Each disturbance signal is a pseudo-random zero mean signal with a period of 184.32 seconds, consisting of a sum of 12 sinusoids spanning the frequency range from approximately 0.1 to 1.0 Hz. Each frequency component is an integral prime multiple of a base frequency of 0.0054 Hz with the alternating primes of an ascending series for these two signals. This interleaving of the two line spectra assures a zero correlation between the two disturbances. A second order shaping filter to approximate a smooth power spectral density function of the form shown in Equation 4.1 is also used, with poles at 0.28 Hz. A

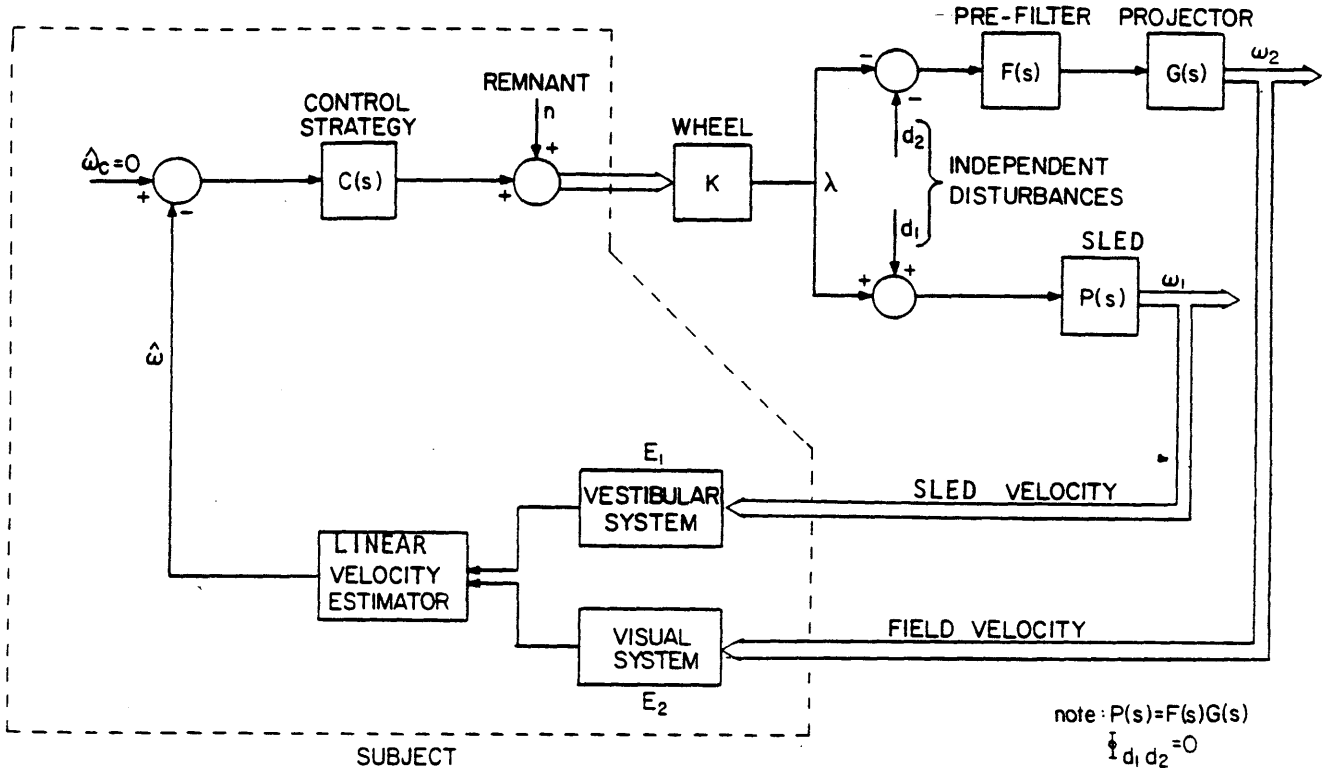

Figure 4.18: Dual input velocity nulling task

(modified from Zacharias and Young (1981)).

summary of the vestibular and visual disturbances are listed in Tables 4.2a and 4.2b respectively. Time histories of the disturbances are shown in Figure 4.19.

Finally, since the projector dynamics are quite the same as the sled response in the tested frequency range, a prefilter F, which is added to the projector drive G, shown in Figure 4.18, is not required.

4.5.2 Experimental Protocol

The same five subjects who participated in the previous sled experiments took part in the current dual-input nulling task. Each subject was instructed to perform the same velocity nulling task and specifically told to keep the sled as motionless as possible by concentrating on his own sensation motion and by providing the appropriate compensatory control wheel deflections. It was also mentioned that the task might become more difficult than in the previous experiments, and if this happened, to simply concentrate more strongly on the sense of self motion and compensate accordingly. Before the experiment, with the control wheel disabled, the disturbance signal was injected into the sled so that the subject, first standing outside the sled and then seated inside, could obtain some estimate of the amplitude and frequency content of the signal he would be asked to null. The subject was seated in the sled, the safety belt tightened, and the head restraint adjusted to fit his head. Then, without a disturbance input, the subject was asked to move the thumb wheel to

SUM OF SINES PROFILE

1.	DURATION OF PROFILE:	184.32 SEC
PARAMETERS OF SINUSOIDS:		
2.	NUMBER OF SINUSOIDS:	12
3.	FUNDAMENTAL FREQUENCY:	0.0054 HZ
4.	EQUAL AMPLITUDE DOMAIN:	0 (-1,P;0,V;+1,A)
5.	SUCCESSIVE PHASE ANGLE:	247. DEG
PARAMETERS OF SHAPING FUNCTION:		
6.	ORDER OF FILTER:	2
7.	POLE:	0.28 HZ
PHYSICAL CONSTRAINTS:		
8.	LENGTH OF TRACK	3.60 M
9.	ALLOWED ACCELERATION	0.41 G
10.	TIME INCREMENT:	0.015 SEC

RESULTING IN THE SUM OF SINUSOIDS:

FREQ [HZ]	AMP [M/S]	ACCEL AMP [G]	PHASE [DEG]
0.016	0.09	0.001	0.
0.038	0.12	0.003	247.
0.071	0.13	0.006	134.
0.103	0.14	0.009	22.
0.157	0.13	0.013	269.
0.201	0.11	0.014	156.
0.255	0.10	0.017	44.
0.331	0.10	0.020	291.
0.450	0.08	0.023	179.
0.613	0.06	0.023	67.
0.884	0.04	0.022	316.
1.242	0.02	0.019	206.

MAXIMUM ACCELERATION IN SIGNAL: 0.104 G
PERCENT USAGE OF TRACK: 100.00%
STARTING POSITION: 0.00

Table 4.2a: Vestibular disturbance used for dual input sled experiment.

SUM OF SINES PROFILE

1. DURATION OF PROFILE: 184.32 SEC

PARAMETERS OF SINUSOIDS:

2. NUMBER OF SINUSOIDS: 12
3. FUNDAMENTAL FREQUENCY: 0.0054 HZ
4. EQUAL AMPLITUDE DOMAIN: 0 (-1,P;0,V;+1,A)
5. SUCCESSIVE PHASE ANGLE: 247. DEG

PARAMETERS OF SHAPING FUNCTION:

6. ORDER OF FILTER: 2
7. POLE: 0.28 HZ

PHYSICAL CONSTRAINTS:

8. LENGTH OF TRACK 3.60 M
9. ALLOWED ACCELERATION 0.41 G
10. TIME INCREMENT: 0.015 SEC

RESULTING IN THE SUM OF SINUSOIDS:

FREQ [HZ]	AMP [M/S]	ACCEL AMP [G]	PHASE [DEG]
0.011	0.06	0.000	0.
0.027	0.09	0.002	247.
0.060	0.11	0.004	134.
0.092	0.10	0.006	21.
0.125	0.10	0.008	268.
0.168	0.10	0.011	155.
0.222	0.09	0.013	42.
0.288	0.08	0.016	290.
0.396	0.07	0.018	177.
0.548	0.05	0.019	64.
0.743	0.04	0.018	312.
1.080	0.02	0.017	200.

MAXIMUM ACCELERATION IN SIGNAL: 0.100 G
PERCENT USAGE OF TRACK: 100.00%
STARTING POSITION: 0.00

Table 4.2b: Visual field disturbance used for dual input sled experiment.

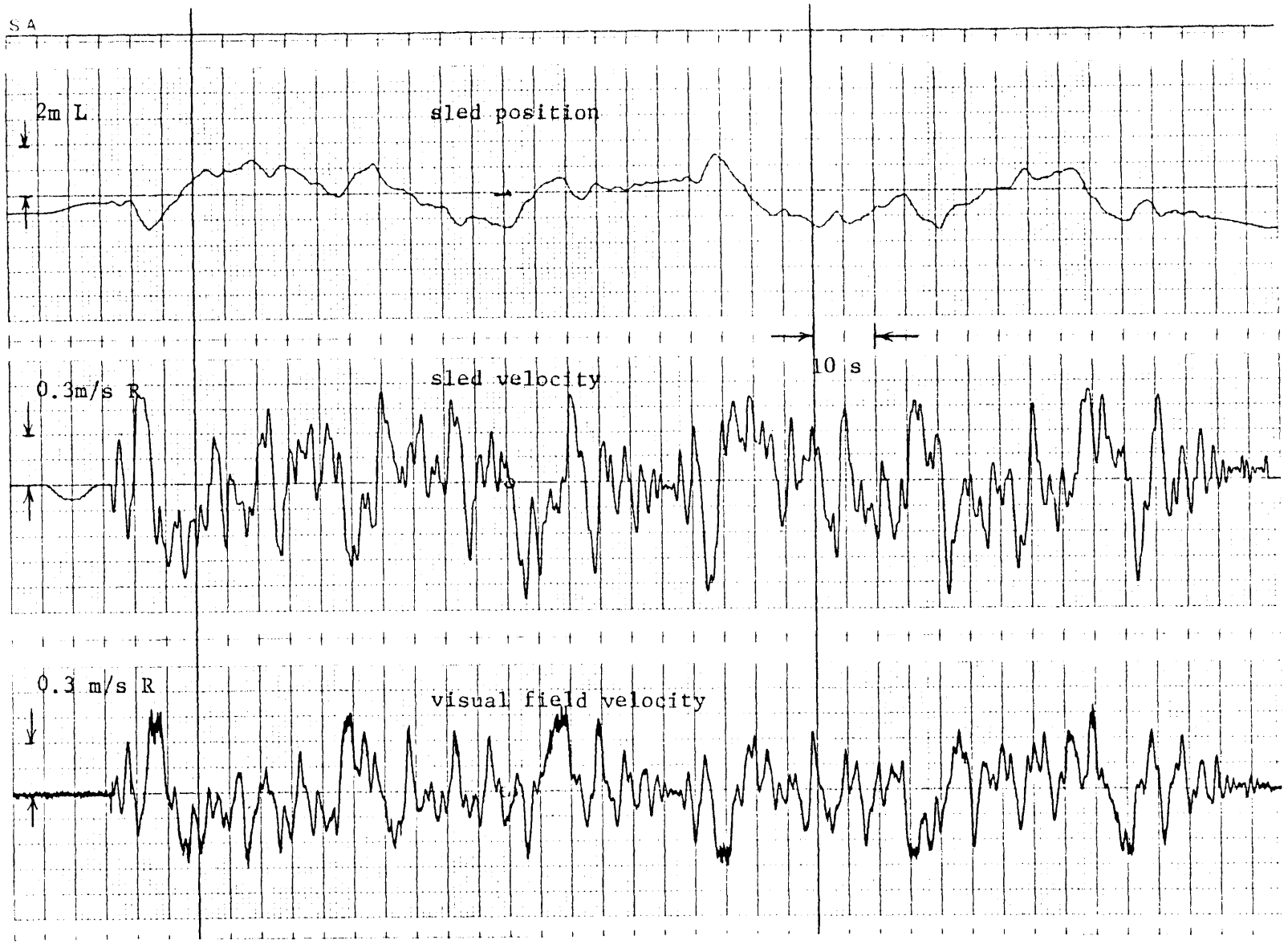

Figure 4.19: Disturbances used for dual input sled experiment

drive the sled so that he could see how well the wheel controlled the sled. During this time, white noise was provided through the headphones and the volume was adjusted to a comfortable level for the subject, assuring that the motor sounds from the sled were inaudible. Finally, the subject was given a practice run with his eyes open in the laboratory. Then, the subject was fitted with goggles which were adjusted so that only the full display could be seen.

The following experiment included four runs for each subject with two runs of each visual field. The visual field alternated between two modes: the countermotion mode (CON), which provides accurate cue confirmation, and the dual-input mode (DI), in which the visual field velocity was determined by adding the subject's wheel signal to the visual disturbance signal as illustrated in Figure 4.18. At the end of the experiment, each subject was questioned as to whether he may have been consciously using other cues besides motion sensation to null the sled velocity. None of the subjects felt that any other cues were available for inferring sled motion.

4.5.3 Experimental Results

4.5.3.1 Time Histories of Subject Response

Figure 4.20 shows a set of typical histories of the vestibular disturbance, visual disturbance, the subject's compensatory wheel deflection, the sled velocity and position, and the visual field velocity. The

subject seems to provide compensatory control mainly to the vestibular disturbance and in this figure it is hard to see whether the subject will null the low frequency portion of the visual field velocity disturbance because of its high variance. The statistical results of the subject's deviation of sled velocity show an average value of 0.127 m/s and one standard deviation of 0.016 m/s for the CON presentation, and an average value of 0.244 m/s and one standard deviation of 0.03 m/s for the dual-input nulling task. The former values are comparable to the previous results from the single input nulling task (Figure 4.4, CON presentation). However, the subject's deviation of sled velocity in the dual-input nulling task is doubled and even higher than that in the CV presentation (Figure 4.4). All the subjects could finish the whole run in the CON presentation, but only 58.4 percent (with one standard deviation of 19.8 percent) of the total run was finished in the dual-input nulling task. This indicates that the task in the dual-input experiment is harder and the performance of the subject is poorer than that shown in any other low frequency visual presentation.

4.5.3.2 Frequency Response

For each run, Fast Fourier Transforms were performed on the sled velocity and wheel deflection in a manner completely paralleling the input-output analysis used in Section 4.3.2. Figure 4.21 shows typical control wheel amplitude spectra in the dual-input nulling task right after the FFT processing. Circles show operator response at the test

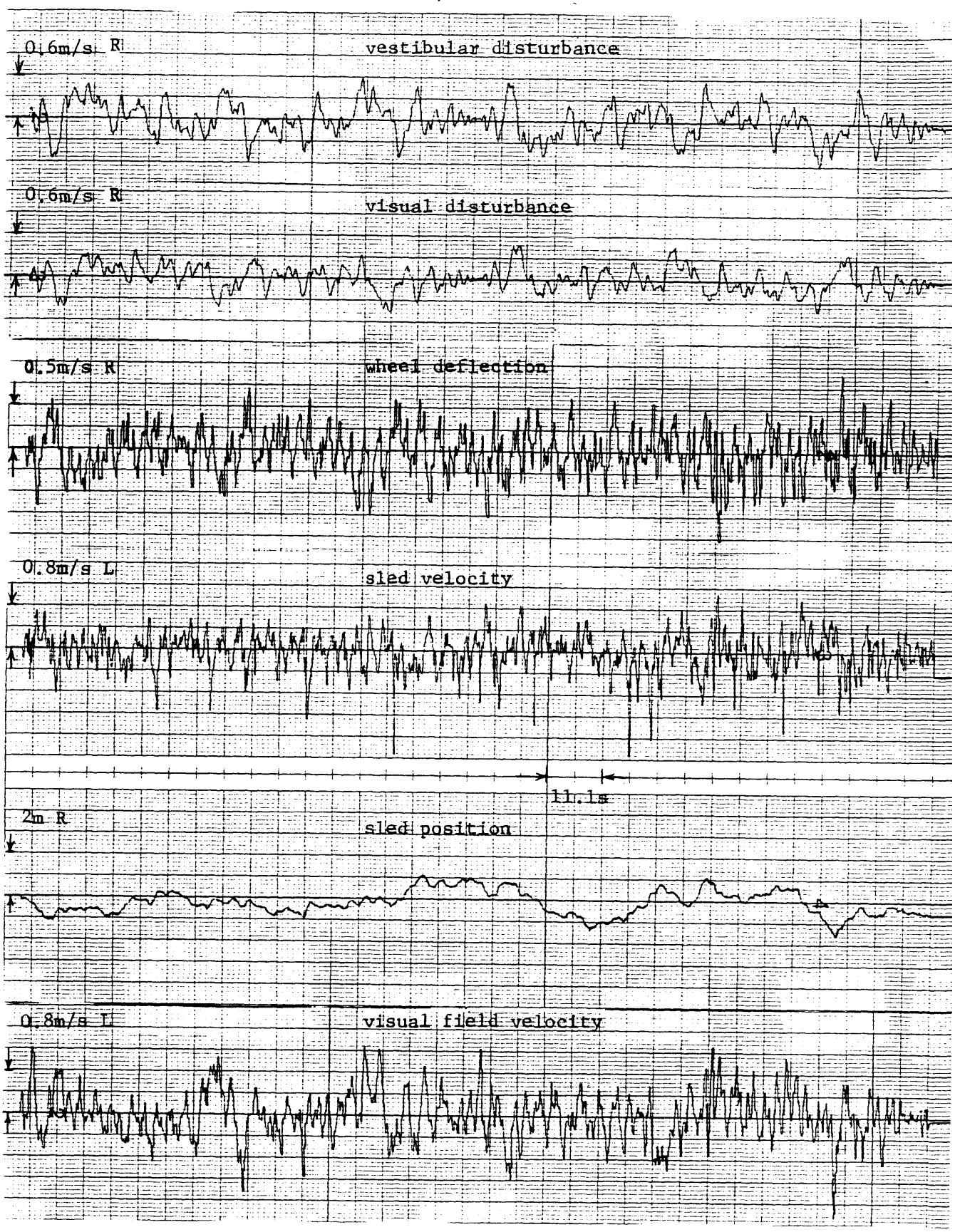

Figure 4.20: Dual input disturbance nulling in sled experiment

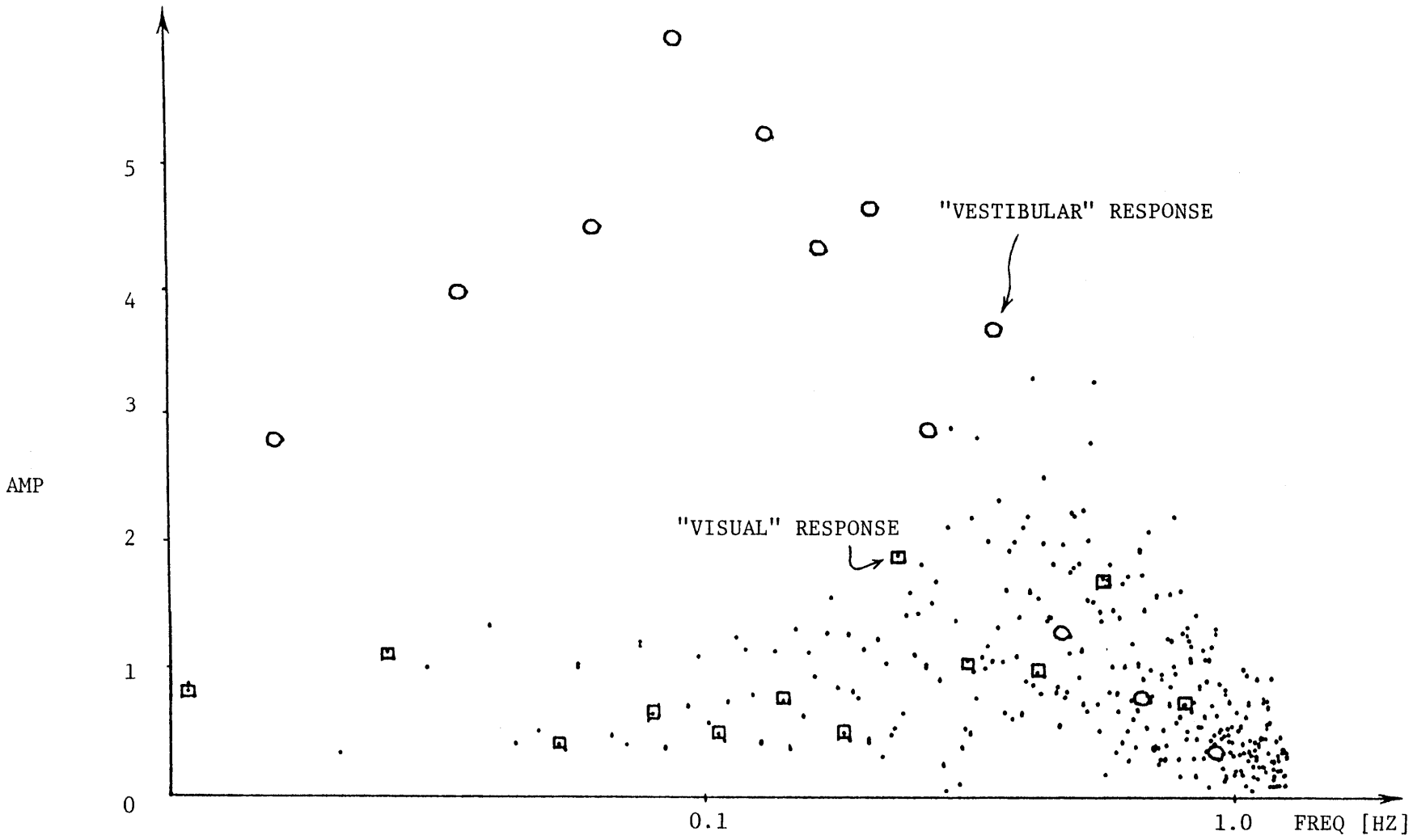

Figure 4.21: Control wheel amplitude spectra in sled experiment

disturbance frequencies contained in the vestibular disturbance and squares show response at the test disturbance frequencies contained in the visual disturbance. The dots indicate response power at all other frequencies which are multiples of the frequency window of 1/184.32 Hz. Although most of the vestibular responses are above the remnant level, most of the visual responses are below it. This infers that the subjects did not provide enough compensatory control over the visual disturbance, even in the low frequency range. Because the visual response is below the remnant level, we cannot derive the estimator of vestibular interaction model is precluded. However, this result must not be interpreted to limit the usefulness of full field visually induced motion in simulation, but is limited only to this experimental set up.

Finally, we perform two psychological tests on those subjects who participated in the sled experiment and comment on their results.

4.6 Field Dependence Tests of the Subjects

As discussed in Section 4.2.2, only five out of eleven subjects were trained successfully to perform the self-velocity nulling task. It may be implied that the perception of spatial orientation of these subjects were mainly based on their body cues rather than on the surrounding field. On the other hand, although no confirming visual cues were provided in the darkness (or when the subject closed his eyes), the subject could still perceive his self-velocity quite well through his body cues and hence

provide suitable compensatory wheel deflections without drifting the sled to the end of the track. This motivates a further study on the extend of field dependence of the subjects who participated in the sled experiment by using two psychological test, the rod and frame test (RFT) and the embedded figure test (EFT).

4.6.1 Background of the Test

Before stating the reasons for choosing the rod and frame (RFT) and the embedded figures test (EFT) in testing our hypothesis, the background of these two tests will be briefly reviewed. First, let us briefly describe what these two tests are. The RFT and EFT are two perceptual psychological tests that have been used for over twenty years (Witkin and Asch, 1948; Witkin, 1959; Witkin et al., 1971). Early on, Witkin and Asch (1948) conducted numerous spatial orientation studies investigating the role of the visual framework in the perception of the upright. This led to the revelation of individual differences and the role of personality factors in perception. In the fourth study of this series, they developed a rod and frame apparatus consisting of a square luminous frame with an adjustable rod mounted in the center. In a completely dark room, the tilting of the frame caused displacement of the visual field and the consequent setting of the rod enabled precise measurement of perception of the upright to be made. The score for the test was the average number of degrees by which the subject's setting of the rod deviated from the true upright position. Witkin then utilized an adaptation of the material used by Gottschaldt to further examine the manner in which individuals

perceived a part within a larger field. In this test (EFT), the subject's task on each trial is to locate a previously seen simple figure within a larger complex figure which has been so designed as to obscure or embed the sought-after simple figure. The subject's score for this embedded figures test was the average of the times taken to locate all the simple figures. In the strictest interpretation, therefore, scores on the EFT reflect the competence in perceptual embedding. Individual differences in EFT performance, however, appear to relate to more than a difference in perceptual functioning. The other test, which is not used here, is the body adjustment test (BAT), in which the subject is seated in a tilted position within a tilted room and must adjust his chair to a position where he perceives himself to be vertical, the room remaining tilted. The RFT and BAT are concerned with orientation toward the upright in space. The EFT, although it in no way involves body position or orientation of the upright, also resembles orientation in the sense that it requires the separation of an item from its organized surrounding field whose framework has horizontal and vertical characteristics and measures characteristics which are both relevant to and may have an influence on the way items (and orientation) are perceived.

Two main results were found in these tests (Witkin et al., 1971). First, high consistency was found in subject's mode of performance across the EFT, RFT, and BAT. The person who takes very long to discover the simple figure in the complex EFT design is also likely to tilt the rod far toward the tilted frame and his own body far toward the tilted room. Second, the high split-half (using 12-trial instead of 24-trial) and test-

retest reliabilities show that an individual remains consistent in his ability to perform this task, not only from item to item on any test occasion (relative stability) but over extended periods of time as well (absolute stability). This allows one to conclude that a person's manner of perceiving does not change easily and represents an ingrained feature of his psychological being--his "perceptual style". Witkin designated this perceptual style as "field dependence-independence". A field independent person shows a capacity to differentiate objects from their background and orients himself to the vertical and horizontal axes of space mainly from his own body sensation. Conversely, a field dependent person reflects a relatively passive submission to the domination of the background and an inability to separate an item from its surroundings. In the general population, scores from any test of field dependence form a continuous distribution.

Testa (1969), in his study of the illness experienced by subjects in a driving simulator, used the RFT and EFT to test his hypothesis which stated that the disparity in incidence of illness could be attributed to differences in perception between extremely field independent and extremely field dependent individuals. The illness experienced in the simulator was presumably caused by the conflict between the apparent motion on the TV screen and the lack of real simulator movement. The results showed that the extremely field independent subjects (one standard deviation above the mean), who were more aware of the conflict, experienced a greater incidence of sickness than the extremely field dependent

subjects (one standard deviation below the mean). This suggests a correlation between the field dependency of the subjects and their performance in the driving simulator.

In conclusion, since field independent people are more sensitive to body cues, we seek to relate the psychological findings to the subject performance of the sled velocity-nulling task. These highly reliable and consistent RFT and EFT, which enable subjects to be classified along a field independent-field dependent continuum, allow us to measure subject's sensitivity to body cues and its relation to the performance of the nulling task.

4.6.2 Experimental Procedures

4.6.2.1 Rod and Frame Test (RFT)

To reproduce the standard RFT(Witkin and Asch, 1948), a portable dark room was built with wood frames covered with black felt (10' x 12' 7.5'). In this dark room, there is a luminous frame (40" x 1") pivoted at its center so that it can be tilted to the left or right. Moving independently of the frame is a luminous (39" x 1") rod, pivoted at the same center. The subject was brought into the test room blindfolded and helped into an upright chair, 9 feet from the apparatus. The floor and walls of the test room were painted with a flat black paint. The subject remained blindfolded while the nature of the test was explained to him. The instructions are as follow:

"The purpose of this test is to determine how well you can establish the vertical under various conditions. Upon uncovering your eyes, you will see a square frame and a rod in an otherwise completely dark room. Your task is to tell me which way to move the rod to make it vertical with respect to the ground and to indicate to me when you perceive the rod to be vertical."

The subject was then told to take off the blindfold and to give the direction of adjustment. After each run, the subject was told to close his eyes, as a small flashlight was turned on to enable the experimenter to take a reading from the voltmeter which was connected to a potentiometer on the shaft of the rod, and to position the rod and frame for the next trial. The above procedure was repeated for eight trials, with two trials for each of four different configurations (frame 28° CCW, rod 28° CW; frame 28° CCW, rod 28° CCW; frame 28° CW, rod 28° CW; frame 28° CW, rod 28° CCW). The test score was the mean of the number of degrees by which the rod deviated from the true vertical for the eight trials.

Three groups containing 13 subjects performed this test. Group S (success) contains five subject, all males, ages between 21 and 30, who were successfully trained to participate in all the experiments described in this chapter. Group F (fail) contains four subjects, ages between 21 and 30, who failed to be trained to perform the sled velocity-nulling task described in Section 4.2.2. Group R (reference) contains four female subjects, ages 17, 30, 40, and 50. After the tests, all subjects were questioned to make sure that no other items were seen during the test

except the rod and frame.

4.6.2.2 Embedded Figures Test (EFT)

The EFT, which is based on the figures developed by Gottschaldt and then modified by Witkin et al. (1971), requires an individual to locate a perceptually obscured simple figure within a larger complex figure. The short form of the test utilized eight simple forms and twelve complex forms as shown in Appendix D. Also included are a simple and complex practice set of figures. The subject's score for the test was the average of the times taken to locate the simple form in the twelve complex figures. The specific instructions are given in Appendix D.

Five groups containing 33 subjects performed the test. Group M1 (male), contains the same five subjects in Group S of the RFT. Group M2 (male) contains seven males, ages 21 to 30, with a comparable educational background to group M1 - MIT students with a scientific major. Group F1 (female) contains nine females, ages 21 to 30, with a scientific background. Group F2 (female) contains seven females, ages 21 to 30, with a non-scientific educational background (MIT secretaries). Finally, Group F3 (female) contains five secretaries, of various ages. These groups are designated to provide a brief study on the factors of sex, age and educational background in contributing to field dependence and to provide a general score for comparison.

4.6.3 Test Results

4.6.3.1 RFT Score

The distribution of individual scores and the mean and standard deviation for each test group are shown in Figure 4.22a. In group R, the results showed that as the age increases, the mean error of the rod also increases. The subject who was 50 years old did perceive a "vertical" rod which was objectively tipped far toward the tilt of the frame. However, groups F and S showed comparable results. Two measurements from the literature (Witkin and Asch, 1948; Testa, 1968) are shown in Figure 4.22b. Testa (1969) used 60 male students, ages 18 to 21. Although the results are comparable to that of group S and group F, six out of our nine subjects of group S and group F are below the mean of Testa's test. This suggests that most of our subjects tend to be field independent. If we compare our results with those from Witkin's test, all our subject tend to be extremely field independent. However, there are clear sex-related and age-related differences in field dependence over the life span (Witkin et al., 1971). Boys and men tend to be more field independent than girls and women observed from many different races. There is also a marked continuous increase in field independence from 8 to 15 years. After age 15, the developmental curves show a levelling off and approach a plateau in the period of young adulthood. After the late 30's, the rate of change toward figure greater field dependence accelerates. From these studies, we would expect to have lower RFT scores in our test and Testa's tests because most of our subjects are male in the period of young adulthood.

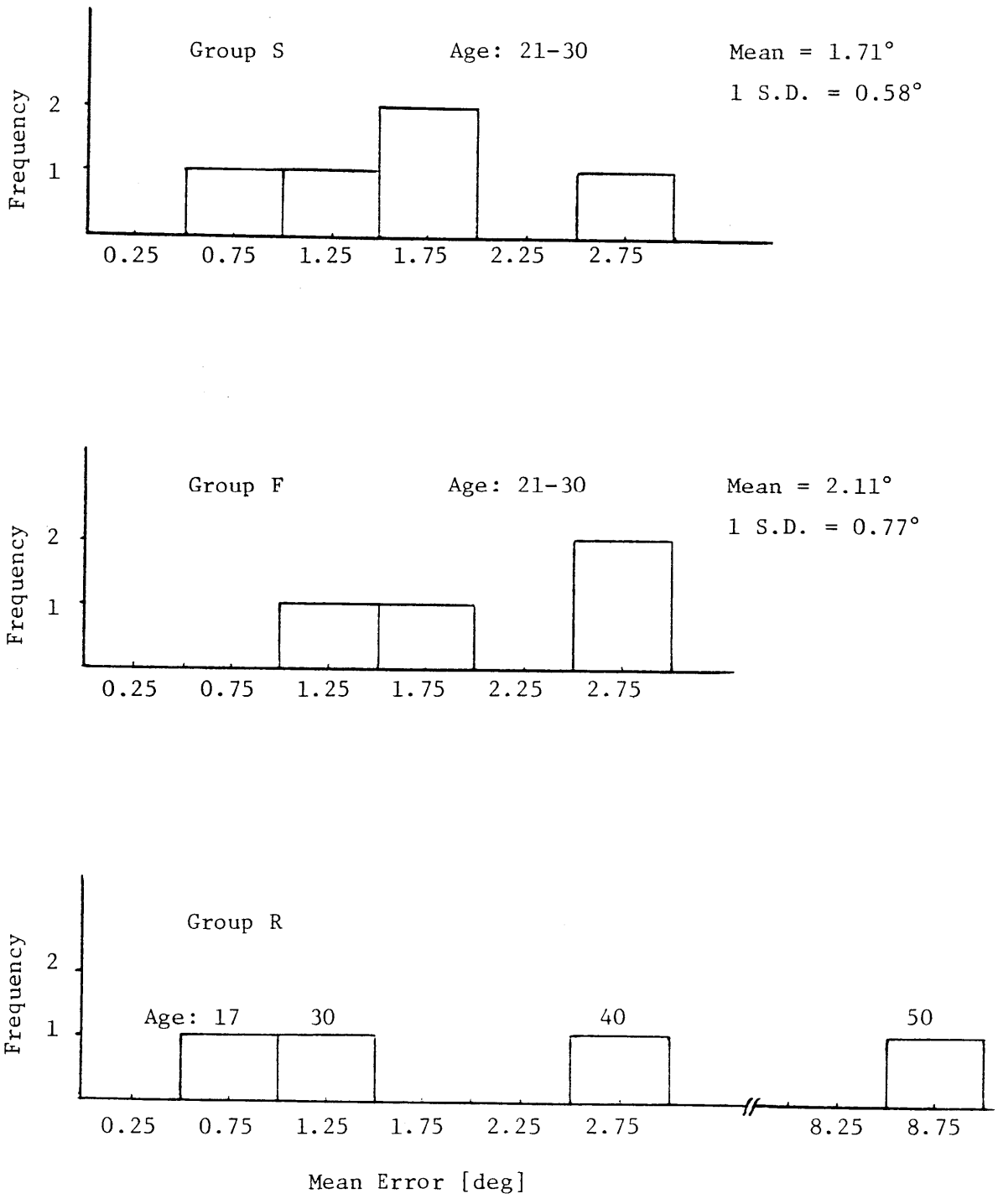

Figure 4.22a: Distribution of individual scores for RFT

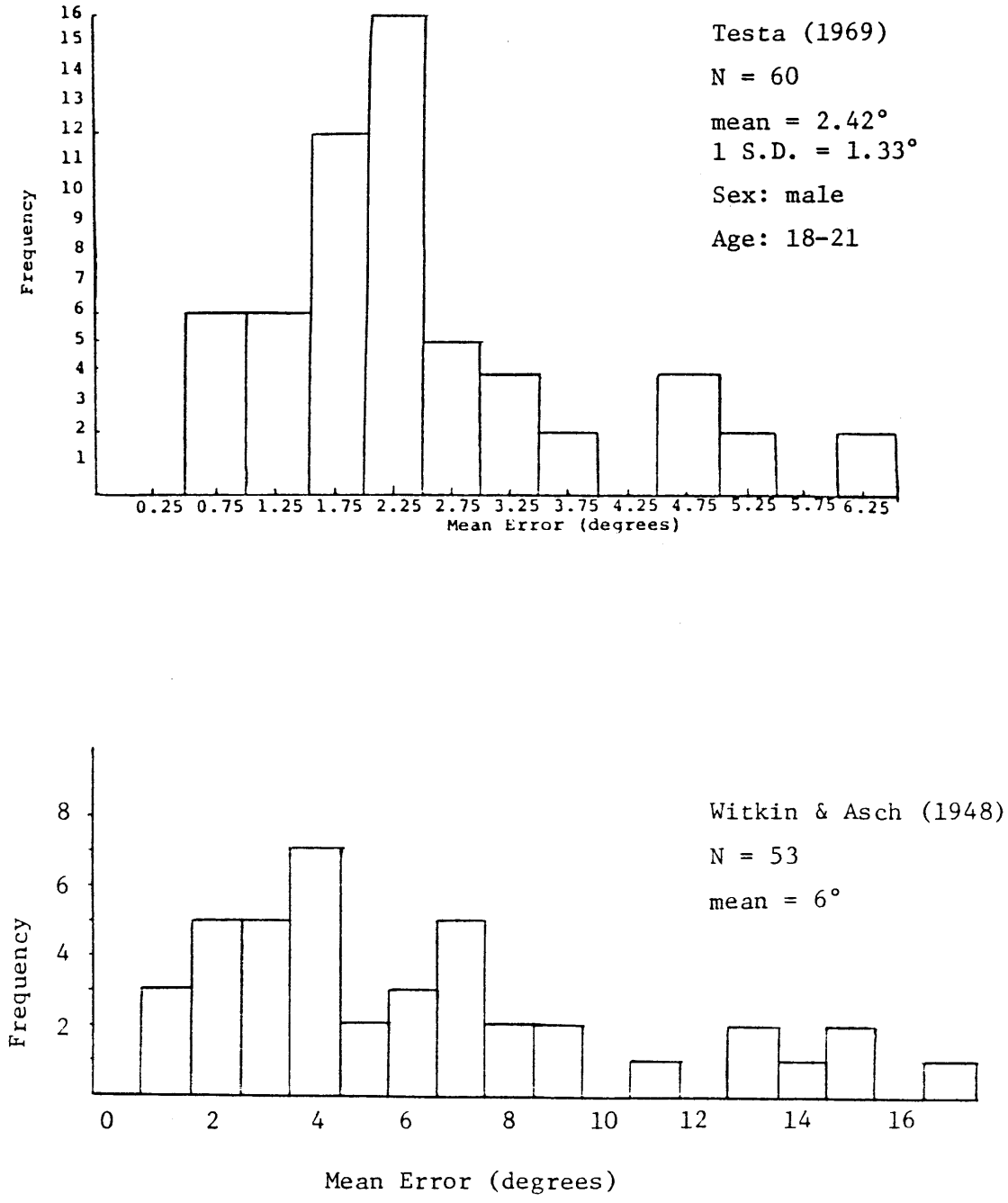

Figure 4.22b: Distribution of individual RFT scores.

The higher RFT scores found in Witkin's test may be caused by the general population which included females and different age groups.

As a result, the RFT scores suggest that most of our subjects who participated in the sled experiments are field independent and no significant difference in field dependency could be observed between those subjects who successfully performed the nulling task and those who failed. However, we don't know whether we bias the subject population by limiting it to the MIT community. This will be discussed in the next section.

4.6.3.2 EFT

The distribution of individual scores and the mean and standard deviations for each testing group are shown in Figure 4.23. First, group F3, which contains five female secretaries, shows that age is an important factor in contributing to field dependence. As the ages increase from 17, the subjects tend to be more field dependent. The subject who has the highest EFT score corresponds to the highest RFT score for the previous section. Groups F1 and F2, both containing female young adults, but with different educational backgrounds (scientific and non-scientific), showed comparable EFT scores. This suggests that educational background is not an important factor in developing field dependence. Groups M1 and M2, both containing male young adults, but with different performance in the sled velocity nulling task, also showed comparable EFT scores. One subject in Group M1 has a particularly high score which may have been related to a fever which he mentioned after the test. This score was thus

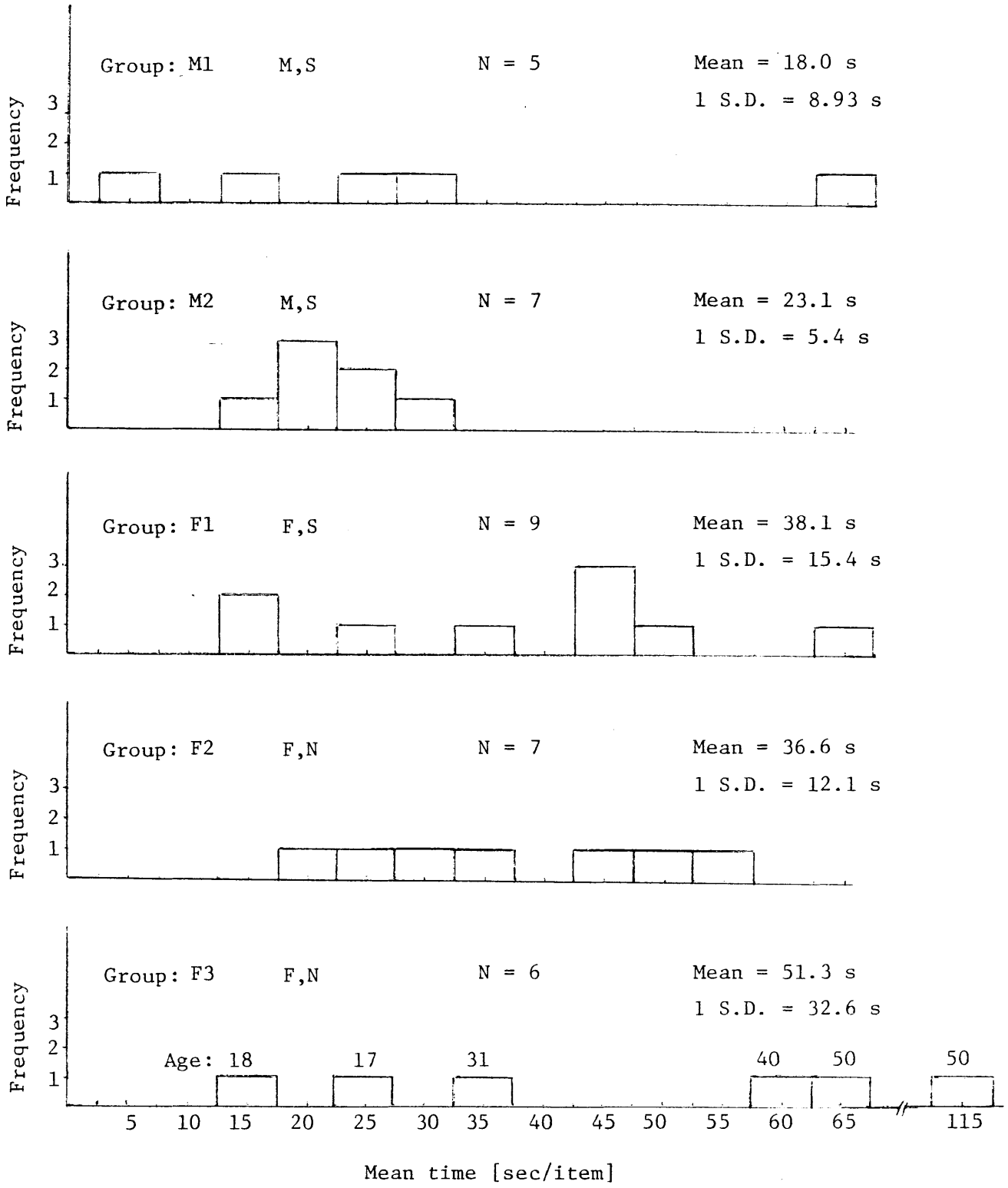

Figure 4.23: Distribution of individual scores for EFT.
(M = Male, F = Female, S = Scientific background
(N =Non-scientific background)

deleted. The results suggest that those subjects (Group M1) who successfully performed the nulling task did not show significantly lower EFT scores compared to those subjects (Group M2) who either failed to be trained or did not participate in the sled experiments. Two male subjects in Group M2, who failed in the nulling task, have EFT scores of 21.0 and 22.1 seconds which is near the mean score of all the male groups (or Group M1) and hence did not show a tendency to be more field dependent. Another two females in Group F1, who also failed in the nulling task, have EFT scores of 36.7 and 44.6 sec, which is also near the mean score of the female groups and hence did not show a tendency to be more field dependent. Finally, if we pool all the male subjects in Groups M1 and M2 and all the female subjects in Groups F1 and F2, the results show that males had significantly lower EFT scores (average 21.3 sec, one standard deviation 7.3 sec) compared to the females (average 37.5 sec, one standard deviation 7.3 sec). This confirmed that sex is an important factor in contributing to field dependence (Witkin et al., 1971).

Table 4.3 Mean and Standard Deviations for the EFT of Young Adults

Source	Sex	N	Mean (sec/item)	S.D.
Witkin et al. (1954)	M	51	45.5	28.5
	F	51	66.9	33.6
Oltmann (1966)	M	34	48.3	22.4
	F	34	69.4	41.0
Karp (1963)	M	150	54.3	36.8
Testa (1969)	M	60	41.1	16.3
Huang (1983)	M	12	21.3	7.3
	F	16	37.5	14.1

However, the EFT scores found in our subjects are lower compared to other findings (shown in Table 4.3) for both sexes. This may suggest that most of our subjects (male and female), chosen from the MIT community may tend to be field independent compared to the general population. The factor that produces these lower values is still uncertain.

As a result, the EFT showed that age and sex are important factors and the educational background is not an important factor in contributing to field dependence, and that all the subjects who participated in the sled experiments tended to be field independent, compared to the general population, no matter how well or poorly they performed the nulling task. It also indicated that we did not chose a group of field independent subjects to participate in our experiment compared to those in the MIT community.

4.7 Conclusions

Measurements were made of human control performance in the closed-loop task of nulling perceived self-velocity about the lateral axis. Four types of visual motion cues were presented on the front screen mounted on a linear acceleration cart. The experimental results showed a better operator performance (based on the value of the variance of the sled velocity) and hence a correspondingly higher gain in the low frequency range in the stationary visual field condition compared to that in darkness. The central spot, fixed in front of the subject, caused an illusion which

is similar to the oculogyral illusion observed in the earth-vertical axis and produced a lower threshold in the illuminated presentation, although the fixed visual field tends to reduce reliance upon vestibular signals.

Describing function data, relating subject compensatory response to actual linear velocity in the dark, was corrected for the dynamics of the operator nulling behavior and the resulting estimator, which is mainly represented by the otolith organs, was linearly modelled in the frequency domain. A Bode plot of the estimator data showed good agreement with a dynamic model of the otolith perception system (Young and Meiry, 1969) when a lead term around 1.5 rad/sec was added.

A further experiment was performed with time-varying visual stimuli in order to develop a human operator dual-input describing function which adequately models a subject's motion perception dependence on combined visual and vestibular linear motion cues. The results showed that the subject didn't provide a compensatory response to the conflicting visual cues, and hence precluded further analysis.

Finally, two psychological tests (the rod and frame test and the embedded figures test) were performed to measure the sensitivity to body cues of the subjects to be classified along a field independent-field dependent continuum. Since field independent people are more sensitive to body cues, a hypothesis was made that the disparity in the human operator performance of the nulling task in the darkness could be attributed to differences in perception between extremely field independent and extremely field dependent individuals. Although the results from over 30

subjects showed that age and sex are important factors and that educational background is not an important factor in developing field dependence, all the subjects who participated in the sled experiments tended to be field independent compared to the general population, no matter how well or poorly they performed the task. However, it also indicated that those subjects are not field independent as compared to those in the MIT community of young adults.

CHAPTER V

SUMMARY AND RECOMMENDATIONS FOR FURTHER WORK

5.1 Summary

The object of this research was to investigate the influence of the visual field on the control engineering characteristics of the vestibular system during rotatory and linear motion. Several experiments were conducted and a model proposed to provide a functional explanation of how vestibular motion cues are integrated with visual field motion cues to result in a subjective sensation of self-motion. Following studies performed for an earth-vertical axis (Zacharias and Young, 1981) and for the roll axis (Huang, 1979), the type of self-motions we investigated here were those involved with the pitch axis and lateral linear motion. The behavioral measure used was the subject's compensatory control response as he attempted to null his own sensation of motion. This closed-loop nulling task required the subject to first estimate his state of spatial orientation, primarily from visual and vestibular motion cues, and then to control his own sensed motion through an appropriate control strategy. Vestibular motion cues were provided to the subject via the use of either a modified aircraft trainer rotated in the pitch axis or a rail mounted linear acceleration cart (the MIT sled). A visual field projection system, mounted on both the trainer and the sled, provided the selected visual motion cues. Both the moving plant and the visual display are

capable of being independently driven to provide the desired motion cues to the subject.

The first experiments investigated the closed-loop task of nulling perceived tilted pitch angles in the face of a pseudo-random vestibular disturbance applied to the trainer drive, combined with one of the following visual fields: (a) counterrotating with respect to the subject so as to be laboratory fixed, thus providing the subject with a visual field motion exactly confirming the vestibular stimulus; (b) stationary with respect to the subject, so that reliance is mainly on vestibular cues; (c) moving at constant velocity upward or downward with respect to the subject; providing him with an illusory sensation of self-motion counter to the actual field motion.

The experimental results are presented in three parts. First, for a visual field moving at constant velocity, the time histories of subject response showed that the subject would bias the trainer in the direction of field rotation, and that this bias was much stronger for pitch backwards with upward stripes than for pitch forward with downward field motion. This may be caused by the directional asymmetry in pitch vection, with a stronger illusion of pitching down. Second, the experimental results also confirmed the importance of visual cues in determining the low frequency components (< 0.3 rad/s) of perceived angles. The high frequency parts of angular motion perception are mainly dominated by the vestibular cues. Describing function data, relating subject compensatory response to actual trainer pitch angle, is shown to be usefully described

by a simple lag-lead transfer function with cascaded dead time, whose parameters varied for the different visual fields used during the nulling task. With confirming visual cues, a high gain was found at low frequency, which drops significantly when the visual field is either held stationary or moving at a constant velocity. Finally, by calculating the correlation between trainer position and subject wheel deflection, both stimulation passing through the semicircular canals and otoliths showed a high correlation with subjective response in the low frequency range (< 1 rad/s). However, the high frequency stimulation is mainly processed through the semicircular canals as compared with the otolith organ. On the other hand, as compared to what we found in the roll axis (Huang, 1979), the results suggested that the subject tends to rely less on the otolith organs in pitch as compared to the roll case.

Next we extended our effort to study how vestibular linear motion cues are integrated with visual field motion cues to result in a subjective sensation of self linear motion. In order to provide visual field cues during the lateral motion, a visual display system has been designed and built to conform with the MIT sled. A type of projector display accompanied by a set of reflecting mirrors could provide linear field motion which is coupled or uncoupled with the sled motion with a field of view of 120° horizontally and 53° vertically.

During the lateral motion, initial experiments investigated velocity-nulling behavior in the face of pseudo-random vestibular disturbances applied to the sled drive, combined with a visual field cue which was

either: (a) countermotion with respect to the subject, thus providing the subject with visual motion cues which confirmed his vestibular sensations; (b) stationary with respect to the subject; (c) moving at constant velocity with respect to the subject; or (d) in the darkness. A single central spot fixed with respect to the subject was also presented except in the case of darkness.

The experimental results showed control with a stationary visual field yielded better operator performance and a higher gain in the low frequency range as compared to control in darkness. This confirmed what we found for earth-vertical rotation (Huang and Young, 1981). The stationary central spot caused an illusion which is similar to the oculogyral illusion observed in the earth-vertical axis and produced a lower threshold in the illuminated presentation, although the fixed visual field tends to reduce reliance upon vestibular signals.

Similar to the pitch experiments, subjects' describing function data is shown to be usefully described by a simple transfer function whose parameters depend on the type of visual field cue presented to the subject during the nulling task. By the use of a second experimental series measuring the tracking or manual control dynamics of the human operator, the describing function found in the dark presentation was then corrected for the dynamics of the operator nulling behavior, and the resulting estimator, which is mainly represented by the otolith organs, was linearly modelled in the frequency domain. A Bode plot of the estimator data showed a good agreement with a dynamic model of the otolith perception

system (Young and Meiry, 1969) by adding a lead term around 1.5 rad/s.

A further experiment was performed with time-varying visual stimuli in order to develop a human operator dual-input describing function which adequately models a subject's sensation in response to combined visual and vestibular linear motion cues. However, the results showed that the subject didn't provide a compensatory response to the conflicting visual field cues, and hence precluded any further analysis. This result must not be interpreted to limit the usefulness of full field visually induced motion in simulation, but is limited only to this experimental set up.

Finally, two psychological tests (the rod and frame test and the embedded figures test) were performed to provide quantitative measures of the extent of field dependence of all the subjects who participated in the sled experiment. The hypothesis stated that the disparity of the human operator performance of the velocity nulling task in the darkness could be attributed to the differences in perception between extremely field independent and extremely field dependent individuals. Although the results from over 30 subjects showed that sex is an important factor and that educational background is not an important factor in contributing to field dependence, all the subjects who participated in the sled experiments tended to be field independent, no matter how well or poorly they performed the task.

5.2 Recommendations for Future Work

1. Visually induced left-right motion sensation

The visual display system, which was built and mounted on the sled, provides a further quantitative study of linearvection in the left right direction. As introduced in Chapter 1, there is an asymmetry in up-down vection (Chu, 1976), in forward and backward pitch (Young et al., 1975) and in the differential effects of upper and lower visual field motion (Young and Oman, 1974)). It will be interesting to investigate whether there is an asymmetry in left right vection.

2. Vestibular-ocular reflex (VOR) during lateral motion

Preliminary tests have shown that it is possible to record horizontal eye movements with the wide-band vestibular disturbance used in Chapter 4, and then perform the Fast Fourier Transform (FFT) analysis. One advantage of this analysis is the simplicity with which the frequency content of the response, obtained by FFT, can be compared to the known frequency components of the stimulus. The eye movements during a velocity nulling task in a supporting or conflicting visual environment would also be interesting to study.

3. The effect of a fixed foveal target on the subjective sensation of lateral motion

In this research, we found that a fixed foveal target can provide more sensitive cues during lateral motion. Similar to the oculogyral

illusion observed in the yaw experiments, the effect of a fixed foveal target on the subjective sensation of lateral motion in the dark can be studied either through the time histories or in the frequency domain (Huang and Young, 1981). A further study of the effects of a moving foveal target on the subjective sensation of lateral motion would be interesting. A similar study performed in the yaw axis was carried out by Sivan and Huang (1981).

4. Washout filter

Since the motion of the sled is mainly limited by the length of the track, a suitable washout filter is necessary to improve our experiments. A kind of U-shaped washout filter, used in the Link trainer (Ish-Shalom, 1982), might be considered.

5. Visual vestibular interaction in the x and z axes

Because the sled is capable of moving a subject in the x and z axes, the experimental and analytical approach used here can be extended to these axes.

REFERENCES

ARROTT, A.P., MIT, Linear Acceleration Facility: Control Program Software Documentation. Man Vehicle Laboratory report, MIT, 1980.

ARROTT, A.P., Torsional Eye Movements in Man During Linear Accelerations S.M. Thesis, Department of Aeronautics and Astronautics, MIT, 1982.

ARROTT, A.P., Manual for the MIT Sled, Man Vehicle Laboratory Report, MIT, in preparation.

BARNHILL, J.H. Surgical Anatomy of the Head and Neck, the Williams and Witkins Co., Baltimore, 1940.

BENSON, A.J. and GUEDRY, F.E., "Comparison of tracking task performance and nystagmus during sinusoidal oscillation in yaw and pitch", Aerospace Med. 42:593-601, 1971.

BERTHOZ, A. JEANNEROD, M., VITAL-DURAND, F. & OLIVERAS, J.L., "Development of vestibulo-ocular responses in visually deprived kittens", Exp. Brain Res. 23:425-442, 1975a.

BERTHOZ, A., BIUZZA, A. and SCHMID, R., Visual-vestibular interaction during linear motion. In: Proceedings of the European Symposium on Life Sciences Research in Space, Cologne/Porz, Germany, 24-26 May,(1977) ESA SP-130, pp. 117-125.

BERTHOZ, A., LACOUR, M., SOECHTING, J. & VIDAL, P.P., "The role of vision in the control of posture during linear motion", Prog. Brain Res. 50:197-21, 1980.

BORAH, J., YOUNG, L.R. and CURRY, R.E., Sensory Mechanism Modeling. AFHRL-TR 78-83. Final Report. Air Force Human Resources Laboratory, 1978.

BRANDT, Th., DICHGANS, J., & BUCHELE, W., "Motion habituation: inverted self-motion perception and optokinetic after-nystagmus", Exp. Brain Res. 16:476-491, 1974.

BREUER, J., "Uber die Funktion der Otolithem-aparates", Pflugers Arch ges Physiol. 48:195-306, 1891.

BRINGHAM, E.O. and MORROW, R.E., "The fast Fourier transform", IEEE Spectrum 4 (12), 1967.

CHAO, A., "Progress Report: Visually Induced Sensation of Vertical Motion", Man Vehicle Laboratory, MIT, 1974.

CHU, W.H.N., Dynamic Response of Human Linearvection, S.M.Thesis, MIT, 1976.

CLARK, B., "Thresholds of perception of angular acceleration in man", Aerospace Med., 38:443-450, 1967.

CLARK, B., "The oculogravic illusion as a test of otolith function", in: The Third Symposium on the Role of the Vestibular Organs in Space Exploration, NASA, SP-152, 1967, pp. 331-339.

CLARK, B., and STEWART, J.D., "Thresholds for perception of angular acceleration about the three major body axes", Fourth NASA Symposium on the Role of the Vestibular Organs in Space Exploration, NASA SP-187, 1968.

COHEN, B., "Vestibulo-ocular relations", In: The Control of Eye Movements, Eds: Bach-y-Rita, P., Collins, C.C. and Hyde, J.E., Academic Press New York and London, 1971.

COLLINS, W.E., SCHROEDER, D.J., RICE, N., MERTENS, R.A. & KRANZ, G., "Some characteristics of optokinetic eye movement patterns: a comparative study", Aerospace Med. 41:1251-1262, 1970.

DAUNTON, N. & THOMSEN, D., "Visual modulation of otolith dependent units in cat vestibular nuclei", Exp. Brain Res. 37:173-176, 1979.

De VRIES, H., "The mechanics of the labyrinth otoliths", Acta Otolaryngol. 49:4, 1958.

DICHGANS, J. & BRANDT, Th., Visual-vestibular interaction and motion perception. In: Cerebral Control of Eye Movement and Motion Perception, Dichgans, J. and Bizzi, E. (Eds.), Basel- New York: S. Karger, 1972, pp. 327-348.

DICHGANS, J. & BRANDT, Th., "Visual vestibular interaction: effects on self-motion perception and postural control", Ch.25, Handbook of sensory Physiology, Vol. VIII, Perception, 1977.

DIENER, H.C., WIST, E.R., DICHGANS, J. & BRANDT, Th., "The spatial-frequency effect on perceived velocity", Vision Res. 16:169-176, 1976.

DINSDALE, P.B., Relative Effects of Roll and Yaw Motion Cues in Manual Control, S.M. Thesis, MIT, 1968.

DIXON, W.J., "BMDP-Biomedical Computer Programs", University of California Press, 1979.

ENGSTROM, H., The first order vestibular neurons. In: Fourth Symposium on the Role of the Vestibular Organs in Space Exploration, NASA SP-187, Washington, D.C., 1968.

EVINGER, C. & FUCHS, A.F., "Saccadic smooth pursuit and optokinetic eye movements of the trained cats", J. Physiol. (London), 285:209-229, 1978.

FERNANDEZ, C. & GOLDBERG, J.M., "Physiology of peripheral neurons innervating otolith organs in the squirrel monkey. I. Response to static tilts and long duration centrifugal force", J. Neurophysiology 39:970-984, 1976a.

FERNANDEZ, C. & GOLDBERG, J.M., "Physiology of peripheral neurons innervating otolith organs in the squirrel monkey. II. Directional selectivity and force response relations", J. Neurophysiology 39:985-995, 1976b.

FERNANDEZ, C. & GOLDBERG, J.M., "Physiology of peripheral neurons innervating otolith organs in the squirrel monkey. III. Response dynamics", J. Neurophysiology 39:996-1008, 1976c.

FERNANDEZ, C., GOLDBERG, J. M. & ABEND, W.K., "Response to static tilts of peripheral neurons innervating otolith organ in the squirrel monkey", J. Neurophysiol. 35:978-997, 1972.

GIBSON, J.J. (Ed.) Motion Picture Testing and Research. Washington, D.C., Government Printing Office, AAF Aviat. Psychol. Program Res. Rep. No. 7, 1974.

GOLDBERG, J.M. & FERNANDEZ, C., "Physiology of peripheral neurons innervating semicircular canals of the squirrel monkey. I, II,III. Variations among units in their discharge properties", J. Neurophysiol. 34:661-684, 1971b.

GUEDRY, F.E., Psychophysics of vestibular sensation. In: Handbook of Sensory Physiology, Vol. VI. Vestibular System. H.H. Kornhuber (Ed.) Berlin: Springer Verlag, 1974 pp.3-154.

HANNEN, R.A., KABRISKY, M., REPLOGLE, C.R., HARTZLER, V.L. & ROCCAFORTE, P.A., "Experimental determination of a portion of the human vestibular response through measurement of eyeball counterroll", IEEE Trans. Biomed. Eng. 13:65-70, 1966.

HENN, V., COHEN, B. & YOUNG L.R., Visual-Vestibular Interaction in Motion Perception and the Generation of Nystagmus, NRP Bulletin 18:459-651,

1980.

HOSMAN, R.J.A.W. & Van der Vaart, J.C., "Vestibular models and thresholds of motion perception. Results of tests in a flight simulators", Report LR-265, Delft Univ. of Techology, April 1978.

HOWARD, I.P. & TEMPLETON, W.B., Human Spatial Orientation, London-New York-Sidney: John Wiley and Sons, 1966.

HUANG, J.-K., Visual Field Influence on Motion Sensation in Yaw and on Manual Roll Stabilization, S.M. Thesis, MIT, 1979.

HUANG, J.-K. & YOUNG L.R., "Sensation of rotation about a vertical axis with a fixed visual field in different illuminations and in the dark", Exp. Brain Res. 41:172-183, 1981.

Integrated Helment and Display Sighting System (IHADSS), Technical Description, Avionico Division, Honeywell, Minneapolis, Minnesota, 1977.

ISH-SHALOM, J., Design of Optimal Motion for Flight Simulator, Ph.D. Thesis, MIT, 1982.

IURATO, S., Submicroscopic Structure of the Inner Ear, Oxford: Pergamon Press Ltd., 1967.

JONGKEES, L.B.W., "On the otoliths: their function and the way to test them", In: Third Symposium on the Role of the Vestibular Organs in Space Exploration, NASA SP-152, 1967, pp. 307-330.

JONGKEES, L.B.W. & GROEN, J.J., The nature of the vestibular stimulus, J. Laryngol. 61:529, 1946.

KARP, S.A., "Field dependence and overcoming embeddedness", J. Consulting Psychology 27:294-302, 1963.

KELLOGG, R.S., "Dynamic counterrolling of the eye in normal subjects and in persons with bilateral labyrinthine defects", The Role of the Vestibular Organ in the Exploration of Space, NASA SP-77, pp. 195-202, 1965.

KRIEGER, H.P. & BENDER, M.B., "Optokinetic after-nystagmus in the monkey", Eletroenceph. Clin. Neurophysiol. 8:97-106, 1956.

LEE, D.N. & ARONSON, E., "Visual proprioceptive control of standing in human infants", Percept. Psychophys. 15:529-532, 1974.

LESTIENNE, F., SOECHTING, J. & BERTHOZ, A., "Postural readjustments induced by linear motion of visual scenes", Exp. Brain Res. 28:363-384, 1977.

LICHTENBERG, B.L., Ocular Counterrolling Induced in Humans by Horizontal Accelerations, Sc.D. Thesis, MIT, 1979.

LICHTENBERG, B.L., YOUNG, L.R. & ARROTT, A.P., "Human ocular counterrolling induced by varying linear accelerations", Exp. Brain Res. 48:127-136, 1982.

LIEBOWITZ, H. & DICHGANS, J., "The influence of luminance level and refractive error on circularvection", in preparation.

LISHMAN, J.R. & LEE, D.N., "The autonomy of visual kenesthesis", Perception 2:287-294, 1973.

LOO, D.K., A Hybrid Controller for a Rail Mounted Sled, S.M. Thesis, MIT, 1978.

MANGNUS, R., "The experimental basis for theories on vestibular function", Roy. Soc. Med. Sect. Laryng. Otol. 11-17, 1924.

MATSUO, V., COHEN, B., RAPHAN, T., DEJONG, V. & HENN V., "Asymmetric velocity storage for upward and downward nystagmus", Brain Res. 176: 159-164, 1979.

MEIRY, J.L., The Vestibular System and Human Dynamic Orientation, Sc.D. Thesis, MIT, 1965.

MELVILL JONES, G., BARRY, W. & KOWALSKY, N., "Dynamics of the semicircular canals compared in yaw pitch and roll", Aerospace Med. 35:984-989, 1964.

MELVILL JONES, G. & MILSUM, J.H., "Characteristics of neural transmission from the semicircular canal to the vestibular nucleus of cats", J. Physiol. 209:295-316, 1970.

MELVILL JONES, G. & YOUNG, L.R., "Subjective detection of vertical acceleration: a velocity dependent response?", Acta Otolaryngologica 85:1, 1978.

MONEY, K.E. & SCOTT, J.W., "Functions of separate sensory receptors of nonauditory labyrinth of the cat", Amer. J. Physiol. 202:1211-1220, 1962.

MORRISON, W., "Link GAT-1 projector system", Man VVehicle Lab. Memo, MVL-751, MIT, 1975.

MURPHY, R.E., A Display System to Induce Self Rotation, S.M. Thesis, MIT, 1972.

MYGIND, S.H., "Static function of the labyrinth attempt at synthesis", Acta Otolaryngol (Stockh.) Suppl. 70, 1948.

ORMSBY, C.C., Model of Human Dynamics Orientation, Ph.D. Thesis, MIT, 1974.

ORMSBY, C.C. & YOUNG, L.R., "Perception of static orientation in a constant gravitoinertial environment", Aviation, Space Environ. Med. 47:159-164, 1976.

PASIK, P., PASIK, T., VALCIUKAS, J.A. & BENDER, M.B., "Vertical optokinetic nystagmus in the split brain monkey", Exp. Neurol. 30:162-171, 1971.

PAVARD, B. & BERTHOZ, A., "Linear acceleration modifies the perceived velocity of a moving visual scene", Perception 6:529-540, 1977.

PETERS, R.A., Dynamics of the Vestibular System and Their Relation to Motion Perception, Spatial Disorientation and Illusions, NASA CR-1309, 1969.

QUIX, F.H., "The function of the vestibular organ and the clinical examination of the otolithic apparatus", J. Laryngol Otol 40:425-443, 493-511, 1925.

SADOFF, M., MATTESON, F.A. & HAVILL C.D., "A method for evaluating the loads and controllability aspects of the pitch up problem", NASA RMA55D06, August 1955.

SCHONE, H., "On the role of gravity in human spatial orientation", Aerosp. Med. 35:764-772, 1964.

SIVAN, R., ISH-SHALOM, J. & HUANG, J.-K., "An optimal control approach to design of moving flight simulators", IEEE Transaction on System, Man, and Cybernetics. Nov. 1982.

SIVAN, R. & HUANG, J.-K., "The effect of a moving foveal target on the subjective sensation of motion", Biological Cybernetics 40:93-99, 1981.

SPOENDLIN, H., "Ultrastructure of the vestibular sense organ", In: The Vestibular System and Its Dieseases, R.J. Wolfson, Ed., Univ. of Pennsylvania Press, 1966, 39-68.

TAKAHASHI, M. & IGARASHI, M., "Comparison of vertical and horizontal optokinetic nystagmus in the sqquirrel monkey", Oto-rhino-laring, 39:321-329, 1977.

TAKAHASHI, M., SAKURAI, S. & KANZAKI, J., "Horizontal and vertical optokinetic nystagmus in man", Oto-rhino-laryng, 40:43-52, 1978.

TESTA, C.J., The Prediction and Evaluation of Simulator Illness Symptomatology, Ph.D. Thesis in Engineering, Univ. of California, Los Angeles, 1969.

VON BEKESY, G., "Pressue and shearing forces as stimuli of labyrinthine epithelium", Arch. Otolaryngol. 84:122, 1969.

VON HOLST, E., "Die Arbeitsweise des Statolithenapparates bei Fischen", S. vergl. Physiol. 32:60-120, 1950a.

VON HOLST, E., "Die Tätigkeit des Statoltithenapparates in Wirbeltierlabyrinth", Naturwissenschaften 37:265-272, 1950b.

WAESPE, W. & HENN, V., "Conficting visual-vestibular stimulation and vestibular nucleus activity in alert monkeys", Exp. Brain Res. 33:203-211, 1977.

WAESPE, B., WAESPE, W. & HENN, V., "Subjective velocity estimation during conflicting visual-vvestibular stimulation", Arch. Psychiat. Nervenkr. 228:109-116, 1980.

WIST, E.R., DIENER, H.C., DICHGANS, J. & BRANDT, Th., "Perceived distance and the perceived speed of self-motion: linear versus angular velocity", Percept. Psychophys. 17:549-554, 1975.

WITKIN, H.A. & ASCH, S.E., "Studies in space orientation. IV. Further experiments on perception of the upright with displaced visual fields", J. of Exp. Psychology 38:762-782, 1948.

WITKIN, H.A., LEWIS, H.B., HERTZMAN, M., MACHOVER, K., MEISSNER, P. & WAPNER, S., Personality Through Perception, New York: Harper, 1954.

WITKIN, H.A., "The perception of the upright", Sci. Amer. February, 1959.

WITKIN, H.A., OLTMAN, P.K., RASKIN, E. & KARP, S.A., A Manual for the Embedded Figures Tests, Consulting Psychologist Press, Inc., PALO ALTO, Cal. 1971.

WOOD, R.W., "The 'haunted swing' illusion", Psychol. Rev. 2:277-278, 1895.

YOUNG, L.R. & MEIRY, J.L., "A revised dynamic otolith model", Aerospace Med 39:606-608, 1968.

YOUNG, L.R., "Role of the vestibular system in posture and movement", in: Medical Physiology, V. Mountcastle, ed., Mosby, St. Louis, 1974.

YOUNG, L.R. & OMAN, C.M., "Model for vestibular adaptation to horizontal rotation", Aerosp. Med. 40:1076-1080, 1969.

YOUNG, L.R. & OMAN, C.M., "Influence of head position and field position on visually induced motion effects in three axes of rotation", Proceedings of the Tenth Annual Conference on Manual Control, 1974.

YOUNG, L.R., OMAN, C.M. & DICHGANS, J., "Influence of head orientation on visually induced pitch and roll sensation", Aviat. Space Environ. Med. 46:264-268, 1975.

ZACHARIAS, G.L., Motion Sensation Dependence on Visual and Vestibular Cues, Ph.D. Thesis, MIT, 1977.

ZACHARIAS, G.L. & YOUNG, L.R., "Influence of combined visual and vestibular cues on human perception and control of horizontal rotation", Exp. Brain Res. 41:159-171, 1981.

ZACHARIAS, G.L., "Motion cue model for pilot vehicle analysis", Report AMRL-TR-78-2, Bolt, Beranek & Newman, Inc., Cambridge, MA, May, 1982.

APPENDIX A

Program Listing for PDP 11/34 Processing

A.1 Programs used in the pitch experiment

MAIN PROGRAM: PITRUN
SUBROUTINES: DISGEN, PARGEN, TABGEN, SINTAB, FILTER,FILER
FILER, ARCFCN, DTOA6, ATOD6, KW

A.2 Programs used in the sled experiment

The programs used for the MIT sled facility were designed and described by Arrott (1980). These programs are then modified for the experiments in Chapter IV. The overlay structure is described as follows:

a. Root (Main Program): CART

b. Region 1: ALPHA, OMEGA, QUERY, CENTRX, ICART, RCARTB, RCARTC, ECART

c. Region 2: MCART, ACART, EOGCAL, EDIPRO, GETPRO, WRIPRO, REPRO, FNAME, QSTEP, QSINE, QSQUAR, QSOS, QDOUBL, QCREAT, QBUFF, QPARAM, QPROJ, QDATA, QMOVE, QVIS, QJOY, QCAM, QEOG, QHELP, STATUS, DVM, QG, QTC

d. Region 3: DISK, DECODR, DIGIN, DIGOUT, MINUS, FLASH, POWER, SUMSIN, ACCEPT, IACCEP, RANS, IANS, IRANSD, IANSD, TTYOUT, IYESNO

e. Region 4: ATOD6, DTOA6, KW, WAIT

The programs used to analyze the data are as follows:

PICK, CONDAT, SPARTA, TRNFCN, CMP320

The programs are listed in alphabetical order.

The CART programs will be listed and described by ARROTT(1983).

```
FORTRAN IV      V02.5-2    Wed 22-Dec-82 00:24:15                PAGE 001

0001          FUNCTION ASIN(X)
      C
      C       IN FILE ARCFCN.FOR
      C
0002          COMMON/ARCCOM/PIHALF
0003          TEMP=ABS(X)
0004          IF(TEMP.LE.1.)  GOTO 5
0006          WRITE(7,100)X
0007      100 FORMAT(5X,'*** ARCFCN ARG VALUE=',E15.5,'   FATAL HALT')
0008          STOP
0009        5 IF(TEMP.NE.1)GOTO 15
0011          ASIN=SIGN(1.,X)*PIHALF
0012          RETURN
0013       15 Y=SQRT(1.-X**2)
0014          ASIN=ATAN(X/Y)
0015          RETURN
0016          DATA PIHALF/1.5707963/
0017          END
ASIN
```

```
        .TITLE  ATOD6       ; ANALOG TO DIGITAL CONVERSION
                            ; OF SIX CHANNELS OF THE LPS
                            ; STARTING WITH CHANNEL 8
        .MCALL  .REGDEF
        .REGDEF

        .GLOBL  ATOD6

        LPSADS=170400    ; A/D CONVERTOR STATUS
        LPSADB=170402    ; A/D CONVERTOR BUFFER

ATOD6:  TST     (R5)+     ; SKIP PAST PARAMETER COUNT
        MOV     (R5),R0   ; GET ADDRESS OF BUFFER
        CLR     @#LPSADS          ; INITIALIZE CONVERTER
        MOV     #4000,@#LPSADS    ; TO CHANNEL 8

1$:     INC     @#LPSADS ; START CONVERSION

2$:     TSTB    @#LPSADS ; WAIT FOR CONVERSION
        BPL     2$       ; TO FINISH

        TSTB    @#LPSADS+1 ; CHECK FOR CONVERSION
        BMI     4$         ; ERROR

        MOV     @#LPSADB,(R0)+ ; SAVE DATA IN BUFFER

3$:     INCB    @#LPSADS+1 ; POINT TO NEXT CHANNEL
        CMPB    @#LPSADS+1,#16  ; CHECK CHANNEL NUMBER
        BLT     1$              ; AND CONTINUE THROUGH
                                ; SIX CHANNELS:
                                ; (8,9,10,11,12,13)
        RTS     PC              ; RETURN


4$:     MOV     #-1,(R0)+ ; FORCE ERRONEOUS DATA TO -1
        BIC     #100000,@#LPSADS ; CLEAR ERROR FLAG
        BR      3$               ; CONTINUE IN LOOP


        .END
```

```
FORTRAN IV      V02.5-2    Wed 22-Dec-82 00:37:10                PAGE 001

0001          PROGRAM CMP320
      C
      C       Author: Jen-Kuang Huang
      C       Date:   13-Mar-82
      C
0002          DIMENSION XIN(2048),OUTAMP(512),OUTPHS(512),AR(320),
             1          GAIN(320),PHASE(320),FREQ(320)
0003          REAL INAMP(512),INPHS(512)
0004          INTEGER SF(2)
      C
0005          EQUIVALENCE (XIN(   1), INAMP(1)),
             1            (XIN( 513), INPHS(1)),
             1            (XIN(1025),OUTAMP(1)),
             1            (XIN(1537),OUTPHS(1))
      C
0006        1 CONTINUE
      C
0007          DEFINE FILE 1 (1,4096,U,NREC)
0008          CALL ASSIGN(1,'TEMP3.DAT')
0009          READ (1'1) XIN
0010          CALL CLOSE(1)
      C
0011          WRITE(7,205)
0012      205 FORMAT(2X,'CONCATE FROM EVERY ? POINTS: '$)
0013          READ(5,207) IPO
0014      207 FORMAT(I2)
0015          TLENTH=TLENTH*IPO/12.
0016          WRITE(7,210)
0017      210 FORMAT(5X,'ENTER SCALE FACTORS(2I1): '$)
0018          READ(5,100) SF
0019      100 FORMAT(2I1)
      C
0020          T1=2.**(SF(2)-SF(1))
0021          DO 5 I=1,NCOMP
0022          J=I+1
0023          IF(INAMP(J) .EQ. 0.0) INAMP(J)=0.01
0025          AR(I)=20.*ALOG10(T1*OUTAMP(J)/INAMP(J)) !CALC AR IN DB
0026          PHASE(I)=(OUTPHS(J)-INPHS(J))*RTD-360.
0027          IF(PHASE(I).GT.360.) PHASE(I)=PHASE(I)-360.
0029          IF(PHASE(I).LT.-360.)PHASE(I)=PHASE(I)+360.
0031          FREQ(I)=I/TLENTH        !CALC FREQ IN HZ
0032        5 CONTINUE
      C
0033          WRITE(7,220)
0034      220 FORMAT(5X,'N',3X,'FREQ',6X,'OUTAMP',7X,'INAMP',
             1          6X,'AR(db)',7X,'PHASE',/)
0035          WRITE(7,230)(I,FREQ(I),OUTAMP(I+1),INAMP(I+1),AR(I),PHASE(I),
             1          I=1,NCOMP)
0036      230 FORMAT(2X,I4,F7.3,4F12.2)
      C
0037          GO TO 1
      C
0038          STOP
      C       DATA NCOMP,TLENTH/320,200.7/
      C       FOR SLED
0039          DATA NCOMP,TLENTH/320,184.32/
0040          DATA RTD/57.296/
0041          END
```

```
FORTRAN IV      V02.5-2    Wed 22-Dec-82 00:32:49                PAGE 001

0001          PROGRAM CONDAT
      C
      C  Author: Jen-Kuang Huang
      C  Creation Date: 8-JUN-82
      C
      C  Concatenates sled data(1 channel, 256 word record, up to 48 blocks)
      C  Method: Window filter (Window: two standard deviation)
      C  Currently assumes input data file has max 12288 ticks long, with
      C   data points per time tick
      C  Program writes out 1024 data points, for two
      C    channels of data  ==> can run SPFFT to do the FFT
      C
0002          DIMENSION INBUF(256),ITEMP(12288)
0003          INTEGER OUT(1024),CASE
      C
0004          WRITE(7,100)
0005      100 FORMAT(' Sled data concatenation',/,
                +  '    Currently accepts maximum of 12288(256*48) samples ')
0006      110 WRITE(7,113)
0007      113 FORMAT(2X,'ENTER NUMBER OF BLOCKS:'$)
0008          READ(5,115) NBLOCK
0009      115 FORMAT(I2)
0010          INTVLE=INT(256*NBLOCK/1024+0.)
0011          WRITE(7,116) INTVLE
0012      116 FORMAT(2X,'Pick up one point from every ',I2,' points.')
0013          DO 117 I=1,12288
0014      117 ITEMP(I)=2048
      C
0015      131 FORMAT(2X,'ENTER FILE1(IN=*.SLD):'$)
0016      132 FORMAT(/,2X,'ENTER FILE2(OUT=*.STK):'$)
0017          CASE=1
0018          WRITE(7,131)
0019      135 CALL ASSIGN(1,,-1)
0020          DEFINE FILE 1 (0,256,U,NREC)
0021          NREC=1
0022          IR=0
0023          SUM=0.
0024          RMSE=0.
      C
0025          DO 152 J=1,NBLOCK
0026          READ(1'NREC,END=200) INBUF
0027          DO 151 K=1,256
0028          ITEMP(256*(J-1)+K)=INBUF(K)
0029      151 CONTINUE
0030      152 CONTINUE
      C
0031          DO 190 L=1,1024
0032          TSUM1=0.
0033          TSUM2=0.
0034          TRMSE=0.
0035          IA=0
0036          IC=INTVLE*(L-1)
0037          DO 170 M=1,INTVLE
0038          P1=ITEMP(IC+M)-2048
```

```
0039          TSUM1=TSUM1+ITEMP(IC+M)-2048
0040          TRMSE=TRMSE+P1*P1
0041      170 CONTINUE
0042          TAVG=TSUM1/INTVLE
0043          TRMS=SQRT(TRMSE/INTVLE)
0044          TSTD=SQRT(TRMS**2-TAVG**2)
0045          ULIM=TAVG+TSTD*2
0046          LLIM=TAVG-TSTD*2
0047          DO 180 N=1,INTVLE
0048          P1=ITEMP(IC+N)-2048
0049          IF(P1.GT.ULIM) GOTO 180
0051          IF(P1.LT.LLIM) GOTO 180
0053          TSUM2=TSUM2+ITEMP(IC+N)-2048
0054          IA=IA+1
0055      180 CONTINUE
0056          OUT(L)=INT(2048+TSUM2/IA)
0057          IR=IR+INTVLE-IA
0058      190 CONTINUE
0059          GOTO 300
      C
0060      200 WRITE(7,210) CASE,J
0061      210 FORMAT(2X,'TEMP',I1,':',I5,' Records(256 words/record)',/,)
0062          GO TO 110
      C
0063      300 IF(CASE.EQ.2) GOTO 301
0065          CALL ASSIGN(2,'TEMP1.DAT')
0066          GO TO 302
0067      301 CALL ASSIGN(2,'TEMP2.DAT')
0068      302 DEFINE FILE 2 (1,1024,U,IREC2)
0069          WRITE(2'1)OUT
0070          DO 305 I=1,1024
0071          P1=OUT(I)-2048
0072          SUM=SUM+OUT(I)-2048
0073          RMSE=RMSE+P1*P1
0074      305 CONTINUE
0075          AVG=SUM/1024
0076          RMS=SQRT(RMSE/1024)
0077          STD=SQRT(RMS**2-AVG**2)
0078          WRITE(7,308) CASE
0079      308 FORMAT('  TEMP',I1,6X,'REJECT(%)',5X,'RMS',5X,'AVG',5X,'STD')
0080          RPC=IR*100./INTVLE/1024.
0081          WRITE(7,309) RPC,RMS,AVG,STD
0082      309 FORMAT(12X,F10.2,F8.2,F8.2,F8.2)
0083          CALL CLOSE(1)
0084          CALL CLOSE(2)
      C
0085          IF(CASE.EQ.2) GOTO 400
0087          CASE=2
0088          WRITE(7,132)
0089          GO TO 135
0090      400 END
CONDAT
```

```
FORTRAN IV      V02.5-2    Wed 22-Dec-82 00:13:09                PAGE 001

0001          SUBROUTINE DISGEN(NOISE)
      C
0002          INTEGER PFLAG,HARM(16),PHASE(16)
0003          INTEGER SINTAB
      C
0004          REAL NOISE
      C
0005          DIMENSION AMP(16),KDIST(16)
      C
0006          COMMON PFLAG,NSTEP,TSEC
0007          COMMON /DCOM/NCOMP,HARM,AMP,PHASE
0008          COMMON /DCOMIN/KDIST
      C
0009          GO TO (100,200,300,300)PFLAG
      C
0010      100 CONTINUE           !FIRST PASS- INIT TABLES
      C
0011          CALL PARGEN            !SET NCOMP,& HARM,AMP,PHASE VECTORS
      C
0012          DO 105 J=1,NCOMP       !CHECK FOR POS HARM, PHASE VALUES
0013          IF(HARM(J).GE.0)GO TO 110
0015          STOP 'A NOISE FREQUENCY IS NEGATIVE'
0016      110 IF(PHASE(J).GE.0)GO TO 105
0018          STOP 'A NOISE PHASE IS NEGATIVE'
0019      105 CONTINUE
      C
0020          CALL TABGEN            !GENERATE SINE TABLE
0021          RETURN
      C
0022      200 CONTINUE           !SECOND PASS
0023          NOISE=0.               !ZERO NOISE
0024          DO 205 J=1,NCOMP       !INITIALIZE INDICES TO PHASES
0025      205 KDIST(J)=PHASE(J)
0026          RETURN
      C
0027      300 CONTINUE           !THIRD OR FOURTH PASS- CALC NOISE
0028          NOISE=0.
0029          DO 305 J=1,NCOMP
0030          KTEMP=KDIST(J)             !GET OLD INDICIES
      C
0031      310 IF(KTEMP.LE.NSTEP) GO TO 315
0033          KTEMP=KTEMP-NSTEP        !KTEMP GT NSTEP;DECR TILL LE NSTEP
0034          GO TO 310
0035      315 CONTINUE                 !KTEMP NOW GE 0 AND LE NSTEP
      C
0036          NOISE=NOISE+AMP(J)*SINTAB(KTEMP)
      C
0037          KDIST(J)=KTEMP+HARM(J)       !INCR K FOR NEXT PASS
0038      305 CONTINUE                     !END J LOOP
0039          RETURN
0040          END
DISGEN
```

```
;       SUBROUTINE DTOA6(IDAT)
;
;       IDAT INTEGER DATA VECTOR, WITH COMPONENTS
;       BETWEEN 0 AND 4095 INCLUSIVE
;
;       IDAT(1) INTO DAC6
;       IDAT(2) INTO DAC5
;               .
;               .
;               .
;       IDAT(6) INTO DAC0
;
        .MCALL  .REGDEF
        .REGDEF

        .GLOBL DTOA6
        DASTAT=170416
        EXTDA=170424
DTOA6:  TST     (R5)+           ;SKIP ARGUMENT COUNT
        MOV     #5,R0
        MOV     (R5),R1
1$:     TSTB    @#DASTAT        ;WAIT FOR LPS DAC
        BPL     1$
        MOV     R0,R2
        ASH     #15,R2          ;SET UP DA SELECT BITS
        BIS     (R1)+,R2
        MOV     R2,@#EXTDA      ;SEND DATA
        DEC     R0              ;ENOUGH DONE?
        BGE     1$              ;NOPE,LOOP
        RTS     PC              ;YES,RETURN

        .END
```

```
FORTRAN IV      V02.5-2    Wed 22-Dec-82 00:22:02                PAGE 001

0001          SUBROUTINE FILER(ICHAN,IDATA)
      C
0002          INTEGER PFLAG,BUFLEN,BUFF1(1024),BUFF2(1024),
             1        BUFF(2048)
      C
0003          DIMENSION IDATA(4)
      C
0004          COMMON PFLAG,NSTEP,TSEC
0005          COMMON /FCOM/IBUFF,JBUFF,KBUFF,IBLOCK,BUFF
      C
0006          EQUIVALENCE(BUFF(   1),BUFF1(1)),
             1           (BUFF(1025),BUFF2(1))
      C
0007          GO TO (100,200,300,400,500) PFLAG
      C
0008        100 RETURN           !FIRST PASS- DUMMY CALL
      C
0009        200 CONTINUE         !SECOND PASS- INITIALIZE:
0010            JBUFF=1          !              BUFFER INDEX
0011            KBUFF=0          !              BUFFER WORD INDEX
0012            ISKIP=0          !              BUFFER SKIP LENGTH
0013            IBLOCK=-2        !              BLOCK INDEX
0014            RETURN
      C
0015        300 RETURN           !THIRD PASS- DUMMY CALL
      C
0016        400 CONTINUE         !FOURTH PASS- FILE STUFF
0017            LBASE=ISKIP+KBUFF
0018            DO 5 L=1,NDATA         !LOAD NDATA WORDS INTO EITHER
0019          5 BUFF(L+LBASE)=IDATA(L)!BUFF1 OR BUFF2
      C
0020            KBUFF=KBUFF+NDATA          !INCR KBUFF
0021            KTEMP=KBUFF+NDATA          !KTEMP IS LOOK AHEAD WORD
0022            IF(KTEMP .GT. BUFLEN)GO TO 10   !TEST IF WE'LL OVER-
0024            RETURN                              !FLOW BUFFER NEXT TIME
      C
0025        500 CONTINUE          !FIFTH PASS- ZERO REST OF BUFFER
0026            IF(KBUFF.EQ. 0)RETURN      !RETURN IF FOURTH PASS FILLED
      C                                      !THE BUFFER; OTHERWISE...
0028            DO 25 L=ISKIP+KBUFF+1,ISKIP+BUFLEN  !ZERO REST OF BUFFER
0029         25 BUFF(L)=0                           !AND WRITE IT OUT
      C
0030         10 CONTINUE             !BUFFER FILLED OR CLOSE TO IT
0031            KBUFF=0              !RESET WORD INDEX
0032            IBLOCK=IBLOCK+4      !INCR BLOCK COUNT
0033            GO TO (15,20) JBUFF  !START A DISC WRITE
      C
0034         15 IBUFF=IWRITE(BUFLEN,BUFF1,IBLOCK,ICHAN) !BUFF1 WRITE
0035            JBUFF=2              !SET UP FOR BUFF2 WRITE NEXT TIME
0036            ISKIP=BUFLEN
0037            RETURN
      C
0038         20 IBUFF=IWRITE(BUFLEN,BUFF2,IBLOCK,ICHAN) !BUFF2 WRITE
0039            JBUFF=1              !SET UP FOR BUFF1 WRITE NEXT TIME
0040            ISKIP=0
0041            RETURN
      C
0042            DATA BUFLEN/1024/,
             1      NDATA/4/
      C
0043            END
```

```
FORTRAN IV      V02.5-2    Wed 22-Dec-82 00:20:07                PAGE 001

0001          SUBROUTINE FILTER(INPUT,OUTPUT,PARAM)
      C
0002          INTEGER PFLAG
      C
0003          REAL INPUT
      C
0004          DIMENSION PARAM(3),COEF(8),
             1          C(4),D(2),E(2),SAVE(6)
      C
0005          COMMON PFLAG,NSTEP,TSEC
0006          COMMON /PCOM/COEF,SAVE
      C
0007          EQUIVALENCE(COEF(1),C(1)),
             1           (COEF(5),D(1)),
             1           (COEF(7),E(1)),
             1           (SAVE(1),X1OLD),
             1           (SAVE(2),X2OLD),
             1           (SAVE(3), UOLD),
             1           (SAVE(4),X1NEW),
             1           (SAVE(5),X2NEW),
             1           (SAVE(6), UNEW)
      C
0008          GO TO (100,200,300,400) PFLAG
      C
0009        100 CONTINUE            !FIRST PASS- CALCULATE COEFFS
      C
0010          GAIN=PARAM(1)               !INPUT BUFFER PARAMS
0011          ZETA=PARAM(2)
0012          W   =PARAM(3)
      C
0013          CONTINUE                    !SECOND ORDER LOW PASS
0014          ATEMP=ZETA*W
0015          BTEMP=W*SQRT(1.-ZETA*ZETA)
0016          PHI=ACOS(ZETA)
0017          T1=(EXP(-ATEMP*TSEC))/BTEMP
0018          T2=BTEMP*TSEC
0019          C(1)=W*T1*SIN(T2+PHI)
0020          C(2)=T1*SIN(T2)
0021          C(3)=-W*W*C(2)
0022          C(4)=-W*T1*SIN(T2-PHI)
0023          D(2)=GAIN*(1.-C(1))/TSEC
0024          D(1)=GAIN*(1.-C(2)/TSEC)-(2.*ZETA/W)*D(2)
0025          E(1)=TSEC*D(2)-D(1)
0026          E(2)=-GAIN*C(3)-D(2)
0027          RETURN
      C
0028        200 CONTINUE            !SECOND PASS- ZERO PLANT STATES
0029          DO 205 I=1,6
0030        205 SAVE(I)=0.
0031          RETURN
      C
0032        300 CONTINUE            !THIRD PASS- CALCULATIONS
0033          UNEW=INPUT                  !BUFFER INPUT
0034          X1NEW=C(1)*X1OLD+C(2)*X2OLD+D(1)*UNEW+E(1)*UOLD
0035          X2NEW=C(3)*X1OLD+C(4)*X2OLD+D(2)*UNEW+E(2)*UOLD
0036          OUTPUT=X1NEW             !BUFFER OUTPUT
0037          RETURN
      C
0038        400 CONTINUE            !FOURTH PASS- UPDATES
0039          X1OLD=X1NEW
0040          X2OLD=X2NEW
0041          UOLD=UNEW
0042          RETURN
      C
0043          END
```

```
        .TITLE  KW              ; CLOCK SET INSTEAD OF SETR

LPSKWS=170404

        .GLOBL  KWSET,KWWAIT

KWSET:  INC     %5              ; CALL KWSET(BUFFER,STATUS)
        INC     %5
        MOV     #LPSKWS,%0      ; BUFFER & STATUS ARE INTEGERS
        CLR     (%0)+           ; TO BE LOADED INTO THE L P S
        MOV     @(%5)+,%1       ; REGISTERS
        NEG     %1
        MOV     %1,@%0
        MOV     @(%5)+,-(%0)
        RTS     %7

KWWAIT: MOV     #LPSKWS,%0      ; IF(KWWAIT().NE.0) STOP 'SYNC ERROR'
        TSTB    @%0
        BMI     2$
1$:     TSTB    @%0
        BPL     1$
        BICB    #200,@%0
        CLR     %0
        RTS     %7
2$:     CLR     @%0             ; TURN CLOCK OFF
        MOV     #-1,%0          ; AND RETURN ERROR FLAG
        RTS     %7
        .END
```

```
0001          SUBROUTINE PARGEN
      C
      C       FREQ USED IN ROLL AND PITCH          17-NOV-79
      C
0002          INTEGER PFLAG,FTYPE,HARM(16),PHASE(16)
0003          REAL MAXVAL
0004          DIMENSION AMP(16),W(16)
0005          COMMON PFLAG,NSTEP,TSEC
0006          COMMON /DCOM/NCOMP,HARM,AMP,PHASE
0007          COMMON /PARCOM/FTYPE,APOLE,RMSDST
      C
0008          DELW=2.*PI/(NSTEP*TSEC)
0009          DO 5 I=1,NCOMP          !CALCULATE DIST FREQUENCIES
0010        5 W(I)=HARM(I)*DELW
0011          WZERO=W(1)*W(1)/W(2)    !CALC FICTITIOUS END FREQUENCIES
0012          W(NCOMP+1)=W(NCOMP)*W(NCOMP)/W(NCOMP-1)
      C
0013          DO 10 I=NCOMP+1,2,-1    !CALCULATE BOX FREQUENCIES
0014       10 W(I)=SQRT(W(I-1)*W(I)) !AND OVERLAY ORIGINAL VALUES
0015          W(1)=SQRT(WZERO*W(1))
      C
0016          GAIN=2.*RMSDST*RMSDST/(PWR(W(NCOMP+1))-PWR(W(1))) *
      C
0017          DO 15 I=1,NCOMP         !CALCULATE AMPLITUDES
0018       15 AMP(I)=SQRT(GAIN*(PWR(W(I+1))-PWR(W(I))))/MAXVAL
      C
0019          NHALF=NSTEP/2           !CALCULATE PHASES
0020          DO 20 I=2,NCOMP,2       !ALTERNATE BETWEEN 0 AND PI
0021       20 PHASE(I)=NHALF
      C
      C       A(I)=AMP(I)*MAXVAL
      C       FREQ(I)=HARM(I)/(TSEC*NSTEP)
      C       AW(I)=A(I)*2.*PI*FREQ(I)
      C       AWW(I)=AW(I)*2.*PI*FREQ(I)
      C       WRITE(7,2)
      C     2     FORMAT(3X,'N',2X,'NF',3X,'FREQ',8X,'AMP',11X,'AMP*W',
      C      1          11X,'AMP*W*W',/)
      C       WRITE(7,3)(I,HARM(I),FREQ(I),A(I),AW(I),AWW(I),I=1,NCOMP)
      C     3     FORMAT(2I4,F7.3,E15.5,E15.5,F15.5)
      C
0022          RETURN
      C
      C       FREQ (ROLL)
      C       DATA HARM/3,5,7,11,17,23,31,43,61,83,107,137,4*0/,
      C       FREQ (PITCH)
0023          DATA HARM/3,5,7,11,17,23,31,43,61,83,107,137,4*0/,
             1      PHASE/16*0/,
             1      NCOMP/12/,
             1      PI/3.14159/,
             1      MAXVAL/32767./
0024          RETURN
0025          END
PARGEN
```

```
FORTRAN IV      V02.5-2    Wed 22-Dec-82 00:30:53                PAGE 001

0001          PROGRAM PICK
      C
      C  Author: Jen-Kuang Huang
      C  Creation Date: 22-APR-82
      C
      C  Pick up sled data(8 channels, 256 word record, 385 blocks)
      C  Currently assumes input data file is 12288 ticks long, with data
      C    points per time tick
      C  Program writes out a data point for every tick, for one specified
      C    channel of data  ==> can run CONDAT to get rid of spikes
      C
0002          DIMENSION INBUF(256),IOBUF(256)
0003          INTEGER OUT1(12288)
      C?
0004          WRITE(7,100)
0005      100 FORMAT(' Pick up input/output sled data ',/,
                +  '    Currently accepts maximum of 12288 samples per channel ')
0006      101 WRITE(7,102)
0007      102 FORMAT(/,2X,'ENTER INPUT FILE:'$)
0008          CALL ASSIGN(1,,-1)
0009          DEFINE FILE 1 (0,256,U,NREC)
      C
0010      110 WRITE(7,111)
0011      111 FORMAT(/,'  CHANNEL NUMBER(-1=EXIT,0=NEW FILE,2=SLD,6=STK):'$)
0012          READ(5,112)INCHN
0013      112 FORMAT(I2)
0014          IF(INCHN.LE.0) GOTO 400
      C
0016          DO 130 K=1,12288
0017      130 OUT1(K)=2048                    ! Initialization
0018          NREC=2
0019          DO 150 J=1,384
0020          READ(1'NREC,END=200) INBUF
0021          ISAVE=32*(J-1)
0022          DO 140 I=1,32
0023          I1=8*(I-1)+INCHN
0024          OUT1(ISAVE+I)=INBUF(I1)
0025      140 CONTINUE
0026      150 CONTINUE
0027          GOTO 300
      C
0028      200 IR=INT((J-2)/8.)+1
0029          WRITE(7,210) J-1,IR
0030      210 FORMAT(2X,I4,' Records(256 words/record) => ',I2,' Records')
0031          WRITE(7,310)
0032          CALL ASSIGN(2,,-1)
0033          DEFINE FILE 2 (IR,256,U,IREC1)
0034          ICT=0
0035          DO 230 I=1,IR
0036          DO 220 K=1,256
0037      220 IOBUF(K)=OUT1(256*(I-1)+K)
0038          ICT=ICT+1
0039      230 WRITE(2'ICT) IOBUF
0040          CALL CLOSE(2)
```

```
FORTRAN IV      V02.5-2    Wed 22-Dec-82 00:30:53                PAGE 002

0041          GOTO 110
      C
0042     300  WRITE(7,310)
0043     310  FORMAT(2X,'ENTER OUTPUT FILE(IN=*.SLD/OUT=*.STK): '$)
0044          CALL ASSIGN(2,,-1)
0045          DEFINE FILE 2 (1,12288,U,IREC1)
0046          WRITE(2'1)OUT1
0047          CALL CLOSE(2)
0048          GOTO 110
      C
0049     400  CALL CLOSE(1)
0050          IF(INCHN.EQ.0) GOTO 101
0052          END
PICK
```

```
FORTRAN IV      V02.5-2    Wed 22-Dec-82 00:01:38                PAGE 001

0001          PROGRAM PITRUN
      C
      C       JEN-KUANG HUANG          25-JUN-80
      C       THIS PROGRAM USED FOR PITCH EXPT
      C       USE PITBAT.BAT TO LINK SUBPROGRAM
      C
0002          INTEGER PFLAG,TMSEC,FTYPE,OUTPUT(6)
0003          REAL KIN(6),KOUT(6),MINVAL,MAXVAL
0004          DIMENSION NULL(256),INPUT(6),SCIN(6),SCOUT(6),
             1          PARAM(3),IDATA(4),VARBLS(4),GAINS(4),IZEROS(6)
0005          COMMON PFLAG,NSTEP,TSEC
0006          COMMON /PARCOM/FTYPE,APOLE,RMSDST
0007          EQUIVALENCE(PARAM(1),GAIN),
             1            (PARAM(2),ZETA),
             1            (PARAM(3),  WN),
             1            (INPUT(1),INTRPT),
             1            (INPUT(2),  MODE),
             1            (SCIN(3),W1),
             1            (SCIN(4),STICK),
             1            (SCIN(5),   THI),
             1            (SCIN(6),   W2),
             1            (SCOUT(1),  W1C),
             1            (SCOUT(2),  W2C),
             1            (SCOUT(3),  DSC),
             1            (SCOUT(4),STKSC),
             1            (SCOUT(5), W1SC),
             1            (SCOUT(6), W2SC),
             1            (SCOUT(3),VARBLS(1))
      C
0008          DEFINE FILE1(66,256,U,NREC)
0009        1 CONTINUE
      C       WRITE(7,95)
      C    95    FORMAT(2X,'IS THIS A DEMO(Y OR N)?:'$)
      C       READ(5,96)IDEMO
      C    96    FORMAT(A1)
0010          IDEMO=INO
0011          TSEC=TMSEC/1000.
0012          PFLAG=1          !FIRST PASS
0013          CALL PITDIS(D)                  !INIT DISGEN TABLE
0014          CALL FILTER(W1CP,W1C,PARAM)     !CALC FILTER COEFFS
0015          CALL DTOA6(IZEROS)              !ZERO D TO A LINES
      C
0016        5 PFLAG=2          !SECOND PASS
0017          IF(IDEMO .EQ. IYES)GO TO 6
      C
0019          WRITE(7,200)
0020      200 FORMAT(2X,'ENTER TYPE OF PROJ(1=CON,2=CVD,3=FIX,4=CVU): '$)
0021          READ(5,86)K
0022       86 FORMAT(I1)
0023       88 WRITE(7,100)                    !OPEN DATA FILE IF NOT A DEMO
0024      100 FORMAT(2X,'ENTER DATA FILEMANE:'$)
0025          CALL ASSIGN(1,,-1)
0026          WRITE(1'1)NULL
0027          ICHAN=ILUN(1)
```

```
0028          CALL FILER(ICHAN,IDATA)        !INIT FILER PARAMS
0029        6 CONTINUE
0030          ICOUNT=0.                       !ZERO THE LOOP COUNT
0031          WHLRMS=0.
0032          TRNRMS=0.                      !ZERO RMS ERROR SCORE
0033          TVLRMS=0.
0034          WHLSUM=0.
0035          TRNSUM=0.
0036          TVLSUM=0.
0037          CALL PITDIS(D)                 !ZERO DIST SIGNAL
0038          CALL FILTER(W1CP,W1C,PARAM)    !ZERO FILTER STATES
      C
0039          PFLAG=3          !THIRD PASS
0040          ISTATE=IWAIT                   !SET STATE TO WAIT
0041          WRITE(7,101)
0042      101 FORMAT(2X,'HIT INTERRUPT TO START')
0043       25 CALL KWSET(TMSEC,'411)         !START CLOCK
      C*****************************************************************
0044       10 CONTINUE                       !TOP OF LOOP
0045          IF(KWWAIT().NE.0)STOP'SYNCH ERROR' !HALT ON SYNCH ERROR
0047          CALL ATOD6(INPUT)               !SAMPLE SIX LINES
0048          IF(INTRPT.LE.INTLVL)GO TO 15   !CHECK FOR INTERRUPT
0050          CALL KWSET(0,0)                !INTERRUPT- STOP CLOCK
0051          CALL KWSET(TMSEC,'411)         !RESTART IT
0052          DO 20 I=1,NTICK                !WAIT NTICK TICKS
0053       20 CALL KWWAIT()
0054          CALL KWSET(0,0)                !STOP CLOCK
0055          IF(ISTATE.EQ.IWAIT)GO TO 7     !IF WE'RE RUNNING,CHECK FOR
0057          IF(IDEMO.EQ.INO)CALL CLOSE(1)  !DEMO,AND CLOSE FILE IF NO
0059          GO TO 76                       !DEMO,THEN TO BOTTOM
0060        7 ISTATE=IRUN                    !IF WE'RE WAITING,CHANGE
0061          GO TO 25                       !STATE AND START RUNNING
0062       15 IF(ISTATE.EQ.IWAIT)GO TO 10    !BACK TO TOP OF LOOP
      C                                     !IF WE'RE IN WAIT LOOP
      C*****************************************************************
      C                                     !LOOP CALCS START HERE
0064          IF(IDEMO.EQ.IYES)GO TO 29      !SKIP COUNT IF A DEMO
0066          ICOUNT=ICOUNT+1                !INCR LOOP COUNTER
0067       29 CONTINUE
0068          DO 30 I=1,6                    !CHECK FOR AD CONV ERROR
0069       30 IF(INPUT(I).LT.0)STOP'AD CONVERSION ERROR'
0071          DO 35 I=3,6                    !SCALE INPUTS TO PROBLEM
0072       35 SCIN(I)=KIN(I)*(INPUT(I)-IZERO)
      C
0073          CONTINUE                       !CALC TRAINER CMD
0074       39 W1CP=D+STICK
0075          CALL FILTER(W1CP,W1C,PARAM)
0076          IF(W1C.LE.12.)GO TO 33
0078          W1C=12.
0079          GO TO 32
0080       33 IF(W1C.GE.-12.)GO TO 32
0082          W1C=-12.
      C
0083       32 CONTINUE                       !CALC PROJ CMD
```

```
0084          IF(IDEMO .NE. IYES)GO TO 98
0086          IDIST=IYES
0087          IF(MODE.LE.MODE3)GO TO 45
0089          W2C=W1                              !CTR(MODE=4,W/ NO DIST)
0090          IDIST=INO
0091          D=0.
0092          GO TO 56
0093       45 IF(MODE.LE.MODE2)GO TO 50
0095          W2C=W1                              !CTR(MODE=3,W/ DIST)
0096          GO TO 56
0097       50 IF(MODE.LE.MODE1)GO TO 55
0099          W2C=CVRATE                           ! CV(MODE=2)
0100          GO TO 56
0101       55 W2C=0.                               !FIX(MODE=1)
0102          GO TO 56
      C
0103       98 GO TO (110,120,130,140) K
0104      110 W2C=W1
0105          GO TO 56
0106      120 W2C=8.
0107          GO TO 56
0108      130 W2C=0.
0109          GO TO 56
0110      140 W2C=-8.
      C
0111       56 CONTINUE                           !CALC STRIP CHART OUTPUTS
0112          DSC=D
0113          STKSC=STICK
0114          W1SC=THI
0115          W2SC=W2
      C
0116          DO 60 I=1,6                         !SCALE ALL OUTPUTS
0117          TEMP=KOUT(I)*SCOUT(I)+ZERO
0118          IF(TEMP .LE. 4095.) GO TO 61          !LIMIT OUTPUT
0120          OUTPUT(I)=4095
0121          GO TO 60
0122       61 IF(TEMP .GE.    0.) GO TO 62
0124          OUTPUT(I)=0
0125          GO TO 60
0126       62 OUTPUT(I)=TEMP
0127       60 CONTINUE
0128          CALL DTOA6(OUTPUT)                   !LOAD SIX DTOA LINES
      C
0129          PFLAG=4                             !FOURTH PASS
0130          CALL FILTER(W1CP,W1C,PARAM)           !UPDATE FILTER STATES
0131          IF(IDEMO .EQ. IYES) GO TO 65
0133          IF(ICOUNT.LE.FITIME) GO TO 65
      C
0135          DO 70 I=1,4                           !SCALE VARBLS FOR FILER
0136          TEMP=GAINS(I)*VARBLS(I)
0137          IF(TEMP .LE. MAXVAL)GO TO 71
0139          IDATA(I)=MAXVAL
0140          GO TO 70
0141       71 IF(TEMP .GE. MINVAL)GO TO 72
```

```
0143          IDATA(I)=MINVAL
0144          GO TO 70
0145       72 IDATA(I)=TEMP
0146       70 CONTINUE
0147          IDATA(4)=ICOUNT   !*********************************
0148          CALL FILER(ICHAN,IDATA)            !STORE VARIABLES
0149       65 CONTINUE
0150          IF(IDIST.EQ.INO)GO TO 67           !SKIP DIST CALC CHECK
0152          CALL PITDIS(D)                     !CALC NEXT DIST POINT
0153       67 WHLRMS=WHLRMS+STICK*STICK
0154          TRNRMS=TRNRMS+THI*THI                !CALC RUNNING RMS ERROR
0155          TVLRMS=TVLRMS+W1*W1
0156          WHLSUM=WHLSUM+STICK
0157          TRNSUM=TRNSUM+THI
0158          TVLSUM=TVLSUM+W1
      C
0159       68 PFLAG=3                          !RESET PFLAG FOR NEXT PASS
0160          IF(ICOUNT.NE.4096)GO TO 10     !CHECK LOOP COUNTER;LOOP BACK
      C                                       !TO TOP IF COUNT .NE. NSTEP
      C*************************************************************
0162          CONTINUE                         !FINISHED THE LOOP;CLOSE UP
      C
0163          PFLAG=5                          !FIFTH PASS
0164          IF(IDEMO .EQ. IYES) GO TO 76
0166          DO 75 I=1,4                          !SCALE VARIABLES FOR FILER
0167       75 IDATA(I)=GAINS(I)*VARBLS(I)
0168          CALL FILER(ICHAN,IDATA)              !LAST VARIABLE STORE
0169          CALL CLOSE(1)                        !CLOSE DATA FILE
0170       76 CONTINUE
0171          CALL KWSET(0,0)                      !STOP CLOCK
0172          CALL DTOA6(IZEROS)                   !ZERO DTOA LINES
      C
0173          WHLRMS=SQRT((WHLRMS/NSTEP))*1.25
0174          WRITE(7,105)WHLRMS
0175      105 FORMAT(2X,'RMS WHEEL POSITION  =',F10.3,'  DEG',)
0176          WHLAVG=WHLSUM*1.25/NSTEP
0177          WRITE(7,106)WHLAVG
0178      106 FORMAT(2X,'AVG WHEEL POSITION  =',F10.3,'  DEG',/)
0179          TRNRMS=(SQRT(TRNRMS/NSTEP))*1.25
0180          WRITE(7,115)TRNRMS
0181      115 FORMAT(2X,'RMS TRAINER POSITION=',F10.3,'  DEG',)
0182          TRNAVG=TRNSUM*1.25/NSTEP
0183          WRITE(7,116)TRNAVG
0184      116 FORMAT(2X,'AVG TRAINER POSITION=',F10.3,'  DEG',)
0185          TRNVAR=SQRT(TRNRMS**2-TRNAVG**2)
0186          WRITE(7,117)TRNVAR
0187      117 FORMAT(2X,'VAR TRAINER POSITION=',F10.3,'  DEG',/)
0188          TVLRMS=SQRT(TVLRMS/NSTEP)
0189          WRITE(7,125)TVLRMS
0190      125 FORMAT(2X,'RMS TRAINER VELOCITY=',F10.3,'  DEG/SEC',)
0191          TVLAVG=TVLSUM/NSTEP
0192          WRITE(7,126)TVLAVG
0193      126   FORMAT(2X,'AVG TRAINER VELOCITY=',F10.3,'  DEG/SEC',)
      C
```

```
0194          DATA NULL/256*0/,
             1     TMSEC,NSTEP/49,4096/,
             1     GAIN,ZETA,WN/1.,0.7,6.28/,
             1     IZERO,IZEROS,ZERO/7*2048,2048./,
             1     IWAIT,IRUN/0,1/,
             1     INTLVL,NTICK/3747,10/,
             1     KIN/2*0.,0.00976,0.00901,-0.00977,-0.03052/,
             1     KOUT/204.8,20.685,4*51.20/,
             1     GAINS/4*100./
             1     MODE1,MODE2,MODE3/2386,3062,3747/,
             1     CVRATE/6./,
             1     SCIN,SCOUT/12*0./,
             1     IYES,INO/'Y','N'/,
             1     MINVAL,MAXVAL/-32767.,32767./,
             1     FTYPE,APOLE,RMSDST/2,1.0,5./
      C
0195          END
PITRUN
```

```
FORTRAN IV      V02.5-2    Wed 22-Dec-82 00:19:10                PAGE 001

0001          INTEGER FUNCTION SINTAB(K)
      C
0002          INTEGER TABLE(1025)
      C
0003          COMMON /TCOM/NHALF,NQUART,TABLE
      C
      C       SINTAB ASSUMES (0 .LE. K .LE. NSTEP)
      C
0004          KDUM=K+1
0005          ISIGN=1
0006          IF(KDUM.LE.NHALF) GO TO 5
0008          KDUM=KDUM-NHALF
0009          ISIGN=2
      C
0010        5 IF(KDUM.LE.NQUART) GO TO 10
0012          KDUM=NHALF+2-KDUM
      C
0013       10 SINTAB=TABLE(KDUM)
0014          GO TO (20,15) ISIGN
0015       15 SINTAB=-SINTAB
0016       20 RETURN
0017          END
SINTAB
```

SPARTA

```
$JOB/RT11
.R SPARTA
*BBU S2 F2 1024
*MOP
*TEMP3.DAT<TEMP1.DAT,TEMP2.DAT
*MIN S1 1024 I1
*DDI S1
*DID
*DLO
*DLO
*DLO
*DLO
*DLO
*DLO
*BSU S2
*FFT S1 S2
*FMP S2 S1 F1 F2
*DDI F1
*MOU F1 512 O1
*MOU F2 512 O1
*MIN S1 1024 I2
*DDI S1
*DLO
*DLO
*DLO
*DLO
*DLO
*DLO
*BSU S2
*FFT S1 S2
*FMP S2 S1 F1 F2
*DDI F1
*MOU F1 512 O1
*MOU F2 512 O1
*MCL
*EXT
$EOJ
```

```
FORTRAN IV      V02.5-2    Wed 22-Dec-82 00:18:11                PAGE 001

0001          SUBROUTINE TABGEN
      C
0002          INTEGER PFLAG,TABLE(1025)
      C
0003          COMMON PFLAG,NSTEP,TSEC
0004          COMMON /TCOM/NHALF,NQUART,TABLE
      C
0005          NHALF=NSTEP/2
0006          NQUART=NHALF/2+1
0007          TEMP=2.*PI/NSTEP
      C
0008          DO 5 I=1,NQUART
0009        5 TABLE(I)=MAXVAL*SIN((I-1)*TEMP)
0010          RETURN
      C
0011          DATA PI/3.1415927/,
             1     MAXVAL/32767/
0012          END
TABGEN
```

```
      C
      C     PROGRAM TRNFCN.FOR
      C
      C     Author: Jen-Kuang Huang
      C     Date:   14-Mar-82
      C
0001        DIMENSION XIN(2048),OUTAMP(512),OUTPHS(512),NF(25),
           1              GAIN(25),PHASE(25),FREQ(25)
0002        REAL INAMP(512),INPHS(512)
0003        INTEGER SF(2)
      C
0004        EQUIVALENCE (XIN(   1), INAMP(1)),
           1            (XIN( 513), INPHS(1)),
           1            (XIN(1025),OUTAMP(1)),
           1            (XIN(1537),OUTPHS(1))
      C
0005      1 CONTINUE
      C
0006        DEFINE FILE 1 (1,4096,U,NREC)
0007        CALL ASSIGN(1,'TEMP3.DAT')
0008        READ (1'1) XIN
0009        CALL CLOSE(1)
      C
0010        WRITE(7,210)
0011    210 FORMAT(5X,'ENTER SCALE FACTORS: '$)
0012        READ(5,100) SF
0013    100 FORMAT(2I1)
      C
0014        T1=2.**(SF(2)-SF(1))
0015        T2=2.*PI
0016        DO 5 I=1,NCOMP
0017        J=NF(I)+1
0018        GAIN(I)=20.*ALOG10(T1*OUTAMP(J)/INAMP(J)) !CALC AR IN DB
0019        PHASE(I)=OUTPHS(J)-INPHS(J)
0020        IF(PHASE(I) .GE. T2) PHASE(I)=PHASE(I)-T2
0022        IF(I.EQ.1)GO TO 3
0024        IF(PHASE(I)*PHASE(I-1).LT.0.)PHASE(I)=PHASE(I)+
           1                                    T2*SIGN(1.,PHASE(I-1))
0026      3 IF(PHASE(I).LE.0.)GO TO 4
0028        PHASE(I)=PHASE(I)-T2
0029      4 PHASE(I)=RTD*PHASE(I)       !CALC PHASE IN DEGREES
      C     PHASE(I)=PHASE(I)+180.
0030        FREQ(I)=NF(I)/TLENTH        !CALC FREQ IN HZ
0031      5 CONTINUE
      C
0032        WRITE(7,220)
0033    220 FORMAT(5X,'N',2X,'NF',3X,'FREQ',8X,'GAIN',7X,'PHASE',
           1       /)
0034        WRITE(7,230)(I,NF(I),FREQ(I),GAIN(I),PHASE(I),I=1,NCOMP)
0035    230 FORMAT(2X,2I4,F7.3,2F12.2)
      C
0036        WRITE(7,240)
0037    240 FORMAT(//,5X,'ENTER OUTPUT FILENAME: '$)
0038        CALL ASSIGN(2,,-1)
```

```
0039          WRITE(2,250)(NF(I),FREQ(I),GAIN(I),PHASE(I),I=1,NCOMP)
0040      250 FORMAT(1X,I3,F5.3,2F8.3)
0041          CALL CLOSE(2)
      C
0042          GO TO 1
      C
0043          STOP
0044          DATA PI,RTD/3.14159,57.296/
      C       USED FOR SLED
0045          DATA NCOMP,TLENTH/25,184.32/
0046          DATA NF/3,5,7,11,13,17,19,23,29,31,37,41,43,47,53,61,73,83,
             +          101,113,137,149,163,181,199/
      C       DATA NF/3,9,21,33,51,75,111,183/
0047          END
.MAIN.
```

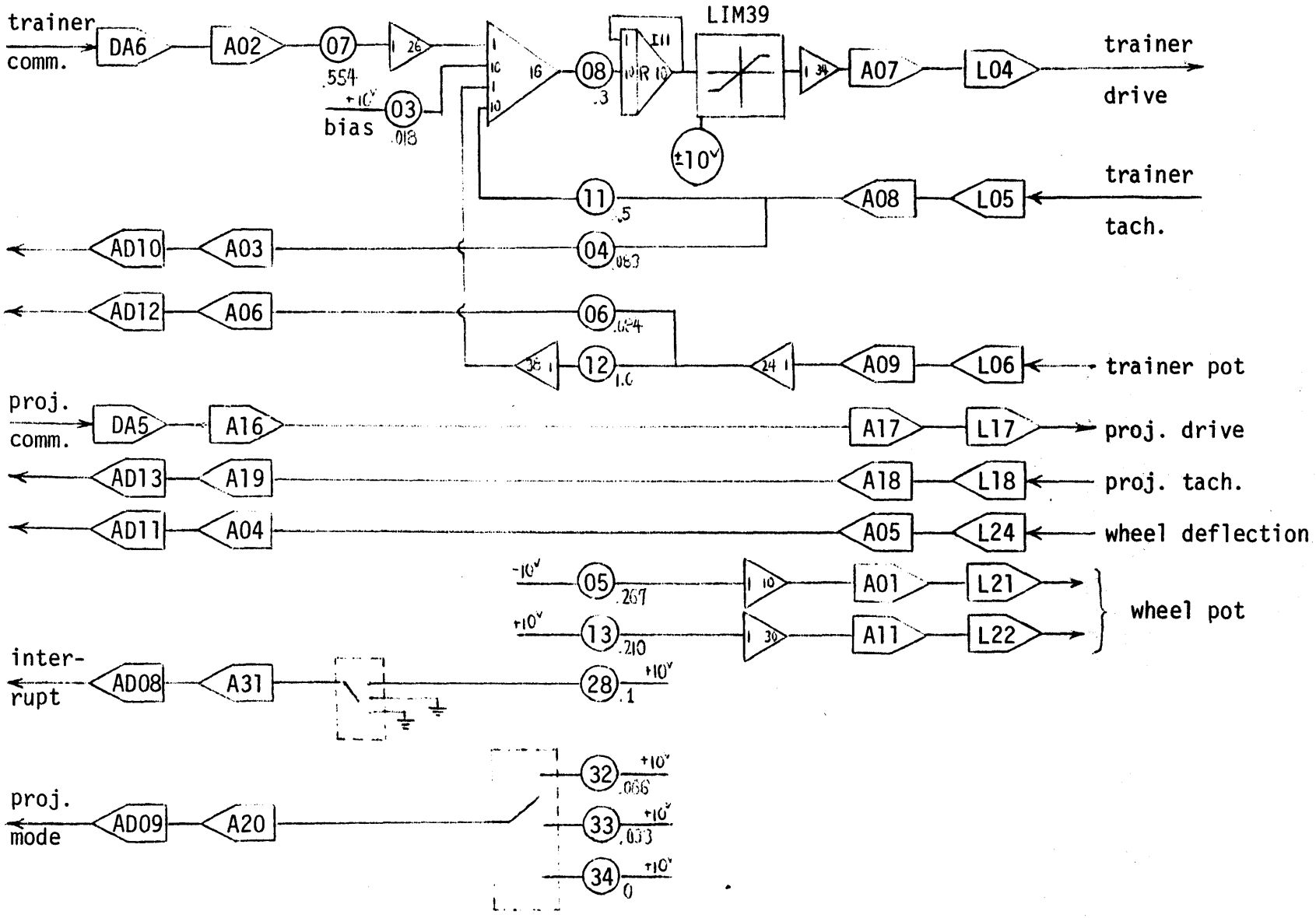

Figure B.1: Analog computer block diagram used in pitch

APPENDIX C

Experimental Procedures for the Computers and Apparatus

C.1 Operating Instructions in Pitch Experiment

C.1.1 Turn on

1. Power up PDP-11, analog computer, strip chart and audio system.
2. Install PITRUN analog patchboard.
3. Check analog wiring; set pots and switches according to Table C.1; set analog computer to COMPUTE
4. Set all four strip chart channels to 0.5 V/div and zero the channels.
5. Boot up the PDP-11 and run PITRUN; respond Y to demonstration question.
6. Install PITRUN trunklike patchboard and set analog amplifier AK with P03 = 0.1834 volts.
7. Proceed to trainer room and ensure that trainer is level in pitch and roll, and that control wheel is approximately centered.
8. Turn on LINK power.
9. Turn on projector power supply and projector bulb, then tighten the film. If the stripe position is not suitable (horizontal), then rotate the stripe by using the stripe control box.
10. Turn on pitch mode switch.
11. Hit interrupt switch on control box to check out system; switch modes 2 through 4 to check out projector control. Refer to Table C.2 for mode definitions.

12. Set control box mode to 1 and start program running; control the trainer via the control wheel.

13. Interrupt program operation and return to computer room. Set analog switch 3 to UP, and repeat step 11, checking trainer and projector responses on the strip chart recorder.

C.1.2 Operation

If a demonstration is desired, simply instruct the subject and begin the run with the interrupt switch. If we want to save the data, terminate program execution and restart the program, then responding appropriately to the program prompts.

C.1.3 Turn Off

1. Interrupt the program to stop trainer.
2. Power down trainer and projector by reversing steps 8 through 10 in section C.1.1.
3. Power down computer room equipment by reversing steps 1 through 6 in section C.1.1.

C.2 Operating Instructions in the Sled Experiments

The operating instructions are described in the "Manual for the MIT Sled" by Arrott.

Table C.1 Analog Computer Settings in Pitch Experiment

POT	VALUE	SWITCH	POSITION
03	1.834	1	Center
04	0.833	2	Center
05	2.667	3	Center
06	0.840		
07	5.54		
08	3		
11	5		
12	10		
13	2.103		
16	1		
17	10		
18	10		
28	1.0		
32	0.67		
33	0.33		
34	0		

Table C.2 Mode Definitions

Mode	Projector	Disturbance
1	CON	absent
2	CON	present
3	CVU	present
4	FIX	present

INFORMED CONSENT STATEMENT

EFFECT OF VISUAL FIELD ON LATERAL MOTION STABILIZATION

We are interested in recording subjective nulling task during linear motion. During the experiment, we will strap you into a chair that moves horizontally. You head will be held immobile with a head restraint device. With different visual field(counter-motion, constant speed, stationary and dark), we may ask you to perform a nulling task(keep the chair stationary as possible as you can) with a control thumb wheel located on the chair. We anticipate that sessions will last no longer than one hour.

The motion during the experiment may produce sensations of dizziness or motion sickness. If this proves troublesome, the experiment will be stopped. Many people get motion sick, so do not hesitate to tell us if you feel any nausea, dizziness or stomach awareness.

You may stop the experiment at any time and withdraw for any reason. You will remain anonymous in any report which describes this work. If you have any questions concerning the purpose,procedures or risks associated with this experiment, don't hesitate to ask them.

CONSENT: I have been informed as to the nature and purpose of the experiments described herein and the risks involved, and agree to participate in these experiments.

I understand that in the event of injury resulting from the research procedures, medical care is available through the MIT Medical Department. The costs of such care will be borne by my own health insurance or other personal resources. Information about the resources available at the MIT Medical Department is available from Laurence Bishoff at 253-1774.
There is no compensation for possible injury, Either financial or insurance, furnished to research subjects merely because they are research subjects.

_____ _____

Subject's Name Signature

Date_____ Witness_____

APPENDIX D

INSTRUCTIONS AND FIGURES USED IN THE EMBEDDED FIGURES TEST

D.1 Instructions

"I am going to show you a series of colored designs. Each time I show you one, I wish you to describe it in any way you wish. I will then show you a simple form which is contained in that larger design. You will then be given the larger design again and your job will be to locate the simple form in it. Let us go through a practice trial to see how it is done."

Show the subject the practice complex figure (P-1) for 15 seconds. Then turn it over and show him the practice simple form (P) for 10 seconds. After that say: "I will now show you the colored design again and you are to find the simple form in it. As soon as you have found the simple form let me know and start tracing the simple form with this stylus. When you are tracing, do not let the stylus touch the surface of the card." Then remove the simple form and present the practice complex figure again. When the subject says that he has found the simple form, note the time but do not stop the watch. If he traces the simple form correctly, record the time at which he found it. If it is not the correct one, note the time followed by an (X). In the latter case, permit the stop watch to continue. If the subject has not found the simple figure in 3 minutes, go on to the next trial and record the score as follows: 180" (F).

"This is how we will proceed on all the trials. I would like to add that in every case the simple form will be present in the larger design. It will always be in the upright position, so do not turn the card around. There may be several of the simple forms in the same design, but you are to find and trace only one. Work as quickly as you possibly can, since I will be timing you, but be sure that the figure you find is exactly the same as the original simple form in size and proportion. As soon as you have found the form, tell me at once and then start to trace it. If you ever forget what the simple form looks like, you may ask to see it again, and you may do so as often as you like. Are there any questions?" Then proceed as above on all subsequent trials. If the subject asks to see the simple form again, stop the watch, but do not reset it. Allow him to see it for 10 seconds, then show the complex figure again and start the watch.

D.2 Figures used in the Embedded Figures Test

The simple figures are designated by a letter; the complex figures are designated by a letter and a number, the letter corresponding to that of a simple figure which it contains. Figures P and P-1 are the practice figures.

The specific colors used in the complex forms are represented by numbers; and wherever necessary the area covered by a given color is indi-

cated by wavy lines radiating from the number. Figure A2 remains uncolored. The colors to which the numbers refer are as follows: 1-red, 2-blue, 3-orange, 4-yellow, 5-brown, 6-dark green. (from Testa, 1969).

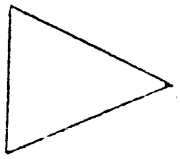

P

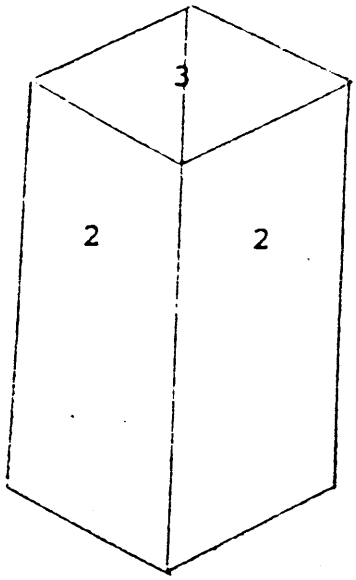

P-1

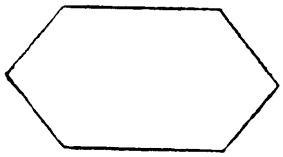

A

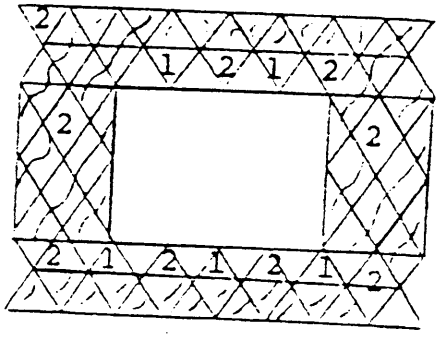

A-1

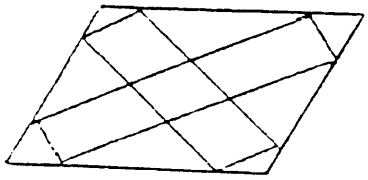

A-2

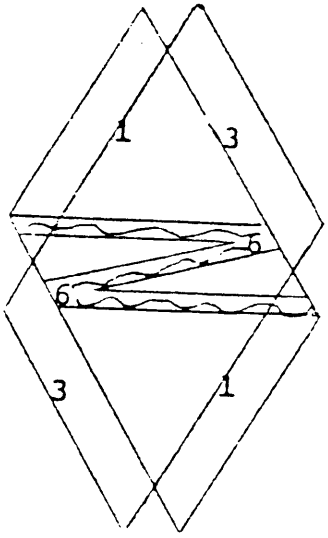

A-3

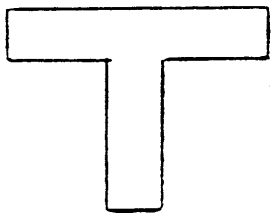

B

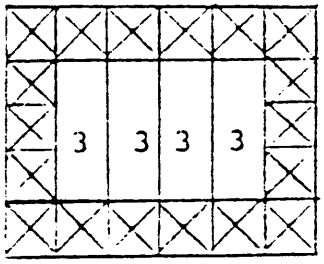

B-1

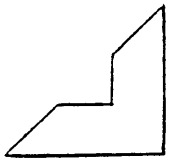

C

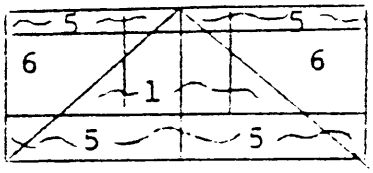

C-1

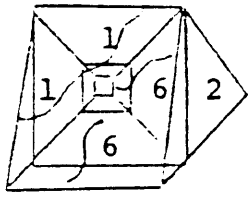

C-2

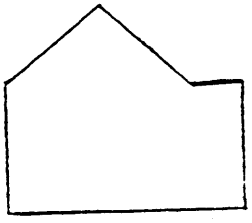

D

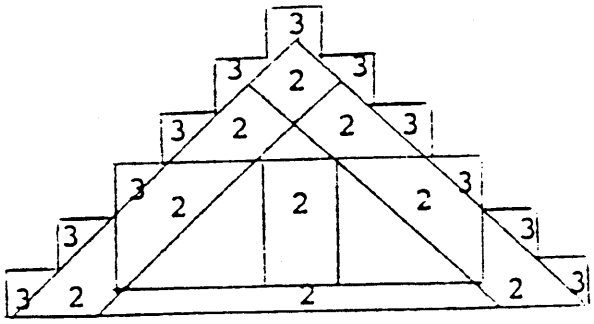

D-1

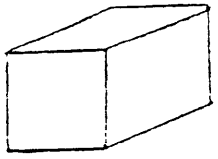

E

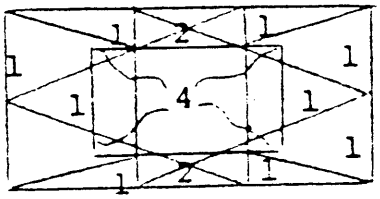

E-1

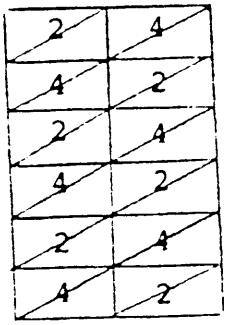

E-2

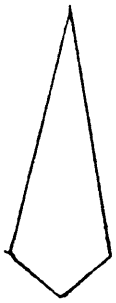

F

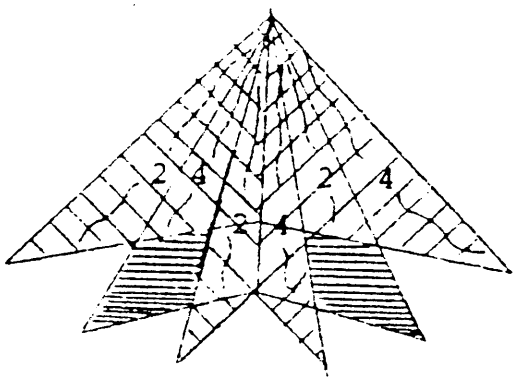

F-1

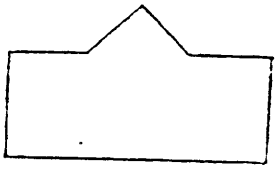

G

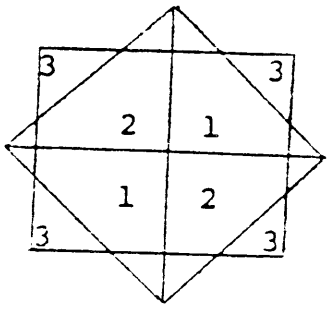

G-1

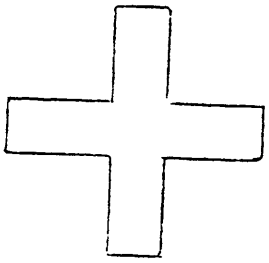

H

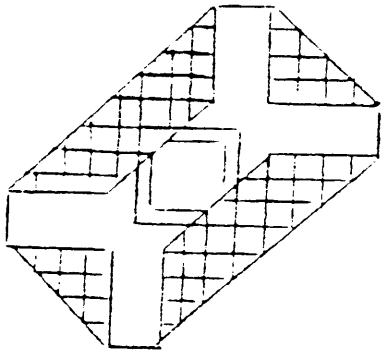

H-1

BIOGRAPHICAL SKETCH

Jen-Kuang Huang was born in Tainan, Taiwan, Republic of China. He received the Bachelor of Science degree from the National Taiwan University in 1975. After graduation, he entered the China Marine Groups and served as a second lieutenant for two years. Upon his return to civilian life, he entered M.I.T. in 1977 and joined the Man Vehicle Laboratory in the Department of Aeronautics and Astronautics to work as a research assistant. He was awarded the Master of Science in 1977 for his work in visual vestibular interaction.

Dr. Huang is married and has a two year old daugher.